A PROTEOMIC APPROACH TO METABOLISM IN THE DIATOM *THALASSIOSIRA PSEUDONANA*

Nicola Louise Hockin

A thesis submitted to the School of Environmental Sciences at the University of East Anglia, for the degree of Doctor of Philosophy

September 2011

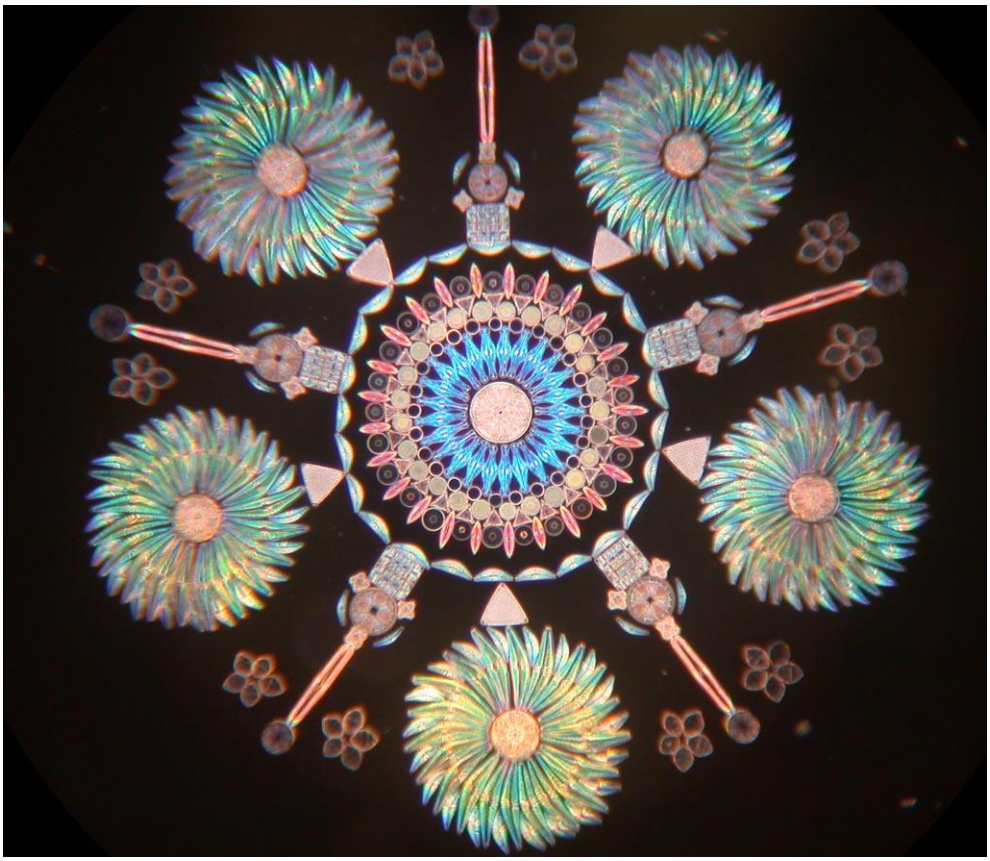

This beautiful image is an arrangement of diatoms by Klaus D. Kemp (www.diatoms.co.uk) and it reminds me how fantastic and diverse these organisms are. Since it has been on the wall beside my desk inspiring me to write it seems appropriate that it has a place in my thesis.

Abstract

Diatoms are thought to be responsible for up to 20 % of global primary productivity and carry out a range of ecosystem services, including an important role in the global sulphur cycle through the production of DMSP, precursor of the volatile sulphur compound DMS. After identifying here that the intracellular concentration of DMSP in *Thalassiosira pseudonana* (CCMP 1335) increased with increased salinity, increased light intensity and nitrogen starvation, these conditions were used in one of the first proteomic studies on the adaptive responses of a marine diatom to different growth conditions. Alongside this, gene expression analysis and enzyme activity quantification were also used to study sulphur metabolism and DMSP synthesis in this species. The findings presented suggest that increased sulphur assimilation is not required for increased DMSP synthesis; instead the availability of carbon and nitrogen substrates may be important in the regulation of this pathway. This is quite different to the regulation of sulphur metabolite synthesis in higher plants, which generally involves the up-regulation of sulphur assimilatory enzymes. Furthermore, changes relating to sulphur metabolism were specific to the individual treatments and little coordination was seen in transcript and protein response across the three growth conditions. Therefore, different patterns of regulation might be responsible for the increase in DMSP concentration seen under each treatment. Nitrogen metabolism is also of great interest since the availability of this nutrient limits primary production in large areas of the world's ocean. Therefore the *T. pseudonana* proteome response to nitrogen availability was investigated further and comparisons were drawn between the transcriptome response of this species, the higher plant Arabidopsis, green alga *Chlamydomonas reinhardtii* and the cyanobacterium *Prochlorococcus marinus* to nitrogen starvation. The results suggest that the response of diatom carbon metabolism to nitrogen starvation has more in common with the cyanobacterium than with other photosynthetic eukaryotes.

Acknowledgments

I would like to thank my supervisors Dr Gill Malin and Dr Stanislav Kopriva, firstly for giving me the opportunity to do this research and for their constructive advice on my thesis. During the project I have learnt a great deal from them and I greatly appreciate the time that they have committed to advising and mentoring me. I am grateful for their enthusiasm for the project and for creating an environment that I've felt confident to put forward my ideas and opinions and follow my research interests. I would also like to thank Dr Thomas Mock, for advising on my supervisory committee and as a co-author on the paper (Chapter 6). He has always brought interesting points to our meetings and I have learnt a lot from our discussions. Within my committee I have been lucky to have such a breadth of knowledge.

I am extremely grateful to Fran Mulholland (who is also a co-author on the paper) and Lynn Olivier, for being so generous with their time in teaching me the 2-dimensional gel electrophoresis techniques that were used in the proteomics study; this formed a large portion of my project.

I would also like to thank members, past and present, of the LGMAC and Kopriva labs for their help during the project and for answering my many questions, especially Anna Koprivova for teaching and practical advice, and Rob Utting and Gareth Lee for their technical assistance. Thanks also to Baldeep Kular for the HPLC analysis of amino acids and also to Mike Naldrett for conducting mass spectrometry analysis for protein identification.

To my friends, thank you for interesting discussions and welcome distractions. The people that I have met through the UEA and JIC have made the last four years in Norwich very enjoyable. The Clarice House 'Women in Science Networking Workshops' that I attended with Elizabeth, Heather and Emma were a highlight of my time here.

To my partner Graeme Kettles, thank you for being there with me through every high and low of the last four years with unfaltering support despite having your own PhD to complete.

To my parents, Jon and Sheila Hockin, and to my sister Lindsey thank you for your constant belief in me and for always telling me that I can do anything. This is not a career that I could have pursued without your support and for that I am grateful every day.

Contents

Table of Figures

Table of Tables

Abbreviations

AMT	Ammonium transporter
APR	APS reductase
APS	Adenylyl sulphate
ATP	Adenosine triphosphate
ATPS	ATP sulphurylase
CbL	Cystathionine-β-lyase
CgS	Cystathionine-γ-synthase
CPS	Carbamoyl phosphate synthase
DMS	Dimethylsulphide
DMSHB	4-dimethylsulphonio-2-hydroxybutyrate
DMSP	Dimethylsulphoniopropionate
Fd	Ferredoxin
GBT	Glycine Betaine
GS	Glutamine synthetase
GOGAT	Glutamate synthase
$^{\bullet}$OH	Hydroxyl radical
MALDI-	Matrix-assisted laser desorption/ionization- time of flight
TOF MS	mass spectrometery
MTHB	4-methylthio-2-hydroxybutyrate
MTOB	4-methylthio-2-oxobutyrate
NADH	Nicotinamide adenine dinucleotide
NADPH	Nicotinamide adenine dinucleotide phosphate
NAT	Nitrate transporter
NiR	Nitrite reductase
NR	Nitrate reductase
OAS	O-Acetylserine

OASTL	O-Acetylserine thiollyase
OPH	O-phosphohomoserine
PEPC	Phosphoenolpyruvate carboxylase
ROS	Reactive oxygen species
SAM	S-adenosyl methionine
SAT	Serine acetlytransferase
SiR	Sulphite reductase
SMM	S-methylmethionine
TCA	Tricarboxylic acid
TS	Theronine synthase

Chapter 1. Introduction

1.1. Overview

In this introduction I will first outline the important contribution that diatoms make to ecological processes. I will then give a brief history of their unusual evolution and describe how this has affected the diatom genome. Since a large proportion of this project was on sulphur and nitrogen metabolism I will discuss the relationship between marine phytoplankton and the cycling of these nutrients and describe what is known about their metabolism in diatoms. We so far do not have a complete understanding of these metabolic pathways in diatoms and I will therefore also describe what is known for photosynthetic eukaryotes generally, which will enable us to draw comparisons between diatoms and other organisms and develop hypotheses about general and specific regulation of nitrogen and sulphur metabolism.

1.2. An Introduction to Diatoms

1.2.1. Ecology

Diatoms are a major group of eukaryotic phytoplankton in the contemporary ocean and with an estimated 200,000 species they are certainly one of the most diverse (Mann and Droop 1996; Kooistra et al. 2007). Individual diatom cells vary in size by three orders of magnitude, from µm to mm, and are classified as either centric or pennate based on their symmetry. Diatoms are characterised by their silica frustule, which is formed by two parts that fit together like a Petri dish. This casing is laid down in very precise, ornate, species specific patterns that are reproduced from generation to generation.

Perhaps owing to their diversity, diatoms are found throughout the world's oceans from tropical to polar latitudes; they exist wherever there are adequate nutrients and light availability. Diatoms are highly successful in coastal and upwelling regions where they can form massive blooms reaching thousands of cells per millilitre (Suzuki et al. 2011). The shear abundance of diatoms in these regions makes them an important basis for marine food webs and they support large-scale fisheries, such as anchovies in the Peruvian upwelling (Bruland et al. 2005). Diatoms are also dominant in sea-ice, where they have adapted to the hypersaline brine channels that form within the ice. Ice cover is generally limiting to terrestrial primary production and in the Arctic and Antarctic both marine and terrestrial food chains are therefore reliant on diatom productivity (Armbrust 2009).

Global primary production based on satellite measurements is estimated to be approximately 104.9 pg carbon per year to which the ocean and terrestrial environments are thought to make roughly equal contributions (Field et al. 1998). It is proposed that diatom productivity accounts for around 40 % of the 45 to 50 pg carbon generated by the ocean, which is comparable to the productivity of all terrestrial rainforests combined (Nelson et al. 1995; Field et al. 1998).

In addition to their contribution to marine food webs, the productivity of diatoms also has a major role in the sequestering of carbon in the deep ocean through the biological carbon pump. This is a major carbon sink and important in the regulation of atmospheric CO_2 levels. The accumulation of settling diatom cells in the deep ocean over geological timescales has formed huge deposits of silica, or diatomaceous earth, which can be more than 1 km thick (Sims et al. 2006).

1.2.2. Evolution

Diatoms are eukaryotic photoautotrophs that belong to the heterokont algae (also known as stramenopiles). Having evolved from a secondary endosymbiotic event diatoms are sometimes grouped with the chromoalveolates, that also includes the coccolithophores and dinoflagellates and although this term can be considered outdated, since this group is now thought to be polyphyletic (discussed in Parker et al. 2008), it is useful for discussion of organisms that evolved by this route.

Members of the chromoalveolates have a fascinating evolutionary history (Figure 1.1). The plastids of the Plantae that enable their phototropic life style were formed by a primary endosymbiotic event involving the engulfment of a cyanobacteria-like photosynthetic prokaryote by a heterotrophic eukaryote around 1.5 billion years ago (Falkowski et al. 2004a; Yoon et al. 2004). These primary endosymbionts diverged into two distinct plastid lines, the chloroplasts of green algae and higher plants and the rhodoplasts of the red algae. Red algal fossil evidence places this split at more than 1.2 billion years ago (Butterfield 2001). The chloroplast line use chlorophyll *a* and *b* for light harvesting, whereas the rhodoplasts contain chlorophyll *a* and phycobilisomes.

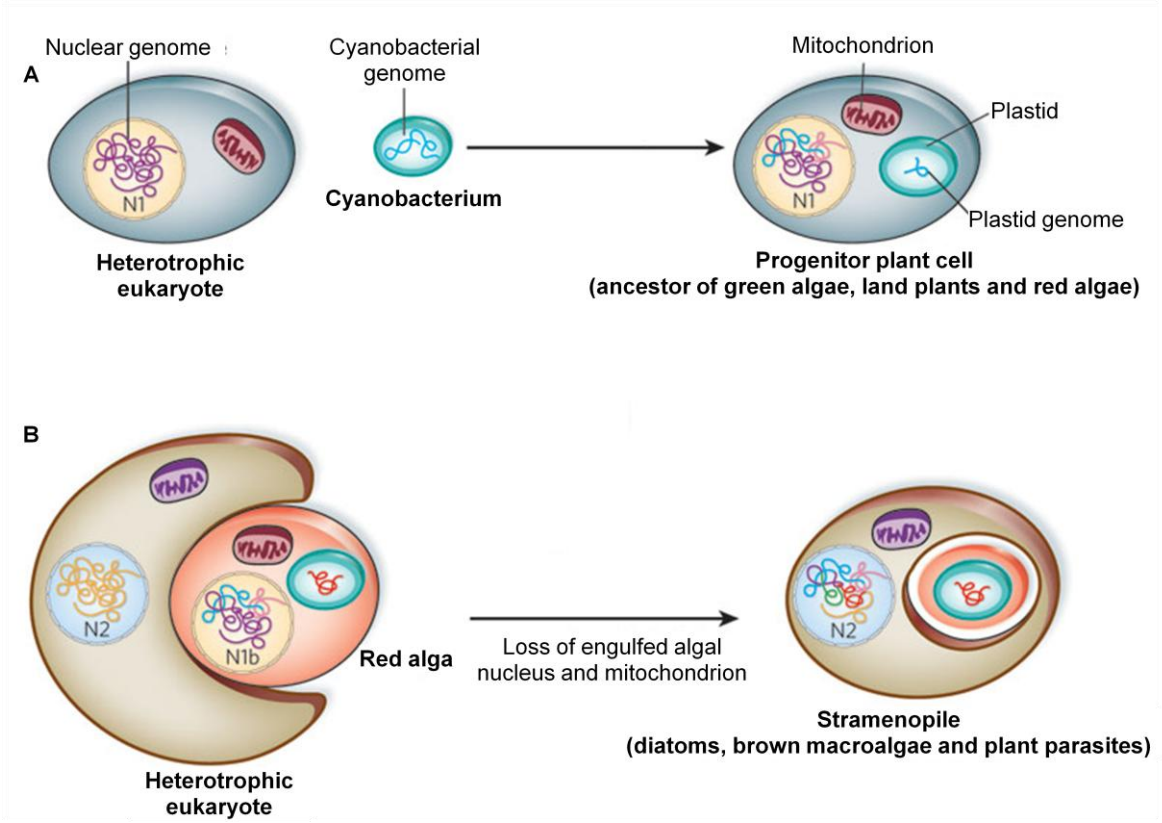

Figure 1.1. A simplified illustration from Armbrust (2009) of a. the primary endosymbiotic event that gave rise to green algae, higher plants and red algae, and b. the secondary endosymbiotic engulfment of a red algal cell, a process which formed the diatoms and other chromoalveolates.

The first milestone in deciphering diatom evolution was the observation of Gibbs et al. (1981) that plastids of diatoms and other chromoalveolates, are surrounded by four membrane layers, compared to the two membranes of plastids in green and red algae and higher plants. This observation was best explained by a hypothesis that the plastids of these algae had evolved from a secondary endosymbiotic event in which a photosynthetic eukaryote was engulfed by a heterotrophic eukaryote. The discovery of residual secondary nuclei (or nucleomorphs) between the second and third membrane layers of some species, further supported this hypothesis (Douglas et al. 2001). Analysis of plastid ribosomal RNA and the comparison of plastid genomes infers a red algal origin of the diatom plastid (Bhattacharya and Medlin 1995).

Molecular clock estimates, based on the divergence of ribosomal gene sequences, place the emergence of diatoms as early as 250 million years ago (Sorhannus 2007). However, the earliest fossil evidence of diatoms are reported to have been found in 180 million year old sponge reef deposits from southern Germany (Rothplez 1896 in Kooistra et al. 2007). Some of the disagreement between molecular and fossil dating might be due to poor preservation of the silica frustules in oceanic habitats. Both molecular clock (Yoon et al. 2004) and fossil evidence (Kooistra et al. 2007) indicate that centric diatoms arose first followed by the pennate form, although there is again some disagreement in dating. Katz et al. (2005) proposed that the emergence of diatoms, along with the coccolithophores and dinoflagellates, brought about important changes in the carbon cycling of the ocean, since these large cells have higher sinking rates than the previously dominant cyanobacteria thereby increasing the rate of carbon capture in the deep ocean.

1.2.3. Genomes

The endosymbiotic theory predicts a great complexity for diatom genomes, which have been formed from at least four sources (bacterial precursors for mitochondria and primary plastids, eukaryotic acceptors of primary and secondary plastids). The sequencing of two diatom genomes, the 32.4 Mb genome of the centric species *Thalassiosira pseudonana* with a predicted 11776 genes (Armbrust et al. 2004) and the 27.4 MB genome of pennate diatom *Phaeodactylum tricornutum*

with a predicted 10402 genes (Bowler et al. 2008), indeed showed that diatom nuclear genes originate from the exo- or endosymbiont of both the primary and secondary event. With each endosymbiotic event genes were transferred from the endosymbiont to the host nucleus (Falkowski et al. 2004a) and because of this the diatom genome is often described as chimeric. This evolutionary history distinguishes diatoms (and other chromoalveolates) from higher plants and green algae.

The diatom photosynthetic apparatus is likely to have been acquired from the original primary prokaryotic endosymbiont, via the secondary red algal endosymbiont, since many diatom proteins shared by all groups of eukaryotic photoautotrophs are found to be involved in chloroplast functions (Armbrust et al. 2004). On the other hand, Armbrust et al. (2004) demonstrated that 806 *T. pseudonana* predicted proteins align with *Mus musculus* (mouse) proteins, but not green plant *Arabidopsis thaliana* or red alga *Cyanidioschyzon merolae* and are thus most probably remnants of the heterotrophic eukaryote acceptors. A surprising discovery in the diatom genome was a complete urea cycle that had not been found in eukaryotes outside the Metazoans (Allen et al. 2006). Both diatom genomes were also found to contain approximately 7.5 % bacterial genes, which is considerably higher than in other eukaryotes (Bowler et al. 2008, Armbrust et al. 2004). These are likely to have been incorporated by horizontal gene transfer, which is not entirely unexpected since there are reports of close associations between diatoms and bacteria (Carpenter and Janson 2000; Zehr and Ward 2002; Schmid 2003). The presence of genes in diatom genomes not found in other photosynthetic eukaryotes provides the potential for novel metabolic processes. Nunn et al. (2009) have now characterised the *T. pseudonana* proteome, demonstrating that many of these proteins of interest are translated and are therefore likely to be active in the cell.

The sequencing of diatom genomes and proteome has provided a wealth of information on the evolution and success of these organisms and has also accelerated the development of a molecular toolbox for these organisms (Armbrust 2009), because of this I have chosen to focus on *T. pseudonana* (strain CCMP1335) in this project, which has become a model organism for centric

species and has been used in physiological studies of diatoms. *T. pseudonana* (CCMP 1335) was originally isolated from Moriches Bay, Long Island, New York.

1.3. Sulphur

1.3.1. Algae and the global sulphur cycle

Marine phytoplankton play a key role in the global sulphur cycle through the synthesis of dimethylsulphoniopropionate (DMSP); the main route for the production of the volatile sulphur compound dimethylsulphide (DMS) is through the lysis of DMSP, a process which also produces acrylate. It is currently thought that DMSP lysis occurs outside the cell and that only a small proportion of DMSP released is from healthy cells and it is more often mediated by viral lysis of the cell or grazing (Wolfe and Steinke 1996; Malin et al. 1998). An external DMSP lyase enzyme has been identified in the prymnesiophyte *Phaeocystis* (Stefels and Dijkhuizen 1996), although it has yet to be confirmed in other species. Marine bacteria are also able to convert DMSP to DMS (Todd et al. 2009) and a large proportion of DMS in the water column is consumed by microbial processes, however, a proportion is released, providing the most substantial biogenic source of sulphur to the atmosphere (Kiene et al. 2000) (Figure 1.2).

The sea-to-air flux of DMS transfers sulphur from the oceans, which are a major sulphur reservoir, to the relatively sulphur-limited land (Lovelock et al. 1972). Furthermore, once in the atmosphere, DMS oxidises to form aerosol particles, which have a cooling affect on the climate (Figure 1.2), directly through the refection of solar radiation and indirectly through the formation of cloud condensation nuclei (Charlson et al. 1987). The global annual flux of DMS from the oceans into the marine atmosphere is thought to be between 15 and 33 Tg sulphur per year (Kettle and Andreae 2000) and Watson and Liss (1998) estimate that DMS emissions have around a 4 °C cooling affect on the planet. Despite the importance of DMSP production in the sulphur cycle and climate regulation, there has been limited research into basic sulphur metabolism in marine phytoplankton.

We have very little direct knowledge of this pathway in most phytoplankton species, including diatoms, and know almost nothing about its regulation.

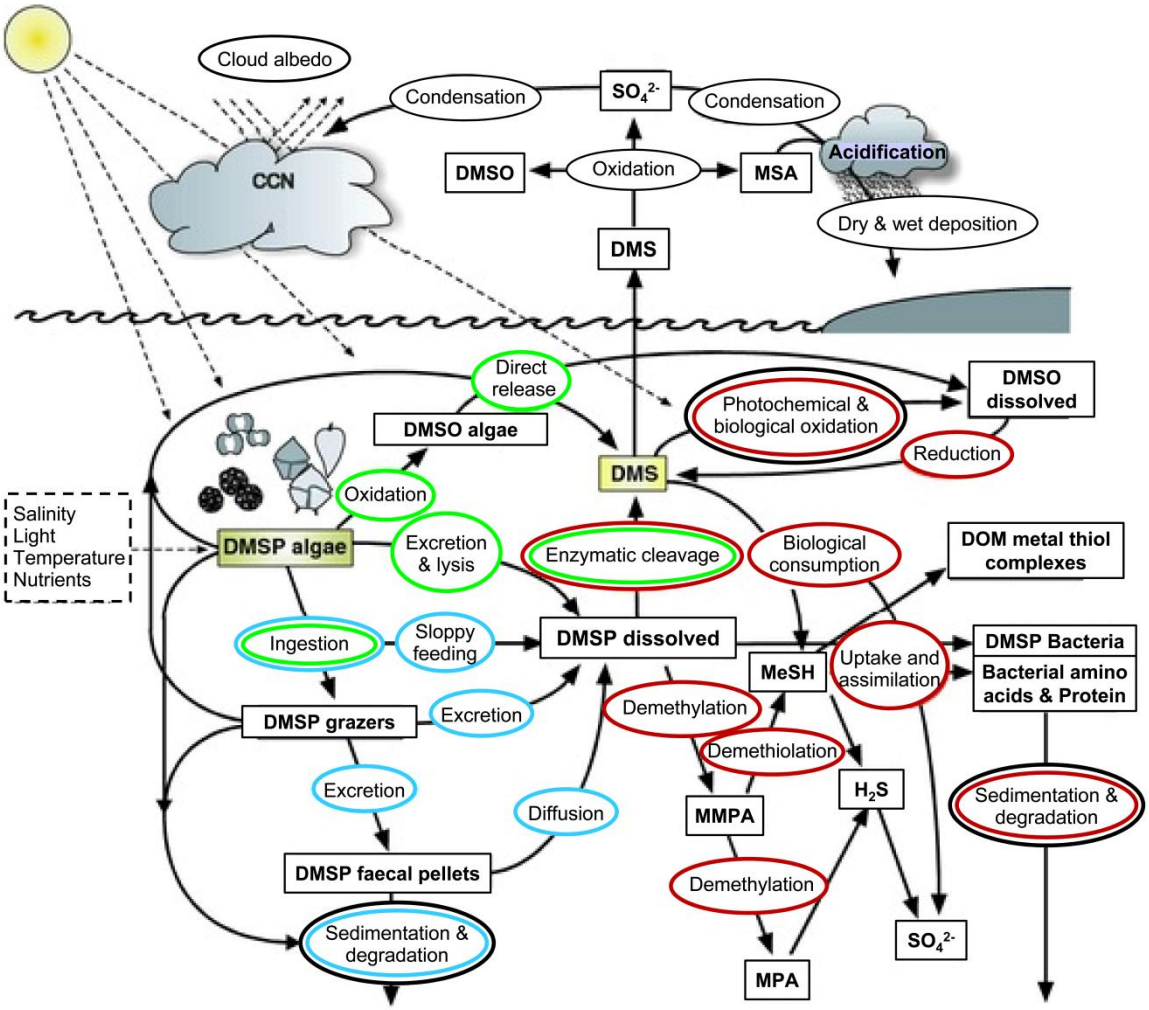

Figure 1.2. Marine biogeochemical cycling of DMS and DMSP (Stefels et al. 2007). Marine phytoplankton take up sulphate from the oceans and convert it to DMSP. This is then broken down by the algal metabolism and microbial interactions to DMS, a volatile sulphur compound. A complex network of interactions then determines how much of this DMS enters the atmosphere through sea-to-air gas exchange, where it is oxidised to form aerosol particles and subsequently cloud condensation nuclei (CNN). Processes dominated by phytoplankton are shown in green ellipses, zooplankton processes are shown in blue, red represents bacterial processes and black ellipses are abiotic factors. Dissolved inorganic matter (DOM); dimethylsulphoxide (DMSO); methanethiol (MESH); mercaptopropionate (MPA); Methylmercaptopropionate (MMPA); methanesulphonic acid (MSA)

Considerable variability in DMSP production has been observed between phytoplankton taxa (Keller et al. 1989). The Dinophyceae and the Prymnesiophyceae are the highest DMSP producers with intracellular concentrations in excess of several hundred mmol l^{-1} in some species, although diatoms and members of other groups can also produce significant amounts. The chlorophytes on the other hand produce very little DMSP (Keller et al. 1989), with the exception of seaweeds such as *Ulva lactuca* (Dickson et al. 1980; Dickson et al. 1982). In addition to taxonomy, external factors, such as nutrient availability, salinity and temperature can cause variations in DMSP production. Multiple cellular functions have been proposed for DMSP and its primary role in the cell remains an area of debate.

1.3.2. The Role of DMSP in the Cell

1.3.2.1. Osmolyte

There is strong evidence that DMSP is involved in osmoregulation; it is notable that DMSP is produced almost exclusively by marine phytoplankton and seaweeds, whereas freshwater algae produce little or no DMSP (Keller et al. 1989), implying that DMSP production is an adaptation for halotolerance. However, there may be additional factors that might contribute to this distinction; sulphur availability is higher in seawater (28 mM) than freshwater (0.01 to 1 mM) (Ratti et al. 2011) and fresh water habitats might be affected less by nutrient limitation. DMSP does have a similar zwitterionic structure as the compatible solutes proline and glycine betaine, which are present in many algae and some halophytic higher plants (Figure 1.3) (Vairavamurthy et al. 1985). The compatibility of DMSP has been confirmed by the study of its effect on enzyme activities in extracts of the prasinophyte *Tetraselmis subcordiformis* (Gröne and Kirst 1991).

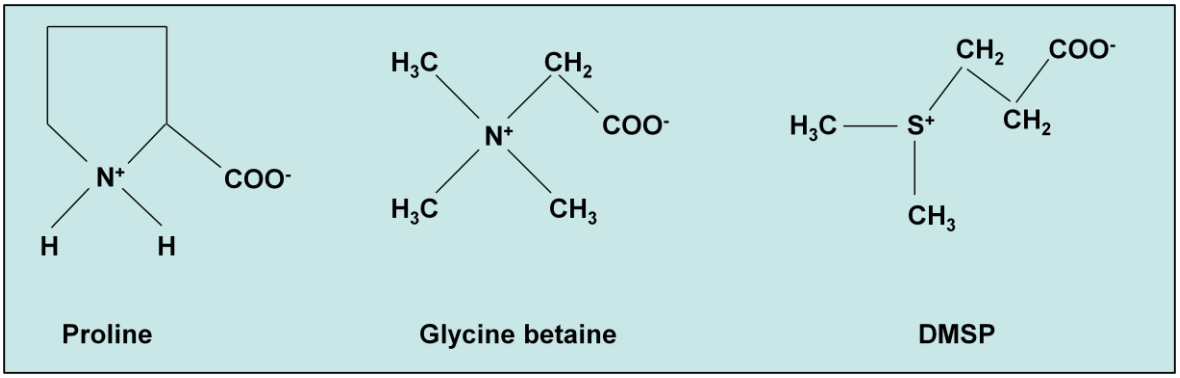

Figure 1.3. Structural formulae for the compatible solutes proline, glycine betaine, and DMSP.

Intracellular DMSP concentration has been found to increase under conditions of increased salinity in a number of algal species including the intertidal macroalga *U. lactuca* (Dickson et al. 1980; Dickson et al. 1982) and in both the coccolithophore *Pleurochrysis carterae* (Vairavamurthy et al. 1985) and the dinoflagellate *Crypthecodinium cohnii* (Kadota and Ishida 1968). The role of DMSP in osmoregulation is further supported by a reduction in the concentration of DMSP in *T. subcordiformis* (Dickson and Kirst 1986) and *P. carterae* (Vairavamurthy et al. 1985) cells when transferred to a lower salinity medium and both groups of authors propose that DMSP is released to the medium.

However, intracellular DMSP levels are not found to increase under hyperosmotic stress in all algal species. Stefels and Dijkhuizen (1996) did not detect any significant changes in the intracellular DMSP concentration of *Phaeocystis* after 6 hour high and low salinity shocks. In the macroalga *Ulva intestinalis* DMSP levels remained stable with increasing salinity while proline and sucrose were found to increase (Edwards et al. 1987), suggesting that these compounds are preferentially used in the hyperosmotic stress response of this species.

Marine phytoplankton rely on a range of osmoregulatory compounds, including quaternary ammonium compounds (e.g. glycine betaine), amino acids (e.g. proline), and the tertiary sulphonium compound DMSP (Stefels 2000). However, not all organic solutes have equal protective properties and the energetic cost and nitrogen and carbon requirements of their

production can differ (Stefels 2000). Solute production may, therefore, depend on the physiological state of the cell and some compounds might be preferentially produced over others. Many of the solutes found in marine phytoplankton are nitrogen based, e.g. proline and glycine betaine (GBT). Since DMSP is sulphur based and does not contain nitrogen it might replace such osmolytes under nitrogen limited conditions. There is evidence suggesting that DMSP production is related to nitrogen availability; three out of four algal species examined by Keller and Korjeff-Bellows (1996) had increased DMSP content when cultures were grown in nitrogen limited conditions relative to nitrogen replete cultures. Similarly, 75 to100 % higher DMSP levels per cell were observed in nitrogen limited *T. subcordiformis* cultures compared to a non-limited control (Gröne and Kirst 1992). In continuous cultures of *T. pseudonana* the intracellular DMSP concentration was inversely related with glycine betaine during nitrogen limited growth conditions (Keller et al. 1999). This relationship, however, was not seen in *Amphidinium carterae* (Keller et al. 1999) so there might be a significant variation in DMSP function.

1.3.2.2. Cryoprotection

The compatibility of DMSP with protein structure is increased at low temperatures (Nishiguchi and Somero 1992), suggesting that, besides its role in osmoregulation, DMSP may also function as an effective cryoprotectant. Supporting this role Sheets and Rhodes (1996) found that intracellular DMSP concentration increased 8-fold with decreasing growth temperature, from 23 to 5 °C, in *T. subcordiformis*. DMSP has also been found to accumulate in *Emiliania huxleyi* cells at low temperatures (van Rijssel and Gieskes 2002). In polar macroalgae intracellular DMSP concentrations were higher in strains cultured at 0 °C compared to strains cultured at 10 °C (Karsten et al. 1992; Karsten et al. 1996). The concentrations found in these strains are thought to be high enough to protect enzymes in the macroalgal tissue after periods of freezing and in extracts from the polar macroalga *Acrosiphonia arcta* DMSP appears to stabilise the activity of malate dehydrogenase at low temperatures (Karsten et al. 1996). A stabilising affect was also observed when DMSP was added prior to freezing and thawing of preparations of the cold labile enzyme

lactate dehydrogenase (Karsten et al. 1996). This stabilising effect increased with increasing DMSP concentration and became stronger than that of proline and sucrose.

1.3.2.3. Antigrazing

A number of grazing experiments have suggested that DMSP may also have a role in chemical defence. When DMSP is broken down, by the enzyme DMSP lyase, DMS and acrylate are produced (Wolfe et al. 2002; Evans et al. 2007). Sieburth (1960) was first to suggest that DMS may be a by-product and that acrylate is produced as a toxin. It has since been demonstrated that during protozoan grazing on the coccolithophore *E.huxleyi*, the conversion of DMSP to DMS by the prey is increased (Wolfe and Steinke 1996). Lysis of ingested *E. huxleyi* cells is thought to initiate the mixing of the algal DMSP and the enzyme DMSP lyase, which are presumed to be separated within the cell (Wolfe and Steinke 1996). Wolfe et al. (1997) observed that although protozoan predators vary in their ability to ingest and survive on prey with high DMSP lyase activity, all grazers tested preferentially selected strains of *E. huxleyi* with low enzyme activity when offered prey mixtures. This suggests that high levels of DMSP lysis deter protozoan herbivores, presumably through the production of highly concentrated acrylate (Wolfe et al. 1997). Interestingly, such lysis reaction has analogy among higher plant and macrophytic defence-mechanisms, such as the hydrolysis of glucosinolates (Bennett and Wallsgrove 1994) and the rapid conversion of halimedatetraacetate to the feeding deterrent halimedatrial upon injury of the marine macroalgae *Halimeda* (Paul and Van Alstyne 1992).

1.3.2.4. Overflow mechanism

In the photic zone of the marine environment, light is not usually a growth-limiting factor; the requirement for nutrients is generally more critical. Stefels (2000) has hypothesised that DMSP may act as an overflow metabolite when growth is unbalanced by nutrient limitation. When captured energy cannot be utilised for growth, DMSP production may allow the dissipation of excess energy into the reduction of sulphate. In the marine environment, sulphate is a nutrient in excess, whereas nitrogen often limits phytoplankton growth. As discussed previously, nitrogen

limitation does appear to result in increased DMSP concentration in a number of algal species. In addition, DMSP production may keep the concentration of cysteine and methionine low, preventing inhibitory feedback mechanisms and allowing the continuation of metabolic pathways (Simó 2001), since intracellular DMSP level is generally much higher than that of methionine and its precursor cysteine.

1.3.2.5. Antioxidant function

In an alternative hypothesis for increased DMSP production under nutrient limitation Sunda et al. (2002) suggest that DMSP might be part of an antioxidant defence system. Reactive oxygen species (ROS; superoxide radicals, hydrogen peroxide and hydroxyl radicals) are formed when reduced components of the photosynthetic electron transport chain react with molecular oxygen to produce singlet oxygen (Foyer and Harbinson 1994). Bucciarelli and Sunda (2003) suggest that disruption of photosynthesis due to metabolic imbalance, e.g. during nutrient limitation, leads to increased ROS production, possibly due to a reduced rate of CO_2 fixation in the Calvin Benson cycle (Govindjee et al. 1973) and/or inefficient electron transport within the photosynthetic electron transport chain. The formation of ROS is also accelerated under stress conditions, such as low temperature and high salinity (Butow et al. 1998; Noctor and Foyer 1998), which have been found to increase DMSP production in algal species, as discussed above.

DMSP and its breakdown and oxidation products (DMS and acrylate, dimethylsulphoxide and methane sulphonic acid) react rapidly with hydroxyl radicals ($^{\bullet}OH$), and thus could serve as effective scavengers of these highly toxic ROS (Sunda et al. 2002). Together these compounds potentially constitute an antioxidant system, which could be more effective at scavenging $^{\bullet}OH$ in high DMSP algae than other well-recognised antioxidants, such as ascorbate and glutathione (Sunda et al. 2002). Exposure to high Cu^{2+} and H_2O_2 also lead to a 9- to 15-fold increase in the intracellular concentration of *E. huxleyi*; indeed, copper catalyses the reaction of H_2O_2 to $^{\bullet}OH$ (Sunda et al. 2002).

Supporting this theory a 20-fold increase in DMSP concentration has been observed in *T. pseudonana* under CO_2 limitation (Sunda et al. 2002), which directly affects the Calvin Benson cycle and has been shown to stimulate the formation of reactive oxygen species in cultured phytoplankton (Vardi et al. 1999). Bucciarelli and Sunda (2003) also measured increases in DMSP concentration in *T. pseudonana* under nitrate, phosphate and silicate limitation, which all cause oxidative stress by decreasing photosynthetic efficiency (Lippemeier et al. 2001). DMSP may also replace nitrogen containing antioxidants, such as glutathione, under nitrogen limitation (Bucciarelli and Sunda 2003).

An antioxidant function would also explain the observed increase in DMSP concentration in *Phaeocystis* at high light intensity (Stefels and Van Leeuwe 1998), since $^{\bullet}OH$ is a by-product of photosynthesis. Intracellular DMSP concentration in *E. huxleyi* increased by 5-100 % and DMS concentration by 2.4- to 36- fold in cultures grown under 30 % solar radiation, with different portions of the UV spectrum removed, relative to cultures grown under similar intensity of fluorescent light with no UV radiation (Sunda et al. 2002). In support of this hypothesis maximum DMS concentrations in oceanic surface waters occur in the summer when solar UV exposure is highest due to higher UV intensity, longer photoperiods, and shallower mixed depths (Simó and Pedrós-Alió 1999).

1.3.3. Sulphur Metabolism

1.3.3.1. Sulphate uptake

Sulphate is the primary source of sulphur available in nature. To utilise sulphate, photosynthetic organisms must take it up and transport it to the plastids where its activation and reduction occur (Figure 1.4). Sulphate uptake is facilitated by a range of sulphate transporters. Higher plants generally use H^+/sulphate co-transporters (Lass and Ullricheberius 1984) and these can be further categorised according to their substrate affinity and localisation (Buchner et al. 2004). In the green alga *Chlamydomonas reinhardtii,* three plant-like H^+/sulphate co-transporters, SULTR1, SULTR2 and SULT3, have been identified (Shibagaki and Grossman 2008).

Prokaryotic organisms, including cyanobacteria, possess a different ATP-dependent sulphate transport complex (Laudenbach and Grossman 1991). A homologue of one of the components of this ABC transporter, SulP, (Green et al. 1989; Laudenbach and Grossman 1991) has been found associated with the chloroplast membrane of *C. reinhardtii* (Chen et al. 2003). This appears to be a major path for sulphate entry to the plastids of this species for reduction and assimilation. A strain with reduced *SulP* expression was found to exhibit responses associated with sulphur starvation and both *SulP* mRNA and protein increased in wild type cells under sulphur starvation (Chen and Melis 2004; Chen et al. 2005). Similar genes have been identified in the chloroplast genomes of a number of green algae and lower plants including *Mesostigma viride, Marchantia polymorphia* and *Anthoceros formosa* (Kopriva et al. 2008). However, no orthologues of this transporter are found in higher plants and the nature of plant plastidic sulphate transporter remains unknown.

A second prokaryotic sulphate transport system of the major facilitator superfamily (MFS) has been found in red algae, such as *C. merolae*. Accordingly, MFS is also present in algae which have a plastid of red algal origin, including the diatom *T. pseudonana*, the haptophytes *Pavlova lutheri* and *Isochrysis galbana* and the dinoflagellate *Karlodinium micrum* (Kopriva et al. 2008).

1.3.3.2. Primary Sulphate Assimilation to Cysteine

ATP-sulphurylase and APS-kinase. Sulphate is a chemically stable compound and must be activated by ATP to 5'-adenylsulphate (APS) before it can be reduced, and this activation is catalysed by ATP sulphurylase (ATPS). The *T. pseudonana* genome appears to encode two isoforms of this enzyme, one of which is plastid targeted, whilst the lack of signal and transit peptide on the other suggests that it is localised in the cytosol (Patron et al. 2008).

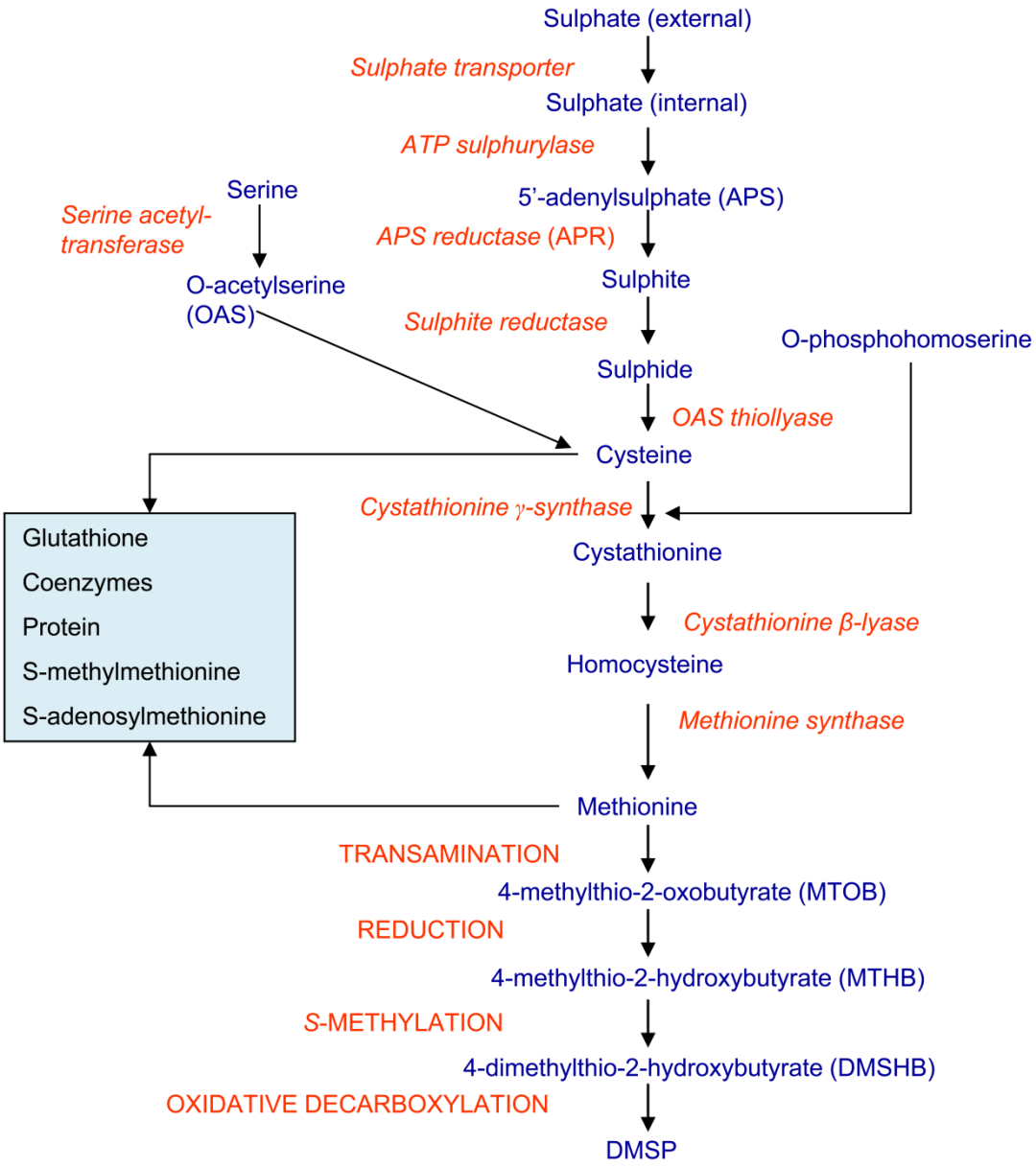

Figure 1.4. A proposed pathway of sulphate uptake and assimilation and the biosynthesis of DMSP in some algae. Metabolites are shown in blue and enzymes are shown in red italic. Enzymes between the methionine and DMSP have not yet been identified. The putative reactions proposed by Gage et al. (1997) are shown in red capitals.

The APS formed in the above reaction can be phosphorylated by APS kinase (APK) to 3'-phosphoadenosine 5'-phosphosulphate (PAPS). Two APK genes have been found in the *T. pseudonana* genome, one of which is localised to the cytosol, while the other is fused to the plastidic ATPS, however, APK activity has not yet been demonstrated in a diatom. In higher plants PAPS can be used by sulphotransferases to catalyse the sulphation of various metabolites including flavanols, choline and glucosides.

APS reductase. Activated sulphate is reduced in two steps. First, the addition of two electrons to APS result in formation of sulphite catalyzed by APS reductase (APR). There are many studies suggesting that APS reduction is a key regulatory step in plant sulphate assimilation (Davidian and Kopriva 2010; Takahashi et al. 2011). The addition of *O*-acetylserine (OAS), sulphide, glutathione and cysteine has been found to regulate APR while other enzymes of the pathway are not affected (Koprivova et al. 2000; Westerman et al. 2001; Vauclare et al. 2002). Using ^{35}S-labelled sulphate Vauclare et al. (2002) have demonstrated that APR is responsible for up to 90 % of the control of flux through the reduction of internal sulphate. Furthermore, the over-expression of APR leads to the accumulation of cysteine and glutathione, sulphite and thiosulphate (Martin et al. 2005), whereas no increase in sulphur metabolites is seen with ATPS or OAS thiollyase (OASTL) over-expression (Saito et al. 1994; Hatzfeld et al. 1998).

APR is considered to be under demand-driven regulation. The activity and/or transcript level of this enzyme is increased under heavy metal stress, salinity, exposure to high light and cold, which are conditions that induce the production of glutathione or other sulphur containing stress defence compounds (Brunner et al. 1995; Lee and Leustek 1999; Koprivova et al. 2008; Queval et al. 2009). On the other hand the addition of cysteine or glutathione reduces APR mRNA, protein levels and activity (Vauclare et al. 2002). The mRNA level of an APR isoform has been found to be increased in mutants over-accumulating OAS, which is a carbon precursor of cysteine (discussed below). Jasmonate and salicylate, which are hormones involved in plants stress response, also increase APR mRNA levels and activity (Koprivova et al. 2008). Transcript levels of

APR generally correlate well with the activity of this enzyme, however posttranslational regulation has been demonstrated by Bick et al. (2001) in response to oxidative stress.

Remarkably, in some algae APR activity is 400-fold higher than typically found in plants (Gao et al. 2000). Although Gao et al. (2000) found that APR activity did not directly correlate with DMSP content, the high APR activity observed may reflect a process for building an intracellular pool of reduced sulphur, which could enable more rapid synthesis of DMSP. The two APR isoforms identified in *T. pseudonana* belong to the APR-B family, discovered recently in lower plants (Kopriva et al. 2007). This APR-B isoform differs from the higher plant enzyme by an absence of iron-sulphur cofactor. The presence of this isoform in diatoms and other marine microalgae might represent an adaptation to limited iron availability in the ocean (Patron et al. 2008).

Sulphite reductase. The sulphite generated by APR is further reduced to sulphide by a plastidic sulphite reductase (SiR). In plants the electron donor for this reduction is ferredoxin, which ties the reduction to photosynthesis, whereas in bacteria it is NADPH (Kopriva et al. 2008). In *C. reinhardtii* there are two genes encoding a eukaryotic-type SiR (*SIR1* and *SIR2*), which use reduced ferredoxin as reductant, and a single gene for a putative bacterial-type enzyme (*SIR3*), which most likely uses NADPH or NADH (Shibagaki and Grossman 2008). The *T. pseudonana* and *C. merolae* nuclear genomes also appear to contain genes encoding both eukaryotic and prokaryotic SiR. (Shibagaki and Grossman 2008).

Serine Acetyltransferase and OAS thiollyase. Cysteine, the first organic compound of sulphur reduction, is formed by the reaction of sulphide with OAS which is catalysed by OASTL. OAS is produced by the activation of the amino acid serine with acetyl-CoA by serine acetyltransferase (SAT). Cysteine synthesis represents a point in the sulphur assimilation pathway where sulphur, nitrogen and carbon metabolism converge. Together OASTL and SAT form the cysteine synthase complex. In higher plants the function of cysteine synthase complex is regulated by metabolite levels. SAT is active when associated with the complex and free SAT has little or no activity,

whereas OASTL is inactive when in the complex and has maximal activity when free (Droux et al. 1998). OAS production by SAT is considered to be a limiting step in cysteine synthesis since OASTL activity levels in the cell are 300-fold higher that SAT (Ruffet et al. 1994) and therefore the binding of SAT determines the rate of cysteine synthesis. The addition of OAS in feeding experiments, mimicking the accumulation of OAS under sulphur deprivation, has been shown to dissociate the complex, thereby inhibiting SAT activity (Droux et al. 1998; Wirtz and Hell 2006), whilst sulphide has a stabilising affect on the complex, maintaining SAT activity and allowing maximum cysteine production (Droux 2003). In addition, SAT is inhibited by physiological concentrations of cysteine, avoiding the accumulation of this amino acid when it is not being consumed by glutathione or methionine synthesis (Droux 2003). Cysteine levels in the cell are maintained in a tight range, since excess might affect the redox potential of the cell (Droux et al. 1998; Wirtz and Hell 2006). OAS has a regulatory effect on genes involved in sulphate uptake and assimilation with APR isoforms in *A. thaliana* and *Lemna minor* up-regulated in response to OAS addition (Koprivova et al. 2000; Kopriva et al. 2002). On the other hand genes involved in these steps are down-regulated by high levels of cysteine and glutathione (Koprivova et al. 2000; Vauclare et al. 2002).

In vascular plants SAT and OASTL are both encoded by multiple genes and unlike the reductive steps of sulphate assimilation, which are localised exclusively in the plastid, there are isoforms of each protein present in the cytosol, plastids and mitochondria (Jost et al. 2000). This adds another dimension to the regulation to cysteine synthesis as ratio of substrates and products and of SAT and OASTL vary between compartments. The *T. pseudonana* genome is also thought to contain three SAT and OASTL isoforms (Kopriva et al. 2008; Shibagaki and Grossman 2008).

1.3.3.3. Cysteine to Methionine

Cysteine serves as the central intermediate from which nearly all cellular compounds containing reduced sulphur are derived. Apart from being the precursor of glutathione, cysteine is also involved in two important metabolic pathways: the synthesis of protein and the *de novo* production

of methionine (Giovanelli 1990). The ability of *P. carterae*, a prymnesiophyte (belonging to the chromoalveolate algae), to grow on cysteine alone as a sulphur source indicates that trans-sulphuration is the main pathway in methionine biosynthesis in this organism (Vairavamurthy et al. 1985) as in higher plants (Thompson et al. 1982) and green algae *Chlorella* sp (Giovanelli et al. 1980), as opposed to direct sulphydration. In the trans-sulphuration pathway sulphide is channelled through cysteine, cystathionine and homocysteine to methionine. On the other hand, metazoans are able to synthesize cysteine from methionine.

Cystathionine γ-synthase. Methionine belongs to the aspartate family of amino acids, along with threonine, lysine and isoleucine, and methionine synthesis therefore represents a second point where sulphur and nitrogen and carbon metabolism meet. The first reaction in the trans-sulphuration pathway, catalysed by cystathionine γ-synthase (CgS), is at a branching point where this enzyme and threonine synthase (TS) compete for their common substrate O-phosphohomoserine (OPH). The relative activities of these enzymes represent an important point in the regulation of methionine synthesis.

Galili and Höfgen (2002) reported that plants overproducing a bacterial feedback-insensitive aspartate kinase, thereby increasing carbon flow to OPH, exhibited higher levels of threonine, but only a slight increase in methionine levels was seen. However plants with a mutation impairing TS did have a 22-fold increased accumulation of free methionine (Bartlem et al. 2000). TS activity is strongly stimulated in plants by S-adenosylmethionine (SAM), a methionine derivative (Curien et al. 1996). It is suggested that CgS might be under post-transcriptional regulation and a region of the *CgS* gene, MTO1, is thought to be involved in the methionine-dependent degradation of CgS mRNA in some higher plants, since a mutation in this region leads to an increase in CgS mRNA, protein and enzyme activity (Inaba et al. 1994; Chiba et al. 1999; Ominato et al. 2002). Over-expression of CgS in *A. thaliana* leads to an increase in free methionine and S-methylmethionine, suggesting that regulation can be overcome by increasing the level of CgS mRNA (Gakiere et al.

2002; Kim et al. 2002). This evidence suggests that CgS is a rate limiting step of methionine synthesis in higher plants.

.

Cystathionine β-lyase. In the second step in methionine synthesis cystathionine β-lyase (CbL) generates homocysteine from cystathionine. Over-expression of CbL in *A. thaliana* resulted in higher levels of CbL peptide, but no increase in methionine levels was seen and therefore CbL is not thought to be rate limiting to methionine synthesis and its activity is most likely regulated by the supply of its substrate cystathionine from CgS (Gakiere et al. 2002).

Methionine synthase. The methylation of homocysteine to form methionine is catalysed by methionine synthase of which there are two forms, vitamin B_{12}-dependent (METH) and vitamin B_{12} -independent (METE). In higher plants methionine synthesis is vitamin B_{12}-independent, whereas the diatom *T. pseudonana* possesses only the METH form making it a vitamin B_{12} auxotroph (Croft et al. 2005). However, this is not the case for all diatoms or even members of the *Thalassiosira* genus and may represent a potential divergence in the regulation of sulphur metabolism (Croft et al. 2005). Interestingly, the *C. reinhardtii* genome appears to encode both the METE and METH forms and Croft et al. (2005) have demonstrated that METH is constitutively expressed whether or not vitamin B_{12} is available, whereas METE is only expressed in its absence. In bacteria it has been shown that METH has a higher catalytic activity and is therefore used preferentially over METE (Gonzalez et al. 1992). This step also represents a crossing point in sulphur and folate metabolism, with 5-methyltetrahydropteroyltri-L-glutamate being a cofactor in methionine synthesis.

1.3.3.4. DMSP Biosynthesis

Along with its incorporation into protein and the utilisation of its methyl group in trans-methylation reactions, methionine is also the precursor for the biosynthesis of DMSP in marine algae and a few species of higher plant (Greene 1962; Pokerny et al. 1970). A significant proportion of sulphur from the sulphate assimilation pathway can be diverted to DMSP synthesis in some phytoplankton species (Shibagaki and Grossman 2008).

There appear to be three possible routes of DMSP biosynthesis from methionine. In the halophytic, strand plant *Wollastonia biflora* (Compositae) the first step of DMSP biosynthesis is the methylation of methionine, yielding S-methylmethionine (SMM) (Hanson et al. 1994), which is then converted to DMSP-aldehyde (James et al. 1995) and is subsequently thought to undergo a decarboxylation reaction catalysed by a dehydrogenase to form DMSP (Trossat et al. 1996). Alternatively, in the saltmarsh grass *Spartina alterniflora* (Gramineae) DMSP-amine has been identified as an intermediate between SMM and DMSP-aldehyde (Kocsis et al. 1998) and the enzymes that catalyse the production and conversion of DMSP-amine are thought to be SMM decarboxylase and DMSP-amine oxidase, respectively (Kocsis and Hanson 2000).

A third entirely different pathway has been identified by radioisotope labelling experiments in the green macroalgae *U. intestinalis*, which has little in common with the pathways found in higher plants (Gage et al. 1997). In the first step of this pathway methionine undergoes transamination to produce 4-methylthio-2-oxobutyrate (MTOB) (Gage et al. 1997) and a 2-oxoglutarate-dependent aminotransferase is thought to catalyse this reaction (Summers et al. 1998). The removal of an NH_3 group at this step could explain the higher levels of DMSP synthesis in nitrogen starved cells (as discussed above); although this theory is complicated by the fact that sulphate uptake requires nitrogen as OAS in the synthesis of cysteine and also in the enzymes that catalyse each step of the pathway. This transamination is followed by NADPH-dependent reduction of MTOB to 4-methylthio-2-hydroxybutyrate (MTHB) (Gage et al. 1997; Summers et al. 1998), which then undergoes methylation to produce the novel compound 4-dimethylsulphonio-2-hydroxybutyrate (DMSHB). The previous two biosynthesis reactions are also present in non-DMSP producers, even if at a much lower level, however DMSHB synthesis is exclusive to DMSP producers and possibly represents the committing step of this pathway (Gage et al. 1997). This reaction is catalysed by a D-MTHB S-methyltransferase (Summers et al. 1998). DMSHB has also been found in the prymnesiophyte *E. huxleyi*, the diatom *Melosira nummuloides* and the prasinophyte *Tetraselmis* sp., suggesting that the same pathway for DMSP synthesis as in *U. intestinalis* is present in a diverse range of algal species (Gage et al. 1997). In the final step of the pathway DMSHB is

converted to DMSP by oxidative decarboxylation (Gage et al. 1997). Although Summers et al. (1998) have been able to measure the putative substrate specific activity of the first three steps of this pathway in *U. intestinalis*, the genes and enzymes that catalyse these steps are yet to be identified.

1.4. Nitrogen

1.4.1. Algae and the Nitrogen Cycle

Nitrogen is an essential macronutrient; it is constituent of all amino acids and is therefore required for protein synthesis, along with the production of nucleic acids, chlorophyll and GBT. Primary production is limited by the availability of nitrogen in large areas of the oceans (Falkowski et al. 1998) and the availability of usable forms of inorganic of nitrogen, nitrate and ammonium, is highly variable in marine systems. In the oligotrophic open ocean gyres concentrations of these compounds are as low as <0.03 to 0.1 µM. Nitrogen is supplied to the upper ocean by mixing from deep ocean water, deposition of nitrogen containing compounds from the atmosphere or by terrestrial runoff (Zehr and Ward 2002; Galloway et al. 2008). Nitrogen fixing bacteria also have a role in creating bio-available forms of this nutrient (LaRoche and Breitbarth 2005). Kudela and Dugdale (2000) demonstrated that temporal variation in nitrogen availability can be an important factor determining productivity in some coastal upwelling regions, such as Monterey Bay, California. The photosynthetic fixation of carbon by marine phytoplankton contributes approximately 50 % to global net primary productivity (Field et al. 1998) and is critical for supporting marine food webs and the global carbon cycle. Understanding the response of phytoplankton to changes in nitrogen availability is therefore of great interest and the more knowledge we gather about the regulation of this response at a cellular level, the better we will be able to predict the effect that changes in availability will have on productivity. This will improve the predications made by climate models for processes such as carbon drawdown.

Diatoms are excellent competitors for nitrate and in ocean upwelling environments, where nutrient rich deep water periodically enriches the surface ocean in wind-driven pulses, they generally dominate the phytoplankton blooms that are formed (Kudela and Dugdale 2000; Bruland et al. 2005). Diatoms have a high capacity to assimilate nitrate and ammonium (Eppley et al. 1969). Falkowski et al. (2004b) suggests that the success of diatoms over other phytoplankton might lie in their possession of a nutrient storage vacuole, which could allow them to rapidly take up and 'hoard' nutrients such as nitrate to be assimilated later, thereby creating a store and denying competitors access to the nutrients. Indeed, there are reports that accumulated nitrate can account for more than 20 % of total cell nitrogen, however evidence from field experiments suggests that in natural populations a value of 0.1 to 4 % is more realistic (Bode et al. 1997).

1.4.2. Enzymes of Nitrogen Assimilation

Considerably more is known about the assimilation of nitrogen by diatoms compared to sulphur. Diatoms are able to use different forms of inorganic and organic nitrogen and have transporters for nitrate, ammonium, amino acids and urea (Armbrust et al. 2004). Hildebrand and Dahlin (2000) identified four copies of nitrate transporter genes (NAT) in the diatom C*ylindrotheca fusiformis* genome and confirmed multiple copies in other diatom species. The *C. fusiformis* genome also encodes two distinct ammonium transporters (AMT): one copy of AMT1 and three copies AMT2 (Hildebrand 2005). These multiple transporter isoforms might have differences in substrate affinities and suggest the potential for differential regulation.

Once in the cell nitrate is reduced to nitrite by a cytosolic NAD(P)H-dependent nitrate reductase (NR). The activity of this enzyme is quantitatively related to nitrate incorporation in five species of diatoms including *T. pseudonana* (Berges and Harrison 1995). Diurnal variation in NR protein abundance and activity has been reported in diatoms, with a midday maxima (Vergara et al. 1998; Jochem et al. 2000). Brown et al. (2009) found that the transcript levels of *nia* (which encodes NR) also follows this pattern suggesting that the changes in protein abundance and activity are regulated at the level of transcription .

Nitrite is taken up into the chloroplast and a single plastid-localised nitrite transporter has been identified in the *T. pseudonana* genome (Armbrust et al. 2004). Like other photosynthetic eukaryotes diatoms possess a ferredoxin-dependent nitrite reductase (Fd-NiR) which uses reductant derived from photosynthetic electron flow for the reduction of nitrite to ammonium. Milligan and Harrison (2000) propose that in high nitrate low chlorophyll (HNLC) regions of the ocean the ability of diatoms to reduce nitrite might be limited by the reduction in photosynthetic electron transport caused by iron limitation. However, the sequencing of the *T. pseudonana* genome revealed that diatoms also possess an NAD(P)H-dependent nitrite reductase (NAD(P)H-NiR) that is cytosolic (Armbrust et al. 2004; Allen et al. 2006). This enzyme is homologous to NiR-B of fungi and bacteria and has not been identified in plants or green algae. Brown et al. (2009) found that mRNA levels of Fd-NiR followed the same diurnal pattern as NR, whereas NAD(P)H-NiR mRNA levels were low during mid day and increased toward the end of the light period.

Finally, glutamine synthetase (GS) catalyses the condensation of ammonium and glutamate. Like plants and green algae diatoms have a chloroplast glutamine synthetase II (GSII), which is of red algal origin (Robertson et al. 1999; Robertson and Tartar 2006; Siaut et al. 2007). However diatoms also have a bacterial-like glutamine synthase III (GS III), which is located in the mitochondria (Robertson and Alberte 1996; Armbrust et al. 2004; Allen et al. 2006; Siaut et al. 2007) and again this enzyme has not been found in higher plants or green algae. The glutamate required for this reaction is provided by the activity of glutamate synthase (GOGAT), however relatively little is known about this enzyme in diatoms and compared to others involved in nitrogen assimilation. Diatoms appear to have NAD(P)H-dependent (NAD(P)H-GOGAT) and plastid localised ferredoxin-dependent (Fd-GOGAT) forms of this enzyme (Clayton and Ahmed 1986; Zadykowicz and Robertson 2005).

NR and the plastid enzymes Fd-NiR and GSII follow the same diurnal regulation suggesting that they might be involved in the assimilation of nitrogen from nitrate reduction. The plastid route of nitrite assimilation is likely to be of primary endosymbiont origin. The cytosolic NAD(P)H-NiR

and mitochondrial GSIII followed identical but different diurnal pattern. There is some speculation as to their roles in the cell and it is possible that these enzymes are involved in the assimilation of nitrite and ammonium that is taken up directly or produced by photorespiration or catabolic cellular processes, such as the degradation of amino acids.

The diurnal variation in *nia* mRNA and NR protein activity and abundance are lost when cultures are transferred to continuous light (Vergara et al. 1998; Jochem et al. 2000; Brown et al. 2009), which suggests that unlike in plants, in diatoms this pattern is not under circadian regulation. Instead changes in cellular nitrogen and carbon pools or metabolites might be an important metabolic control as is seen in prokaryotes and fungi through 2-oxoglutarate, which is a tricarboxylic acid cycle (TCA cycle) metabolite (Commichau et al. 2006). Alternatively, Giordano et al. (2005) has found that signalling mechanism that responds to the redox status of the chloroplast might be responsible for the diurnal patterns of regulation seen in *C. reinhardtii*.

1.4.3. Regulation of the Assimilation of Different Nitrogen Sources in diatoms

Nitrogen assimilation is an energetically demanding process and as in other photosynthetic eukaryotes enzymes of this pathway are regulated at multiple levels. The uptake and assimilation of different nitrogen sources requires different levels of energy input; with reference to energy derived from photosynthesis nitrate requires approximately 32 mol photons per mol, whereas the more reduced form ammonium only requires only 9.45 mol photons per mol (Raven 1985). Accordingly differences in the regulation of enzymes are seen.

In the uptake of nitrogen Hildebrand and Dahlin (2000) found that NAT mRNA levels are high when grown with nitrate and also under nitrogen starvation, however lower levels were measured in cultures grown with nitrite and there was only minimal expression in the presence of ammonium chloride or ammonium nitrate. Transcript levels of AMT1 were always higher than AMT2, with the highest levels measured in nitrogen starved cells and cells grown with nitrate as a sole source of nitrogen (Hildebrand 2005).

In *C. fusiformis* NR is transcribed under nitrogen starvation however nitrate is required for its translation and in the presence of ammonium NR transcription is repressed and the protein abundance and activity are reduced (Poulsen and Kroger 2005). Neither NR enzymatic activity or protein was detected in *Thalassiosira weissflogii* grown with ammonium as the sole source of nitrogen and addition of ammonium to cells growing on nitrate decreased both protein level and enzyme activity by 40 % within 2 hours (Vergara et al. 1998).

When cultured in media containing both ammonium and nitrate, the uptake of nitrate by *Skeletonema costatum* began once the ammonium concentration had fallen below 2 µM and in these experiments GSII transcription only increased once nitrate in the medium began to be depleted (Takabayashi et al. 2005), providing further evidence that the plastid GSII is linked to the assimilation of ammonium produced by nitrate reduction and not that taken up directly. These experiments demonstrate a clear preference for ammonium assimilation over nitrate.

1.4.4. The Urea Cycle

Urease activity had been detected in diatoms (Peers et al. 2000) and it was known that some members of this group (Ferguson et al. 1976; Berman and Chava 1999), with the exception of *C. fusiformis* (Hildebrand and Dahlin 2000), were able to grown on urea as a sole source of nitrogen. However, the discovery of genes encoding a complete urea cycle was an unexpected discovery in the genome of *T. pseudonana* (Figure 1.5) (Armbrust et al. 2004). Prior to this the urea cycle had not been found in eukaryotes outside the metazoans, where it is generally responsible for the conversion of ammonium to urea for excretion, since the ammonium is highly toxic in animal systems. However, as discussed above, nitrogen is a limiting nutrient in the oceans and the diatom urea cycle is likely to fulfil an entirely different role in these cells. Phylogenetic analysis of the mitochondrial carbamoyl phosphate synthase (CPS), which is the first enzyme of the urea cycle, suggests that the heterotrophic secondary endosymbiotic host in diatom evolution shared a common ancestor with the metazoans (Allen et al. 2011).

The integration of the urea cycle into diatom cell metabolism has created quite novel possibilities and metabolites of this pathway might link to other cell processes (Armbrust et al. 2004). Ornithine is a precursor in the synthesis of polyamines, which have diverse functions in eukaryotic cells and have also been implicated in silica precipitation in the formation of diatom frustules. The enzyme ornithine cyclodeaminase can convert ornithine into the amino acid proline, which is an osmolyte in diatom cells and in addition the *T. pseudonana* genome was also found to encode many proline-rich and proline binding proteins. Furthermore, the synthesis of nitric oxide, which has a role in pathogen defence in higher plants, requires arginine. Allen et al. (2011) have demonstrated that the impairment of the *P. tricornatum* mitochondrial CPS affects the ability of the diatom to synthesise proline and precursors of long chain polyamines. These authors propose that the urea cycle could be an important cellular hub for the redistribution and turnover of carbon and nitrogen from catabolism and photorespiration. This ability to link catabolic and anabolic metabolism might increase the efficiency of nitrogen usage and be an important factor in the success of diatoms during upwelling events.

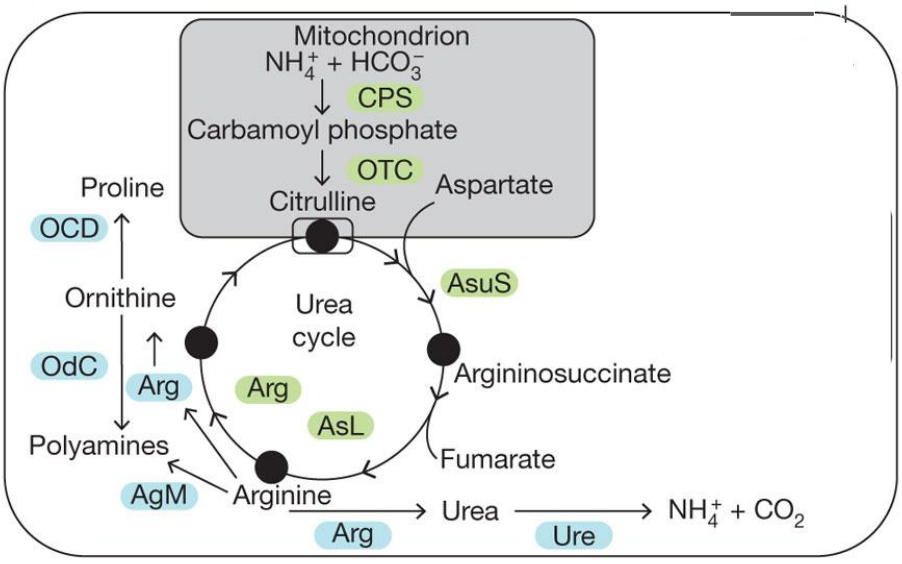

Figure 1.5. A schematic showing how the urea cycle might function in the *P. tricornatum* cell, modified from Allen et al. (2011). AgM, agmatinase; Arg, arginase; AsL, argininosuccinate lyase; AsuS, argininosuccinate synthase; CPS, carbamoyl phosphate synthase; OCD, ornithine cyclodeaminase; OdC, ornithine decarboxylase; OTC, ornithine transcarboxylase; Ure, urease.

From the research discussed above we have a relatively good understanding of the processes of nitrogen assimilation in diatoms, compared to sulphur metabolism, however we know less of how this pathway interacts with other aspects of cell metabolism, such as carbon metabolism. Since there are many aspects of nitrogen metabolism that are unique to diatoms it is likely that these interactions will be quite different to higher plants and green algae.

1.5. Project Objectives

The world's oceans are facing changes in temperature, acidity and stratification and it is important that we understand how marine organisms influence biogeochemical cycles, and that we are able to predict how they will respond to the changes. A key component in making such predictions is a detailed knowledge of the metabolic pathways involved in primary production and the processing of nutrients. Although a great deal of information has been gained from genome and proteome studies of diatoms, we now have to investigate their adaptive response to changing conditions. This information could be used to improve predictive climate models. There is also great interest in the processing of nutrients with regards to agricultural crop productivity. The knowledge obtained by studying the nutrient metabolisms of diverse photosynthetic eukaryotes and identifying similarities as well as differences in these pathways could be applied to manipulate the metabolic pathways of crop species to improve nutrient use efficiency. For example Napier (2007) discusses the introduction of new fatty acids into plant oils. However, the information on marine phytoplankton nutrition is fragmented and obtained with a large number of different species, making it difficult to draw general conclusions. To fully use the potential of genomics and molecular tools for model microalgal species it is necessary to complement them with physiological studies. This thesis combines physiological and molecular studies over a range of environmental conditions to obtain new deeper understanding of the sulphur and nitrogen metabolism of the centric marine diatom *T. pseudonana* and its regulation.

The first objective of this project was to identify a range of growth conditions that affect the intracellular concentration of DMSP in *T. pseudonana* to establish an improved understanding of the response of one species of diatom. For this I tested sulphur deprivation, increased salinity, increased light intensity, and nitrogen starvation (Chapter 3).

With the exception of sulphur deprivation all of the conditions tested were found to increase the intracellular DMSP concentration of *T. pseudonana* and I then used these to study sulphur metabolism and DMSP synthesis. The aim of this work was to identify proteins involved in DMSP synthesis and also to increase our understanding of the regulation of diatom sulphur metabolism. For this I used a broad proteomic approach alongside the more focused approaches of qRT-PCR and enzyme activity measurements (Chapter 4). This is one of this first studies on the adaptive response of the diatom proteome to changing growth conditions.

A basic question regarding DMSP synthesis is whether it is produced in the dark. I therefore quantified the intracellular DMSP concentration of *T. pseudonana* over a light:dark cycle along with cysteine and glutathione concentrations and the activity of APR (Chapter 5).

Since the metabolism of nitrogen by phytoplankton is of interest due to its strong influence on the distribution of primary production in the ocean I further investigated the response of the *T. pseudonana* proteome to nitrogen starvation with particular reference to carbon metabolism. I then compared these findings with the transcriptome response of *T. pseudonana* to nitrogen starvation, reported by Mock et al. (2008) in a study of biosilification, and also to the response of the higher plant *A. thaliana*, the green alga *C. reinhardtii* and the cyanobacterium *Prochlorococcus marinus* to this growth condition. The aim of this work was to determine whether the unique combination of genes possessed by this diatom result in the differential regulation of metabolic pathways (Chapter 6). A paper on this aspect of the research is published in Plant Physiology (Hockin et al. 2012).

Chapter 2. Materials and Methods

2.1. Culturing

Axenic *Thalassiosira pseudonana* (CCMP 1335) were grown in batch culture in ESAW (enriched seawater artificial water) artificial seawater medium (Tables 2.1 and 2.2) (Harrison and Berges 2005). Unless otherwise stated, cultures were grown in MLR-351 Plant Growth Chambers (Sanyo E&E Europe BV, Loughborough, UK) at 15 ^{o}C under a 14:10 light:dark cycle with an irradiance of ca. 115 µmol photons m^{-2} s^{-1} based on an immersed measurement with a Scalar PAR Irradiance Sensor QSL 2101 (Biospherical Instruments Inc., San Diego, USA). Cultures were growth in Erlenmeyer flasks with the exception of 3 L cultures, which were grown in 5 L Duran bottles.

Cell counts and volumes were taken with a Multisizer 3 Coulter Counter (Beckman Coulter Ltd, High Wycombe, UK), for which 1 ml of culture was diluted with 9 ml of 0.45µm filtered seawater and three technical replicates were taken for each count. A blank of 10 ml, 0.45µm filtered seawater was also run and the background was subtracted. The ratio of variable to maximum fluorescence (Fv/Fm), an estimate of the maximum efficiency of photosystem II or capacity for noncyclic photosynthetic electron flow, was measured on a Walz Phyto-Pam phytoplankton analyser (Heinz Walz GmbH, Effeltrich, Germany). Culture aliquots of 3 ml of culture were first dark adapted for 30 min and then transferred to a quartz vial for analysis.

Table 2.1. The constituent salts in ESAW artificial seawater and their final concentration.

Salts	**Chemical Formula**	**Mass per litre (g)**	**Final Concentration (mM)**
Sodium chloride	NaCl	21.19	363
Sodium sulphate	Na_2SO_4	3.55	25
Potassium chloride	KCl	0.599	8.04
Bicarbonate	$NaHCO_3$	0.174	2.07
Potassium bromide	KBr	0.0863	0.725
Boric acid	H_3BO_3	0.023	0.372
Sodium fluoride	NaF	0.0028	0.0657
Magnesium chloride	$MgCl_2{\cdot}6H_2O$	9.592	47.2
Calcium chloride	$CaCl_2{\cdot}2H_2O$	1.344	9.14
Strontium chloride	$SrCl_2{\cdot}6H_2O$	0.0218	0.082

Table 2.2. Nutrients added to ESAW artificial seawater and their final concentration.

Nutrient	**Chemical formula**	**Mass per litre (mg)**	**Final Concentration (µM)**
Nitrate	$NaNO_3$	46.47	549
Phosphate	$NaH_2PO_4{\cdot}H_2O$	3.09	21
Silicate	$Na_2SiO_3{\cdot}9H_2O$	15	105
Iron	$FeCl_3{\cdot}6H_2O$	1.77	6.56
	$Na_2EDTA{\cdot}2H_2O$	2.44	6.56
Trace metals	$Na_2EDTA{\cdot}2H_2O$	3.09	8.29
	$ZnSO_4{\cdot}7H_2O$	0.073	0.25
	$CoSO_4{\cdot}7H_2O$	0.016	0.057
	$MnSO_4{\cdot}4H_2O$	0.54	2.42
	$Na_2MoO_4{\cdot}2H_2O$	0.0015	0.0061
	Na_2SeO_3	0.000173	0.0001
	$NiCl_2{\cdot}6H_2O$	0.00149	0.0063
Vitamins	Thiamine HCl	0.1	0.297
	Biotin	1.0	0.0041
	B_{12}	2.0	0.0015

All culture work was conducted using sterile technique in a Class-II laminar flow cabinet (Walker, Glossop, UK). Surfaces were wiped with 70 % ethanol and bottle necks were flamed on opening and closing. The cultures were regularly checked for bacterial contamination by staining subsamples with 4',6-diamidino-2-phenylindoledihydrochloride (DAPI), a stain that binds to DNA (Porter and Feig 1980). For this 1 to 3 ml of culture, depending on cell density, were fixed with 3 µl ml^{-1} lugols solution (5 % iodine w/v and 10 % KI w/v in distilled water) and 50 µl ml^{-1} formalin (20 % formaldehyde and 100 g l^{-1} hexamine in distilled water). To discolour the iodine 3 µl ml^{-1} 3 % sodium thiosulphate was added. Samples were incubated at room temperature for 20 min in the dark with 10 µl ml^{-1} of 1 mg ml^{-1} DAPI solution made in distilled water, before being collected by filtration onto 25 mm black nucleopore membranes with 0.2 µm pores (Whatman Plc, Maidstone, UK). Filters were rinsed with filtered seawater to remove excess dye and then examined under an epifluorescence microscope (model BX40; Olympus, Essex, UK). To avoid bacterial contamination during the procedure all solutions and seawater were 0.2 µm filter sterilised.

2.2. Measuring Intracellular DMSP Concentration

2.2.1. Sampling

Depending on the cell density, 3 to 7 ml of culture was collected by filtration onto 25 mm nucleopore track-etch membranes with a 1 µm pore (Whatman) at a pressure no greater than 15 KPa. The filters were folded and positioned in the top of a 4 ml glass vial containing 3 ml 0.5 M sodium hydroxide, this was done quickly to avoid the filter drying, which might cause cells to lyse and therefore lose DMSP. A polyethylene screw cap, with a Teflon coated septum was tightened before the filter was shaken down into the sodium hydroxide to cleave the DMSP in cells to release the volatile compound DMS (cold alkali hydrolysis), which then partitions between the aqueous and head phases of the vial.

Sunda et al. (2002) found that intracellular DMSP concentrations measured for *E. huxleyi* reduced with increasing volumes of culture filtered, this loss of DMSP was considered to be due to cell lysis

caused by filtration. Although in the same study this problem did not occur for *T. pseudonana*, I also tested the effect of filtering different volumes of *T. pseudonana* culture on the intracellular DMSP concentration measured to ensure that this was not an issue, especially since I was using a different filter type from the GF/F filters used in that study. Samples of 2, 3, 5 or 10 ml were taken from a 1.44 x 10^6 cell ml^{-1} culture (n=5). The intracellular DMSP concentration was then measured (described below) (Figure 2.1). No difference in intracellular DMSP concentration was observed between the different volumes filtered, demonstrating that there is no increase in cell breakage and DMSP loss when different volumes within this range are filtered. As was concluded by Sunda et al. (2002), this is most likely due to protection from the diatom's strong silica frustule. Based on this finding throughout this study the volume of cells filtered was between 2 and 10 ml, depending on the growth conditions and cell density of the culture.

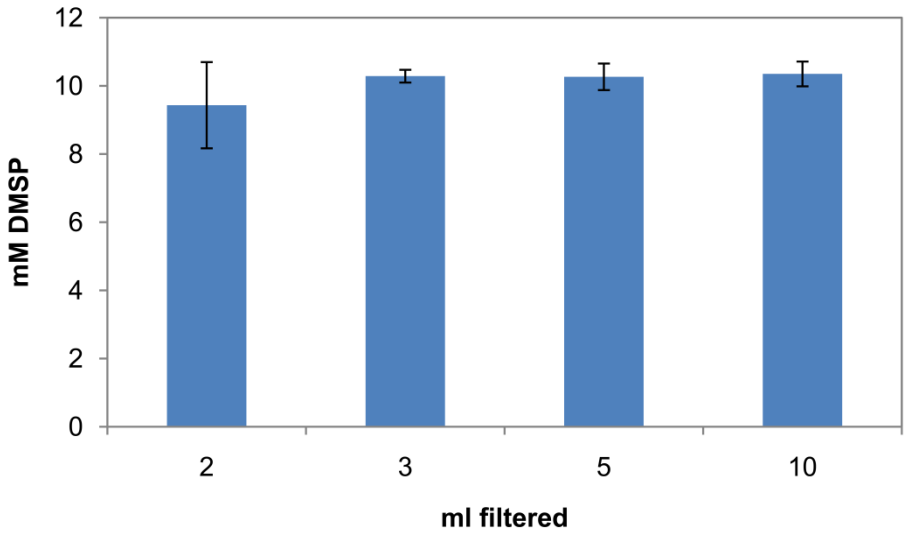

Figure 2.1. The intracellular DMSP concentrarion, established by the measurement of the volatile compound, DMS, derived from the cold alkali hydrolysis of DMSP, by gas chromatography,when different volumes of *Thalassiosira pseudonana* culturewere collected by the filtration of . Bars show the mean of 5 samples ± standard deviation.

2.2.2. Calibration

Standards ranging from 0.025 to 2.50 µM DMSP (Figure 2.2) were made by adding volumes of a stock DMSP solution to 3 ml 0.5 M sodium hydroxide in the same 4 ml vials used above. To avoid loss of DMS the DMSP standard was pipetted into the lids, which were used to quickly close the vials, which were then inverted to mix the standard and sodium hydroxide. Standards were run before samples for every batch of analyses.

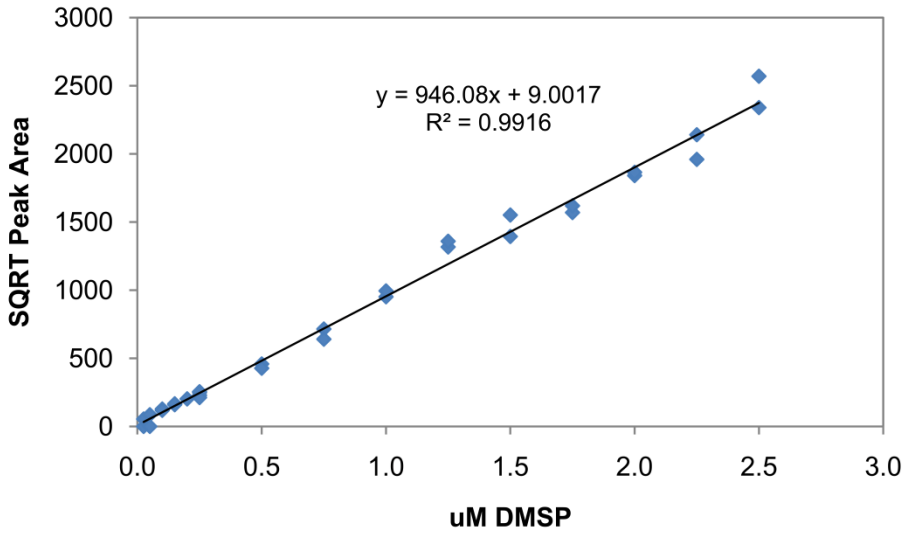

Figure 2.2. A typical standard curve used in the analysis of intracellular DMSP concentration, established by the measurement of the volatile compound, DMS, derived from the cold alkali hydrolysis of DMSP, by gas chromatography.

2.2.3. Analysis

Prior to analysis all samples and standards were incubated at 30 ^{o}C overnight to equilibrate the DMS concentration in the aqueous phase with that in the headspace of the vial. Samples were run on a gas chromatograph (GC-2010; Shimadzu, Milton Keynes, UK) fitted with a fused-silica capillary 30 m × 0.53 mm column (CP-SIL 5CB; Varian, Oxford, UK) and DMS was quantified using a flame photometric detector (FPD). An automatic multipurpose sampler (Gerstel GmbH & Co.KG, Mülheim an der Ruhr, Germany) with a 250 µl gas-tight syringe (Gerstel) was used to take

150 µl of headspace gas from each vial. The injector, column and detector temperatures were set to 200, 120 and 250 °C respectively. The carrier gas, helium, was set to 34.7 ml min^{-1}.

DMS gives a single peak the area of which was square rooted, because the response of the FPD detector is not linear and follows a square root function, and then compared to the calibration curve to calculate the total moles of DMSP in the sample. This was divided by the number of cells filtered and the mean volume of a cell to give a micromolar intracellular concentration of DMSP.

The detection limit for DMSP in the 3 ml volumes with 0.5 M sodium hydroxide, detected by sampling its volatile lysis product DMS in the headspace, was equivalent to approximately 0.025 µM in the aqueous phase. This was determined by running calibration curve standards with different amounts of DMSP in the aqueous phase (see example in Figure 2.2). However since the biological samples contained different numbers of cells it is not possible to quote a constant detection limit for intracellular DMSP concentration. The density of the culture and the expected DMSP concentration of the cells under a given growth condition was always taken into consideration when deciding how much culture to filter for each analysis. There were a number of samples for which the concentration of DMSP was very low and there was no detectable peak i.e. the sample was below the limit of detection. These are marked with an x in the figures.

2.3. Two Dimensional Gel Electrophoresis

2.3.1. Sample Collection

Cells were collected by filtering 250 ml of culture onto 47 mm diameter nucleopore membrane filters with a 1.0 µm pore size, at a pressure of 35 KPa. Filters were then immediately folded into 2 ml eppendorf tubes and frozen in liquid nitrogen. Samples were stored at -80 ^{o}C.

2.3.2. Protein extraction

Proteins were extracted based on the method of Contreras et al. (2008). Cells were washed from the filter with 800 µl extraction buffer (1.5 % w/v polyvinyl pyrrolidone, 0.7 M sucrose, 0.1 M potassium chloride, 0.5 M Tris-HCl pH 7.5, 250 mM EDTA and 0.5 % 3-[(3-cholamidopropyl)dimethylammonio]-1-propanesulfonate (CHAPS)] and 8 µl protease inhibitor cocktail (Sigma-Aldrich Company Ltd, Dorset, UK) was added. Cells were disrupted by sonication (three times for 10 sec at ca. 15 microns on ice with a Soniprep 150 probe; MSE, London, UK), followed by addition of 16 µl mercaptoethanol. An equal volume of Tris-HCl pH 8 saturated phenol was added and samples were shaken on ice for 20 minutes. Samples were then centrifuged at 6600 g and 4 ^{o}C for 30 minutes. The upper phenol phase was removed to a 15 ml glass tube and kept on ice, while the lower buffer layer was re-extracted with phenol. Proteins were precipitated by addition of 7.5 ml ice cold 0.1 M ammonium acetate in methanol and 3 hours incubation at -20 ^{o}C, followed by 20 min centrifugation at 10000 g at 4 ^{o}C. The supernatant was removed and the pellet was resuspended in 2 ml ice cold 0.1 M ammonium acetate in methanol, and incubated for a further 20 minutes at -20 ^{o}C. The protein was collected by 5 min centrifugation at 6600 g at 4^{o}C. The pellet was rinsed 4 times in ice cold acetone and stored at -80^{o}C.

2.3.3. SDS-PAGE gel casting

Two clean glass plates were sealed together, with spacers between, with a silicon sealant. This was allowed to dry for two days. The glass plates were then positioned in the casting box and the acrylamide solution (table 2.3) was poured in. The top of each gel was overlaid with 1.5 ml water saturated butanol and the gels were left to polymerise for 2 to 4 hours.

Once polymerised the butanol was poured off and the tops of the gels were rinsed with milliQ water. The gels were then removed from the casting box and the external glass plates were rinsed well with milliQ water. The tops of the gels were then rinsed three times with 0.3 mM Tris buffer.

Table 2.3. Acrylamide solution sufficient for making 11 SDS-PAGE gels.

Solution	Volume
30 % Duracryl 0.65 % Bis (Genomic Solutions)	344.75 ml
1.5 M Tris buffer	257.79 ml
MilliQ water	425.5 ml
10 % SDS	10.87 ml
TEMED	0.0520 ml
10 % Ammonium persulphate	2.64 ml

Gels were then stored at 2 ^{o}C, in heat sealed bags with 50 ml diluted 0.3 mM Tris buffer to stop them drying out, for a minimum of 2 weeks before using. Through practical experience it has been found that gels stored after casting are more robust and less prone to distortion when fitted in the running tank.

2.3.4. Two-dimensional separation

For the first dimension, 100 µg protein (extracted as above and quantified with an Ettan 2-D Quant kit; GE Healthcare, Chalfont, UK) was mixed with immobilized pH gradient (IPG) rehydration buffer (7 M urea, 2 M thiourea, 2 % CHAPS, 18 mM dithiothreitol (DTT), bromophenol blue (trace amount to give blue colour) and 2 % pH 4-7 IPG buffer; final volume 450 µl) before loading onto 24 cm pH 4-7 Immobiline DryStrips (GE Healthcare). Following overnight rehydration, isoelectric focusing was performed for 44.7 kVh at 20 °C over 8 h 45 min using the IPGphor system (GE Healthcare). Prior to the second dimension, the focussed strips were conditioned in 122 mM Tris-acetate equilibration buffer supplemented with 5 mg ml^{-1} SDS, 360 mg ml^{-1} urea and 300 mg ml^{-1} glycerol. To reduce and alkylate cysteine residues, the strips were sequentially treated with equilibration buffer containing 8 mg ml^{-1} DTT, and then equilibration buffer containing 25 mg ml^{-1}

iodoacetamide (each treatment consisted of 9 ml of buffer, 30 min with gentle shaking). For the second dimension, 10 % Duracryl gels (28 x 23 cm; 1 mm thick) were prepared (as described in section 2.3.3) for use in the Investigator 2nd Dimension Running System (Genomic Solutions, Huntington, UK); with cathode buffer (200 mM Tris base, 200 mM Tricine, 14 mM SDS,) and anode buffer (25 mM Tris/acetate buffer, pH 8·3). Electrophoresis was carried out using 20 W per gel.

2.3.5. Staining Imaging and Analysis

The gels were gently shaken overnight in 400 ml fixing solution (40 % methanol, 10 % acetic acid) and then in 330 ml Sypro-Ruby overnight (Invitrogen Ltd, Paisley, UK). All steps involving Sypro Ruby were carried out in the dark. The stain was then removed and replaced with 400 ml destaining solution (10 % methanol, 6 % acetic acid) and gels were gently shaken for at least 1 hour.

Gel images were captured with a Pharos FX+ Molecular Imager with Quantity One imaging software (Invitrogen). A 532 nm excitation laser was used with a 605 nm band pass emission filter and gels were scanned at 100 µm resolution to produce a 16 bit image. For each gel the laser strength of the photo-multiplier tube was optimised; this was usually in the range of 49 to 50 % laser strength.

Gel images were compared using Progenesis SameSpots analysis software (v4.1; Nonlinear Dynamics Ltd, Newcastle Upon Tyne, UK). Spots were detected and the gels were aligned. Interfering marks, such as excess stain, were removed from the analysis. Data on protein spots with altered levels of expression under any treatment was exported to Microsoft Excel where spots were sorted by significance (based on t-test) and fold change in each experiment.

2.3.6. Protein Identification

Spots of interest selected for identification, based on their fold change and P-value, were excised from the gel using a ProPick excision robot (Genomic Solutions). The protein was then manually

in-gel trypsin digested by first washing twice in 100 µl 400 mM ammonium bicarbonate : 100 % acetonitrile (1:1) for 20 min to equilibrate the gel to pH 8 and to remove the stain. Aqueous solutions were then removed by washing briefly with 100 µl acetonitrile. The gel was washed again in 100 µl acetonitrile for 15 min to shrink the gel before air drying for 10 min. The protein was digested by the addition of 50 ng trypsin in 5 µl 10 mM ammonium bicarbonate (modified porcine trypsin, Promega, Madison, USA) and samples were incubated at 37 °C for 3 h. Samples were acidified by incubating with 5 µl 5 % formic acid for 10 min, before flash freezing and storing at -80 ^{o}C.

Tryptic digests were analysed by peptide mass fingerprinting (Pappin et al. 1993); this was conducted by the John Innes Centre Proteomics Facility. The acidified digests were spotted directly onto a pre-spotted anchor chip (PAC) target plate (Bruker UK Ltd, Coventry, UK) which is pre-coated with α-cyano-4-hydroxycinnamic acid matrix. Mass analysis was carried out on an Ultraflex MALDI-ToF/ToF mass spectrometer (Bruker UK). A 50 Hz nitrogen laser was used to desorb/ionise the matrix/analyte material, and ions were automatically detected in positive ion reflection mode, first with and then without the use of fuzzy logic programming. The calibrated spectra were searched against a monthly updated copy of the SPtrEMBL database, using an in-house version (v2.2) of the MASCOT search tool (reference: http://www.matrixscience.com).

2.4. qRT-PCR

2.4.1. RNA Extraction

Samples were collected by filtering 250 ml culture as described in section 2.3.1. Cells were washed from the nucleopore membrane (Whatman) with 500 µl RNA extraction buffer (80 mM Tris pH 9, 5 % SDS, 150 mM LiCl, 50 mM EDTA), transferred to a 1.5 ml eppendorf tube and homogenised, with a further 100 µl buffer used to rinse the piston. To the homogenate 500 µl phenol chloroform (1:1) was added before vortexing and shaking for 5 min. The phases were then separated by 25 min centrifugation at 11100 g and 20 °C. The upper buffer phase was removed to a fresh tube and extracted twice more by vortexing and shaking with 500 µl phenol chloroform. After the third

extraction the upper phase was incubated with 140 µl 8 M lithium chloride at -80 °C for 2 hr to precipitate the RNA, which was then collected by 30 min centrifugation at 11100 g at 4 °C. The supernatant was removed, leaving 10 to 20 µl as the pellet is unstable at this stage. The pellet was dissolved in 300 µl distilled water by incubation at 65 °C for 10 min and the RNA was re-precipitated with 100 µl 8 M lithium chloride at -20 °C over night. The RNA was collected by 30 min centrifugation at 11100 g at 4 °C and the supernatant was removed. The pellet was washed with 400 µl 70 % ethanol for 5 minutes before 5 min centrifugation at 11100 g at 4 °C. The ethanol was removed and the pellet was air dried for 5 min. The RNA was dissolved in 30 µl distilled water by incubation at 65 °C for 15 min, although the volume was adjusted depending on the size of the pellet.

The concentration RNA was determined using a NanoDrop (ND-1000; ThermoScientific, Waltham, MA, USA), with 1.5 µl RNA solution pipetted onto the pedistall. The ratio of absorbance between 260 and 280 nm was compared to check for protein contamination. The ratio of absorbance between 230 and 280 nm was also compared as contaminants including carbohydrate and phenol have maximum absorbance close to 230 nm. Acceptable ratios were $A_{260}/A_{280} > 1.8$ and $A_{260}/A_{230} > 2.0$ as advised by Udvardi et al. (2008). The integrity of RNA was also tested by running samples on a gel. RNA samples were stored at -20 °C.

2.4.2. cDNA synthesis and DNase treatment

These steps were carried out with a QuantiTect kit (Qiagen, Valencia, USA). Samples that had previously been stored were defrosted on ice. RNase free water was added to 1 ng RNA to make the total volume up to 12 µl to which 2 µl DNA wipe-out buffer were added. Samples were incubated at 42 °C for 3 min. Meanwhile, the reverse transcription master-mix was prepared, with 1 µl Quantiscript reverse transcriptase, 4 µl Quantiscript reverse transcription buffer and 0.9 µl reverse transcription primer mix per sample. To each 14 µl DNase treated sample 5.8 µl of this master-mix was added, keeping everything on ice before transferring to 42 °C for 30 min followed

by 3 min at 95 °C to stop the reverse transcription. The resulting concentration of cDNA was 50 ng ml^{-1}, which was then diluted to the working concentration for the qRT-PCR reaction, 2.5 ng μl^{-1}, by addition of 380 µl distilled water.

Table 2.4. Primers used in qRT-PCR studies. Length (L), melting temperature (MT), % GC content (GC), product size (PS), efficiency (E).

	Gene	Sequence	L	MT	GC	PS	E
Actin	ACT	L:CATTTACGAGGGGTATGCTCTC	22	59.99	50.00	143	2.07
		R:TATCACGGACAATCTCACGTTC		60.00	45.45		
Beta Tubulin	TUB	L:AAGGAGGTGGATGATGAGATG	21	58.95	47.62	152	2.03
		R:ATGCAGGTGGAGTTACCAATG	21	59.87	47.62		
Sulphate Transporter 1	Trans1	L:CATTGTCGGTATCGCATCTG	20	60.10	50.00	137	2.02
		R:TCGACATTGAACCACTCACTG	21	59.74	47.62		
Sulphate Transporter 2	Trans2	L:TGTTCACCATCTTGTTGACGAC	22	61.00	45.45	121	1.97
		R:GCACTGATTGTGGTGGACTG	20	60.16	55.00		
ATP Sulphurylase 1	ATPS1	L:AATGGAAGTTCAAAAGGCACTC	22	59.64	40.91	100	1.98
		R:GTTGAAGAAGGGTGTTCCGTAG	22	60.03	50.00		
ATP Sulphurylase 2	ATPS2	L:GATGATGTTGACGTGGTTGC	20	59.97	50.00	129	2.04
		R:GTAGGATGGACGAGGACAACTC	22	60.00	54.55		
APS Reductase 1*	APR1	L:AGTTGGCACGTGAAAATGTG	20	59.62	45.00	127	1.99
		R:GGCTGTACGACAAGTAAGCAAG	22	59.11	50.00		
APS Reductase 2	APR2	L:GAGAGTGCTGGAGTTCCTGTG	21	60.04	57.14	102	2.01
		R:GATGAAGTTGACAGTAGGGAAGC	23	59.30	47.83		
OAS Thiollyase 1*	OASTL 1	L:CAATACTTGAAACCTCGCAATC	22	58.77	40.91	156	1.92
		R:CGTCGATTAGAGAAGTGTCTGC	22	59.15	50.00		
OAS Thiollyase 2	OASTL 2	L:TGCTTCCTGACACTGGTGAG	20	60.02	55.00	109	1.92
		R:ATCCAACTGGGAGTGCTACG	20	60.13	55.00		
OAS Thiollyase 3	OASTL 3	L:GGATTGTTCGTCGGATCAAG	20	60.46	50.00	109	1.87
		R:GCCCTCCATCACATACAACAG	21	60.39	52.38		
Serine Acetyltrans-ferase 1	SAT1	L:AGTTCTCGCGCATTACCTACAG	22	60.81	50.00	121	1.91
		R:CTCTCCAATAACGATCCCTGTG	22	60.87	50.00		
Serine Acetyltrans-ferase 1	SAT2	L:CTCTCGGAGGTACGGGTAAAG	21	60.13	57.14	104	2.01
		R:GCCAACAAAGATATTTCCCAAG	22	59.84	40.91		
Serine Acetyltransf-erase 3	SAT3	L:GAATGGCAATGTATGTGCAAAG	22	60.38	40.91	120	2.05
		R:TTTCACCAATCACCACTCCTC	21	59.96	47.62		
Sulphite Reductase	SiR	L:CCGTGTACTCCTCAACAAGATG	22	59.66	50.00	101	1.96
		R:CCAATTCTGCCATGTAAGGAC	21	59.44	47.62		

*Indicates that the region of amplification includes an intron.

2.4.3. Primer Design, Preparation and Efficiency

Primers for qRT-PCR were designed using primer3 (version 0.4.0; http://frodo.wi.mit.edu/primer3/) based on the criteria outlined in Udvardi (2008). Primers (Table 2.4) were 20 to 23 bp in length, with a melting temperature of 58 to 61 °C. The primer GC content was set at 40 to 60 % and a 1 base GC clamp was used. The maximum nucleotide repeat allowed was 3. Two primer pairs were designed to include an intron to test for DNA contamination.

All primers were supplied by Sigma-Aldrich in a dry form. These were centrifuged briefly to ensure the contents were at the bottom of the tube, before resuspending in distilled water to achieve a final concentration of 100 µM. To ensure the primers were completely dissolved, the solution was incubated for 10 min at 65 °C, vortexed, returned to 65 °C for a further 5 min and vortexed once more. This solution was stored at -20 °C. The efficiency of each primer pair was calculated using linear regression through the points of exponential amplification of at least 6 reactions. The melting curve of each PCR product was checked for evidence of primer dimer formation.

2.4.4. Reaction

The PCR reactions were run on 96 well plates. A 10 µM working stock was prepared for each primer pair using distilled water. Each reaction contained 4 µl 10 µM primer mix, 1 µl of 2.5 ng μl^{-1} cDNA and 5 µl SYBR Green JumpStart *Taq* Ready Mix (Sigma-Aldrich), with the cDNA and SYBR Green were prepared as a mastermix. The qRT-PCR reaction was run on an MJ Research Opticon 2 continuous fluorescence detector (Bio-Rad, Hemel Hempstead, UK) the reaction settings are described in table 2.5.

2.4.5. Analysis

Results of the reaction were viewed using MJ OpticonMontior Analysis Software (V.3.1; Bio-Rad). A threshold was set and the point at which the fluorescence of each reaction crosses the threshold is called the Ct value. The relative difference in transcript abundance between the control samples and the treatment samples was calculated using the ΔΔCt method.

Table 2.5. The qRT-PCR reaction settings

Step	Temperature	Time	Description
1	94 °C	3 min	Initial denaturing.
2	94 °C	15 sec	Denaturing.
3	60 °C	30 sec	Annealing.
4			Plate Read.
5	72 °C	30 sec	*Taq* extension.
			From here the reaction returns to step 2 for 39 cycles.
6	65 to 95 °C	2 sec per 0.5 °C	Melting curve.

First for each sample the Ct value of the reference gene was subtracted from the Ct value of the target gene (ΔCt). The stability of both actin and beta-tubulin was tested for the growth conditions investigated in this study using geNorm software (Vandesompele et al. 2002). Both were considered stable, however the beta-tubulin gene show slightly more consistent expression and was therefore used as the reference gene. This normalisation controls for experimental variation between the reactions of different samples e.g. small differences in the quantity of template from the cDNA synthesis step.

Next the average ΔCt of the controls is subtracted from the ΔCt of all samples (ΔΔCt) which makes all values relative to the controls. Finally the ΔΔCt are converted to relative transcript abundance using the principle that after a given number of cycles (n) the increase in transcript abundance will be E^n, where E is the efficiency of the reaction (primer efficiency). Significance was tested by t-test.

$$\text{Ratio} = E^{-\Delta\Delta Ct} \text{ (where E = reaction efficiency)}$$

2.5. APS reductase activity

APS reductase (APR) activity was measured as the production of [^{35}S]sulfite and assayed as acid volatile radioactivity formed in the presence of [^{35}S]APS and dithioerythritol as reductant (Kopriva

et al. 2007). Depending on the cell density, 5 to 15 ml of culture were collected by centrifugation at 5380 g, snap frozen in liquid nitrogen and stored at -80 °C. Samples were resuspended in 500 µl of extraction buffer (45.45 mM Na/KPO_4, 27 mM Na_2SO_3, 0.45 mM AMP, and 9.1 mM DTE). They were then disrupted by sonication (as detailed above) and spun for 5 minutes at 11100 g and 4 °C to remove cell debris. Five µl of the extract was added to 140 µl of reaction assay (100 mM Tris/HCl pH 9, 800 mM $MgSO_4$, 8 mM DTE, 0.075 mM [^{35}S]APS) in 1.5 ml tubes without a lid, vortexed, and incubated at 37 °C for 30 min. After 30 minutes 50 µl 1M Na_2SO_3 was added and each reaction tube was transferred to a scintillation vial, containing 1ml 1M TEA to trap the evolved [^{35}S]SO_2. Then 200µl 1M H_2SO_4 was added to each tube and the lids were put on immediately. The vials were incubated at room temperature over night.

The tubes were removed from the vials and the outside was washed with 200 µl H_2O into the vial. 2.5 ml Optiphase II scintillation cocktail (Perkin Elmer, Waltham, USA) was added and vials were shaken well before determination of radioactivity in a liquid scintillation counter (Wallac-1409; Perkin Elmer). The protein concentration in each sample was measured according to Bradford assay (Bradford 1976) using a Bio-Rad Protein kit.

2.6. Amino Acids Measurements

Samples were collected by filtering 250 ml culture as described in section 2.3.1. Cells were washed from the filter with 410 µl of methanol:buffer (3.5:0.6 v/v; buffer: 20 mM HEPES, pH 7.0, 5 mM EDTA, 10 mM NaF) and 150 µl chloroform was added. Samples were shaken at 4 °C for 30 min and 300 µl water was added, before shaking for a further 30 min at 37 °C. Samples were then centrifuged for 15 min at 11100 g at room temperature and the upper aqueous phase was taken. The lower chloroform phase was re-extracted with 300 µl water. Samples were dried in a speed vac at 37 °C and resuspended in 500 µl water. Of this, 15 µl was derivatised according to the AccQ Tag chemistry package (Waters Ltd, Elstree, UK) and 10 µl of the final solution was injected into a Waters 2695 HPLC, fitted with an AccQ-Tag (3.9 x 150 mm) column and a 474 fluorescence

detector (Waters). Derivatisation and HPLC measurements were carried out by the John Innes Centre Metabolite Services. Amino acid concentrations were compared by t-test.

2.7. Thiol Measurements

Samples were collected by the filtration of 20 ml onto GF/F filters (Whatman), snap frozen in liquid nitrogen and stored at -80 °C. To extract the thiols, filters were placed directly into 2 ml 10 mM methanosulphonic acid (MSA) at 70 °C for 2 min and homogenised on ice with a tissue grinder. The homogenate was centrifuged at 11100 g and 4 °C and 800 µl of the supernatant was transferred to a new eppendorf tube. The solution was adjusted to pH 9 by adding 84 µl of 100 mM tetraborate buffer containing 10 mM diethylenetriaminepentaacetic acid. To 50 µl of this extract 1 µl 0.1M DTT was added to reduce oxidised thiols and samples were incubated in the dark for 15 min at 37 °C before adding 35 µl water, 10 µl 1M Tris pH 8 and 5 µl 100 mM monobromobimane (Calbiochem GMBH, Bad Soden, Germany). After a further 15 min incubation in the dark at 37 °C 100 µl of 9 % acetic acid was added and samples were centrifuged for 15 min at 11100 g and room temp. From the supernatant 180 µl were transferred to HPLC vials and 80 µl was injected into a Waters 2695 HPLC, fitted with a Spherisorb (4.6 x 250 mm) column (Waters).

Alongside the samples standards for glutathione and cysteine were also run. These were prepared by mixing 5 µl 10 mM glutathione and 10 mM Cys with 495 µl 0.1M HCl. From this 25 µl was taken and neutralised with 25 µl 0.1 M NaOH before adding 35 µl water, 10 µl 1M Tris pH 8 and 5 µl 10 mM MB. Samples were incubated in the dark for 15 min at 37 °C and 900 µl 5 % acetic acid was then added. For analysis 200 µl was put into a HPLC vial and 10, 20, 40, 50 µl aliquots were injected to form a standard curve.

2.8. Nitrate Measurements

Twenty five mg aliquots of polyvinylpolypyrrolidone (PVPP) were incubated with 1 ml deionised water over night at 4 °C. Diatom cells, collected by the filtration of 250 ml culture (as described in

section 2.3.1), were washed from the filter with 500 µl of deionised water and centrifuged at 1500 g at 4 °C for 5 min. The supernatant was removed and cells were resuspended in 500 µl of the PVPP incubated water. They were then disrupted by sonication (as detailed above). The homogenised sample was returned to the water-PVPP mix. Samples were shaken at 4 °C for 1 hour and then heated at 95 °C for 15 min. Finally they were centrifuged at 11100 g for 15 min at 4 °C and 100 µl was injected into a Waters 2695 HPLC, fitted with an ION-Pack ion exchange column (Waters). The ions were resolved in an isocratic flow (0.8 ml^{-1} min^{-1}) of Li-gluconate buffer and detected with a conductivity detector (Waters) as described in (North et al. 2009).

Chapter 3. The Effect of Sulphate Availability, Salinity, Light Intensity and Nitrogen Limitation on Intracellular DMSP Concentration in *Thalassiosira pseudonana*

3.1. Introduction

Diatoms have an important role in the global sulphur cycle through the production of DMSP, the major precursor of the volatile sulphur compound DMS. Although this group are not generally considered to be major DMSP producers, the synthesis of this compound in *T. pseudonana* has been shown to be up-regulated under certain growth conditions (Keller et al. 1999; Bucciarelli and Sunda 2003). This means that diatoms might contribute more to DMSP production than was previously suggested by studies on actively growing nutrient, replete batch cultures (Keller et al. 1989). The ability to up-regulate DMSP production is also a useful characteristic for investigating the regulation of the pathway at a cellular level.

Environmental factors have been shown to be important in determining the production of DMSP, which potentially has multiple roles within the phytoplankton cell (discussed in Chapter 1.3.2). DMSP is proposed to act as a compatible solute (Vairavamurthy et al. 1985), cryoprotectant (Karsten et al. 1996), antioxidant (Sunda et al. 2002) and as an overflow mechanism (Stefels 2000) and in addition its breakdown product, acrylate, may be a grazing deterrent (Wolfe and Steinke 1996).

A detailed understanding of the biological mechanism of DMSP production is now required to improve our ability to predict how environmental factors might affect this process and to enable more detailed equations on the relationships between biological processes and physiological factors for climate models. Although there have been many studies on the effect of different environmental conditions on DMSP concentration in many different species of marine phytoplankton (as discussed in Chapter 1.3.2), the variation observed in the responses of different organisms and the variety of methods used makes it difficult to establish a clear understanding of how DMSP levels are responding. One aim of this chapter was to establish a more complete understanding of the response of one species of diatom, *T. pseudonana,* to different conditions.

Molecular techniques are now widely available for various species of phytoplankton and comparing cell protein and transcript abundance could offer new insight into the pathway of DMSP biosynthesis, and its regulation, in marine phytoplankton. *T. pseudonana* is an excellent model for diatom biology, due to availability of various molecular tools for this species and it has also been used in some previous DMSP studies. To test whether it could also be a suitable model for addressing questions about DMSP in the present study, I measured intracellular DMSP concentration in *T. pseudonana* under conditions reported to affect the intracellular DMSP concentration in this species and others; these were sulphur deprivation, increased salinity, increased light intensity and nitrogen starvation.

3.2. Methods

3.2.1. Culturing

Axenic cultures of *T. pseudonana* were grown as described in Chapter 2.1 unless otherwise stated. Cell number, volume and the ratio of variable to maximum fluorescence (Fv/Fm) of cultures were measured daily (see Chapter 2.1).

3.2.2. Sulphur Deprivation

T. pseudonana cultures were grown in either standard ESAW media, which has a sulphate concentration of 25 mM, or in media with a reduced sulphate concentration of 5 mM. To achieve 5 mM sulphate in the media the amount of sodium sulphate added was reduced and sodium chloride was used to maintain the ionic strength. Intracellular DMSP concentration was measured daily in the control cultures, whereas the concentration of the reduced sulphate cultures was measured on alternate days (see Chapter 2.2).

3.2.3. Salinity

The salinity of the growth medium was adapted by either increasing or decreasing the concentrations of all salts in the ESAW artificial seawater base recipe (see Chapter 2, Table 2.1) with the exception of bicarbonate. This was because the bicarbonate concentration alters the availability of carbon in the media and changes in its concentration affected culture growth rate and yield.

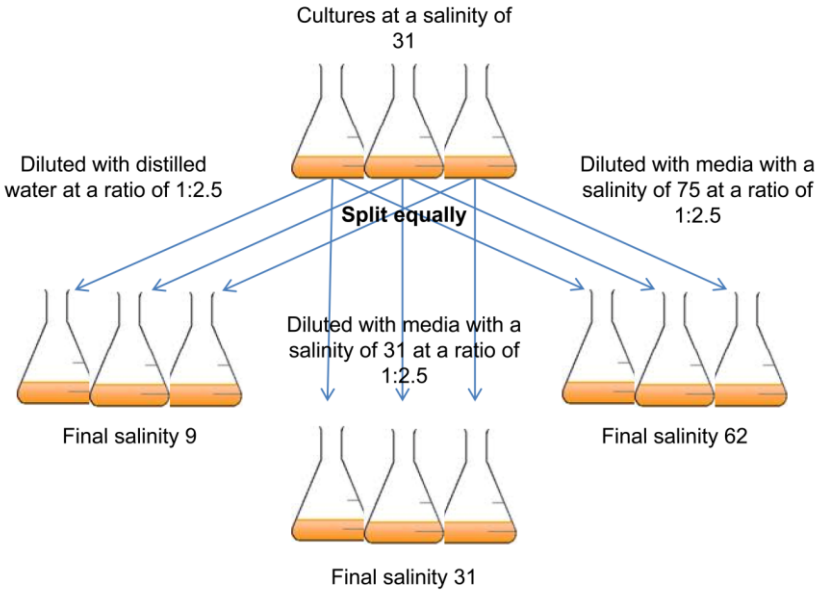

Figure 3.1. Experimental design for the initial experiment testing the affect of different salinities on intracellular DMSP concentration in *Thalassiosira pseudonana*.

In a preliminary experiment *T. pseudonana* cultures were grown to ca. 1.75 x 10^6 cells ml^{-1} in triplicate 600 ml cultures, each of which were then split to three 130 ml subcultures. To these 325 ml of either distilled water, standard ESAW media, or a concentrated stock of ESAW salts was added to achieve final salinities of 9, 31 or 62 (Figure 3.1). Intracellular DMSP concentration was measured on the day prior to the salinity change and then for the following four days according to the protocol described in Chapter 2.2.

For the further comparison of transcript or protein abundance it is preferential to use growth conditions that up-regulate DMSP synthesis as opposed to decreasing its concentration in the cell. I therefore conducted a second experiment with triplicate 600 ml *T. pseudonana*, previously acclimated to a salinity of 10 for a minimum of four subcultures, grown to a cell density of ca. 1 x 10^6 cell ml^{-1}. At this point they were split to two 300 ml subcultures and to one an equal volume of medium with a salinity of 10 was added to maintain the salinity, while to the other 300 ml of medium with a salinity of 60 was added to adjust the final salinity to 35 (Figure 3.2). Intracellular DMSP concentration was measured on day 3, prior to altering the salinity, and then for the following four days according to the protocol described in Chapter 2.2.

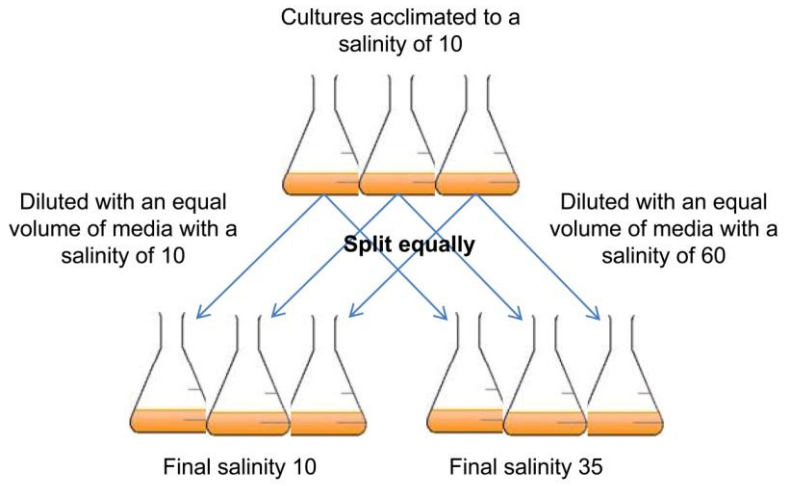

Figure 3.2. Experimental design used to increase the salinity of *Thalassiosira pseudonana* cultures to increase the intracellular concentration of DMSP.

I chose to adjust the salinity of ESAW media to 10 by the dilution of all salts because it is a more environmentally relevant treatment than only changing levels of sodium chloride, however this also decreased the concentration of sulphate from 25 mM, in standard ESAW media, to 7 mM. The effect of reduced sulphate availability on *T. pseudonana* was tested and found not affect intracellular DMSP concentration in this species (discussed in section 3.3.1).

3.2.4. Light Intensity

T. pseudonana cultures, acclimated to a low light intensity of 50 µmol photons m^{-2} s^{-1} (achieved using a neutral density filter) for a minimum of four subcultures, were grown in triplicate 1.2 L cultures to a density of ca. 5 x 10^5 cells ml^{-1}. At this point the cultures were split to two 600 ml aliquots (Figure 3.3). One was kept at 50 µmol photons m^{-2} s^{-1} and the other was exposed to a high light intensity of 900 µmol photons m^{-2} s^{-1}. Intracellular DMSP concentration was measured on day 3, prior to altering the light intensity, and then for the following five days according to the protocol described in Chapter 2.2.

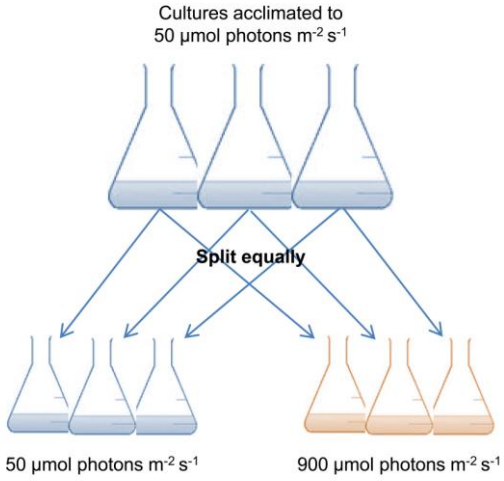

Figure 3.3. Experimental design for testing the affect of increased light intensity on intracellular DMSP concentration in *Thalassiosira pseudonana*.

3.2.5. Nitrogen Limitation

The growth of *T. pseudonana* cultures started with different initial concentration of nitrate was measured in preliminary tests and it was found that cultures started with 30 µM nitrate were yield-limited at ca. 1 x 10^6 cell ml^{-1} whilst cultures with an initial concentration of 550 µM nitrate (standard ESAW) were still in logarithmic growth. Hence, triplicate cultures were started with initial concentrations of 550 µM or 30 µM nitrate. Samples for the analysis of intracellular DMSP concentration were taken from day 3 for four days according to the protocol described in Chapter 2.

3.3. Results and Discussion

3.3.1. Sulphate Deprivation

Since sulphur is an essential nutrient, at a high ~28 mM concentration in seawater, and is required for DMSP synthesis I was interested to test how reduced sulphate availability (5 mM) would affect the growth and intracellular DMSP concentration of *T. pseudonana*. Surprisingly, no reduction in growth was seen over the first 4 days and slightly higher cell numbers were seen between days 4 and 9 in the low sulphate treatment (Figure 3.4 A). Fv/Fm and intracellular DMSP concentration were consistent between the treatments throughout the whole growth curve (Figure 3.4 B and D).

Sulphur is required for the biosynthesis of cysteine and methionine, both of which have an important role in protein biosynthesis and other cell processes and a reduction in their synthesis might be expected to affect culture growth. It was especially surprising that photosynthetic efficiency appeared to be unaffected by the reduced availability of sulphate because the reductive assimilation of sulphate requires energy and reductants, which are products of photosynthesis. A reduction in their consumption by sulphate assimilation would lead to an accumulation of these components, causing increased levels of oxidative stress (Logan et al. 1999) and a reduction in photosynthetic activity would therefore be expected under reduced sulphur assimilation. Reduced photosynthetic efficiency under sulphur deprivation has been reported for green algae and higher plants (Gilbert et al. 1997; Wykoff et al. 1998). One of the major cellular antioxidants, glutathione,

is also a product of sulphur metabolism and any limitation in its production would reduce the cellular capacity to scavenge ROS that are a by-product of photosynthesis, leading to increased levels of oxidative stress. In addition, sulpholipids are a component of photosynthetic membranes (Benning 1998) and again a reduction in their synthesis would also be expected to negatively impact on photosynthesis. This evidence suggests that in this study a reduced sulphate concentration of 5 mM is not limiting to *T. pseudonana* growth or DMSP synthesis.

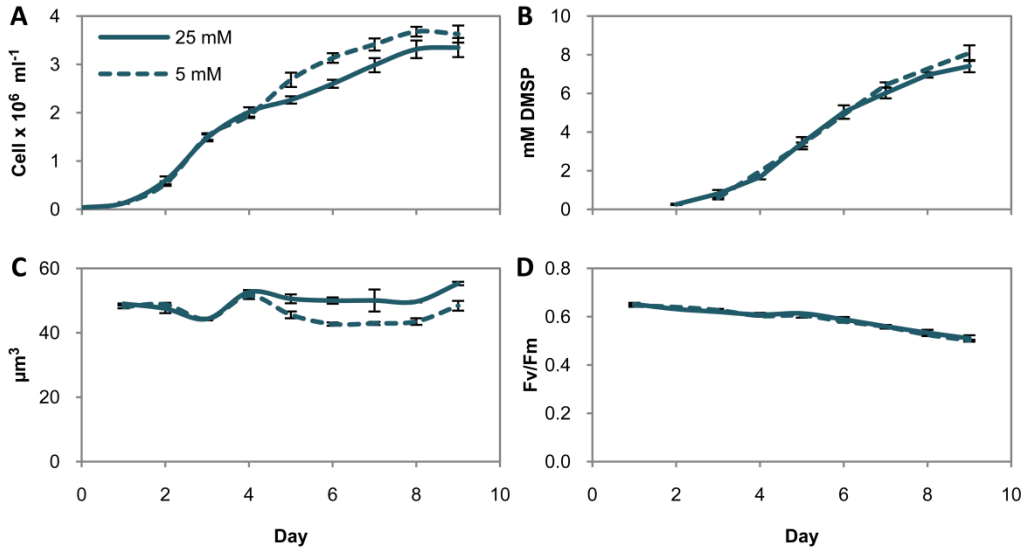

Figure 3.4. A. cell number B. intracellular DMSP concentration, C. volume per cell, D. Fv/Fm of *Thalassiosira pseudonana* cultures with an initial concentration of either 5 mM or 25 mM sulphate. Results are shown as means ± standard deviation from 3 independent cultures.

Interestingly *E. huxleyi* cultures grown with an initial sulphate concentration of 5 mM, as was used here, do become yield-limited in growth with declining Fv/Fm and a reduced intracellular DMSP content compared to cultures with 25 mM sulphate (Michal Bochenek, University of East Anglia and John Innes Centre, personal communication). How does *T. pseudonana* grow normally at this concentration? *T. pseudonana* might have a much lower demand for sulphur; *E. huxleyi* is reported to maintain intracellular DMSP concentrations of more than 150 mM (Keller et al. 1989) whereas in *T. pseudonana* levels 1 to 10 mM are normal under standard growth conditions. However, Ratti et al. (2011) found that the diatom *T. weissflogii* does not have a lower S:C ratio than *E. huxleyi*. If this is the case where is the sulphur going in the diatom cell? We know that it is an important

component of lipids and cell protein, however degradation of these compounds might be expected to affect growth and photosynthesis. Alternatively, one theory as to the success of diatoms over other chromoalveolate algae, such as the coccolithophores, is their possession of a nutrient storage vacuole (Falkowski et al. 2004b). This enables diatoms to hoard inorganic nutrients, keeping them from competitors and saving them for when nutrients are scarce, hence their success in regions with fluctuating nutrient regimes where they are poised for immediate growth when a limiting nutrient becomes available (Falkowski et al. 2004b). Although it would not be necessary to store sulphate for nutrition, since it is never limiting in seawater, it might be involved in maintaining the osmolarity of the vacuole. Further research would be requires to confirm or disprove such this hypothesis. An initial test would be to grow the *T. pseudonana* cultures with 5 mM sulphate over a longer time period and multiple subcultures, if these cells are relying on stored sulphur it would be outstripped at some point. Also measuring sulphate concentration in the media and cells throughout the experiment would tell us whether uptake is actually reduced under reduced sulphate availability or whether *T. pseudonana* generally has a limited requirement for sulphate.

3.3.2. Salinity

There are several examples of altered DMSP content with changing salinity regimes in the literature. I therefore tested whether changes in salinity affect DMSP concentration of *T. pseudonana*. In an initial experiment I increased and decreased the salinity of the growth media of cultures from 31, which is the same as standard ESAW medium, to 9 and 62. The growth of cultures was reduced with both increased and decreased salinity (Figure 3.5 A). There was little difference in the Fv/Fm of cultures adjusted to a salinity of 9 compared to the control cultures that were maintained 31 (Figure 3.5 D). However the cultures adjusted to a salinity of 62 had an initial decreased in Fv/Fm on day 7, before recovering to the level of cultures at 9 and 31, and then decreased relative to cultures at 9 and 31 over days 11 to 13. The intracellular DMSP concentration of the cultures at a salinity of 31 showed an initial decrease at day 7, possibly due to the dilution of the culture with fresh medium on day 6, and then a steady increase (Figure 3.5 B), as is generally

seen in a standard growth curve; as growth rate decreases intracellular DMSP concentration generally increases (for example see Figure 3.4 B). A 1.9-fold (t-test, P = 0.014) higher DMSP concentration was seen in the cultures adjusted to a salinity of 62 compared to those at 31 after 24 hours, but in contrast to the controls, the DMSP content did not increase further. Intracellular DMSP concentration decreased 3.1-fold (t-test, P = 0.0072) in the cultures adjusted to a salinity of 9 and this reduced concentration was maintained over the three days of DMSP measurements.

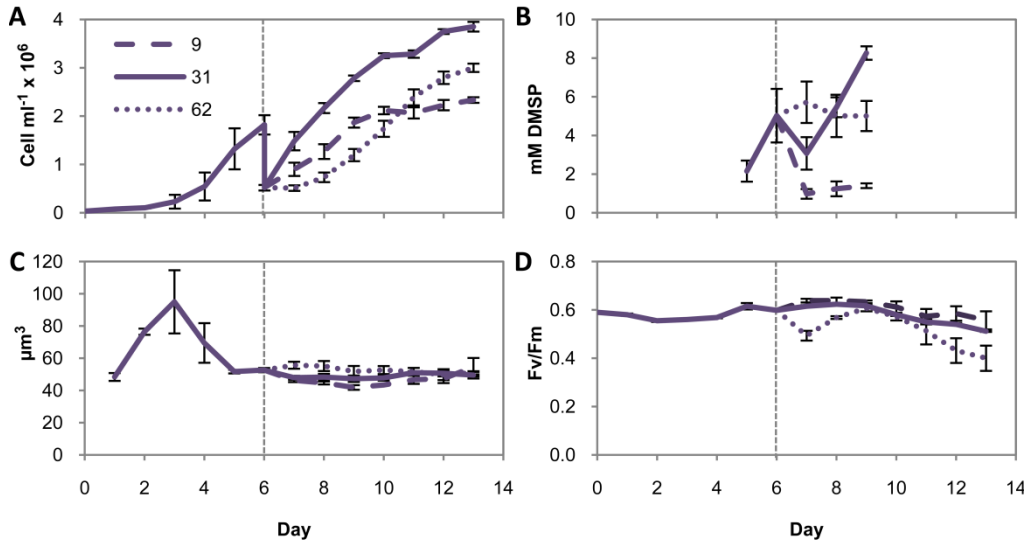

Figure 3.5. The affect of increasing and decreasing salinity on *Thalassiosira pseudonana* showing A. cell number, B. intracellular DMSP concentration, C. volume per cell, D. Fv/Fm. Results are shown as means ± standard deviation from 3 independent cultures. The vertical line indicates the point at which the salinity of the cultures was adjusted.

Whilst there was a clear difference in the intracellular DMSP concentration of cultures at a salinity of 31 and 9, for further investigation of DMSP synthesis at a cellular level, for example through gene expression analysis or measurement of protein abundance, it was preferential to identify a growth condition that induced production rather than repressed it. Therefore the effect of increasing salinity to 35 on the intracellular DMSP concentration of *T. pseudonana*, previously acclimated to a salinity of 10, was tested (Figure 3.6). The cell numbers of cultures adjusted to a salinity of 35 increased more rapidly than those kept at a salinity of 10, but the overall culture yield was the same (Figure 3.6 A). There was very little difference in the Fv/Fm of cultures grown under these

conditions until days 9 and 10 when the Fv/Fm of cultures at a salinity of 35 was lower than those maintained at 10 (Figure 3.6 D). Cells at a salinity of 35 had a ca. 1.3-fold larger volume than those at a salinity of 10 (Figure 3.6 C). The DMSP concentration of cells acclimated to a salinity of 10 was below the level of detection on days 3 to 5 and remained low throughout the experiment, reaching a maximum of 1.08 mM. In contrast, within 48 h the intracellular DMSP concentration of cultures that were adjusted to a salinity of 35 reached 3.83 mM, and on day 7 the DMSP concentration was 12.8-fold (t-test, $P<0.001$) higher than in the cultures maintained at a salinity of 10 (Figure 3.6 B).

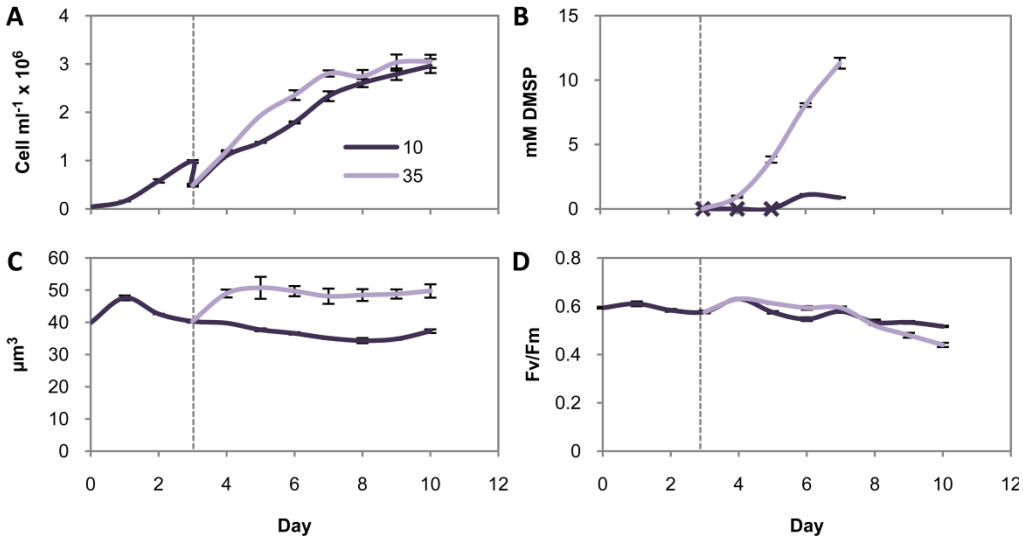

Figure 3.6. The affect of increased salinity on *Thalassiosira pseudonana*, previously acclimated to 10, showing A. cell number, B. intracellular DMSP concentration, with points below the level of detection marked ×, C. volume per cell, D. Fv/Fm. Results are shown as means ± standard deviation from 3 independent cultures. The vertical line indicates the point at which the salinity of the cultures was adjusted.

Our results agree with reports showing an increasing DMSP content with increasing salinity in a diverse range of algae including the green macroalga *U. lactuca* (Dickson et al. 1980), the prasinophyte *P. subcordiformis* (Dickson and Kirst 1986), the coccolithophore *P. carterae* (Vairavamurthy et al. 1985), the dinoflagellate *C. cohnii* (Kadota and Ishida 1968) and the diatom *P. tricornutum* (Dickson and Kirst 1987). However, no significant difference in DMSP levels were measured in *U. lactuca* under a fluctuating salinity regime, designed to mimic an estuarine

environment where salinity varied between 30 % and 100 % seawater over a 24 hour cycle (Dickson et al. 1982). This may be due to a slow synthesis and accumulation of DMSP. Dickson and Kirst (1986) noted a lag period prior to the response of DMSP levels to increased salinity in *P. subcordiformis*.

It is interesting that the intracellular DMSP concentration of *T. pseudonana* measured here showed such a large difference between the salinities of 10 and 35, but no sustained increase was found between the salinities of 31 and 62. In agreement with our study, Van Bergeijk et al. (2003) found that the DMSP content of the benthic diatom *Cylindrotheca closterium* increased with salinity from 11 to 44, but at higher salinities it did not increase further. A number of compatible solutes and inorganic ions can be used to regulate osmotic potential in marine phytoplankton (Dickson and Kirst 1987). It is likely that DMSP acts in combination with these to regulate the osmotic potential of the cell and therefore, there may not be a straightforward linear response of intracellular DMSP concentration to salinity in all cases.

3.3.3. Light Intensity

High light leads to an increased production of reducing equivalents which in absence of sufficient electron acceptors form ROS and thereby increase levels of oxidative stress (Jakob and Heber 1996). From the proposed functions for DMSP, two are particularly relevant for the response to high light intensity: defence against oxidative stress (Sunda et al. 2002) and an overflow mechanism for when nutrient availability and growth are unbalanced (Stefels 2000). I therefore tested the effect of increased light intensity on intracellular DMSP concentration in *T. pseudonana* by exposing cultures previously adapted to a low light intensity of 50 µmol photons m^{-2} s^{-1} to a high light intensity of 900 µmol photons m^{-2} s^{-1} (Figure 3.7). Although little effect was seen on growth rates (Figure 3.7 A), the Fv/Fv of cultures exposed to the high light intensity decreased rapidly (Figure 3.7 D). After 48 hours the intracellular DMSP concentration was 2.25-fold higher (t-test, $P = 0.007$) in the high light intensity cultures compared to those that remained at the low light intensity (Figure 3.7 B). Although the intracellular DMSP concentration of cultures at the low

light intensity gradually increased through the experiment, as is seen in a standard growth curve (see Figure 3.4 B for example), the difference was maintained with the intracellular DMSP concentration 1.82-fold higher (t-test, $P < 0.001$) in the high light intensity cultures on day 8 of the experiment.

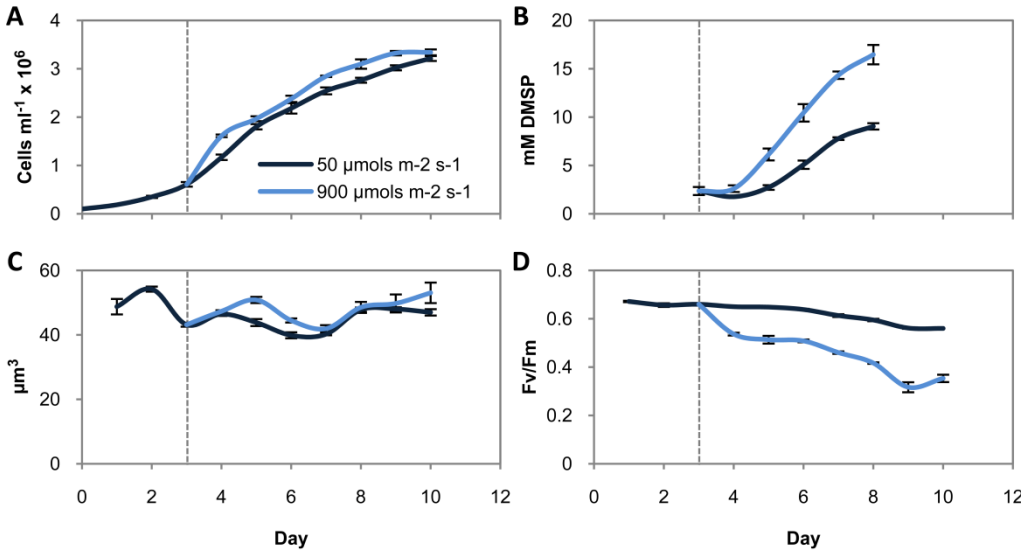

Figure 3.7. The effect of increased light intensity on *Thalassiosira pseudonana* previously acclimated to a low light intensity, showing A. cell number, B. intracellular DMSP concentration, C. volume per cell, D. Fv/Fm. Results are shown as means ± standard deviation from 3 independent cultures. Vertical line indicates the point at which the light intensity of the cultures was adjusted.

Karsten et al. (1991) also noted increased DMSP levels in the tissues of a number of macroalgal species with increased light intensity. Stefels and van Leewe (1998) found higher intracellular DMSP concentrations in *Phaeocystis* cultures exposed to higher light intensities than those kept at a lower light intensity. However, in *E. huxleyi* no increase in intracellular DMSP concentration was found with increasing light intensity (van Rijssel and Gieskes 2002), although in that study the highest light intensity tested was 150 µmol s^{-1} m^{-2}, which is not considerably higher than the irradiance of standard growth conditions used in this study (described in Chapter 2.2).

3.3.4. Nitrogen Limitation

There is evidence that intracellular DMSP content increases under nitrogen limited conditions in a number of marine phytoplankton including: *T. subcordiformis* (Gröne and Kirst 1992), *Chrysochromulina, Minidiscus triculatus, Heterocapsa pygmaea* (Keller and Korjeff-Bellows 1996) and *Thalassiosira oceanica* (Harada et al. 2009). I therefore compared the intracellular DMSP concentration of nitrogen starved cultures to that of nitrogen replete cultures, with initial nitrate concentrations of 30 µM and 550 µM respectively (Figure 3.8). On day 3 the growth of the low nitrate cultures was reduced, having only reached 4.7 x 10^5 cells ml^{-1} compared to 5.2 x 10^5 cells ml^{-1} in the nitrogen replete cultures (Figure 3.8 A) and the Fv/Fm of these cultures was 0.60 compared to 0.63 (Figure 3.8 D), suggesting that they were becoming yield limited. At this point the cultures grown in medium with a low nitrate concentration already had a 2-fold higher intracellular DMSP concentration than the nitrogen replete cultures (Figure 3.8 B). This difference was maintained and DMSP levels were still 1.67-fold higher in nitrogen starved cultures on day 6.

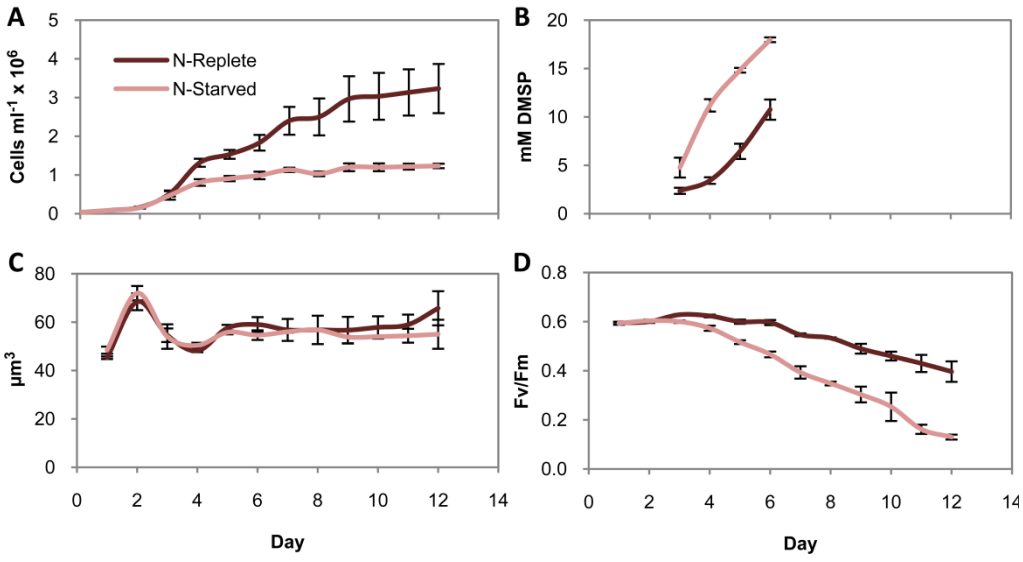

Figure 3.8. The effect of nitrogen starvation on *Thalassiosira pseudonana* A. cell number B. intracellular DMSP concentration, C. volume per cell, D. Fv/Fm of *T. pseudonana* cultures with an initial concentration of either 30 µM of 550 µM nitrate. Results are shown as means ± standard deviation from 3 independent cultures.

Andreae (1986) first suggested that increasing DMSP content with nitrogen limitation might be part of a reciprocal relationship with GBT. DMSP does not contain nitrogen and may therefore be favoured over nitrogen containing osmolytes under conditions of nitrogen limitation, especially since the sulphur required for DMSP synthesis is found at high concentrations throughout the world's oceans and is almost never limiting. DMSP levels were shown to be inversely related to those of the nitrogen containing osmolytes GBT and homarine in continuous cultures of *T. pseudonana* with respect to nitrogen availability (Keller et al. 1999). However, this relationship was not seen in *E. huxleyi* or *A. carterae*. In these species DMSP was the primary compatible solute, with nitrogen containing osmolytes accounting for only a small portion of the osmotic potential, and so nitrogen deprivation may therefore have little effect on the osmolyte content of these cells (Keller et al. 1999).

Bucciarelli and Sunda (2003) also found that the intracellular concentration of DMSP in *T. pseudonana* cultures increased with nitrogen limitation, but they suggested an alternative hypothesis to explain this finding. As discussed above, there is evidence that DMSP may be involved in an antioxidant defence cascade (Sunda et al. 2002). Nitrogen limitation may increase oxidative stress by negatively affecting photosynthesis, since many enzymes involved in light harvesting and CO_2 fixation are nitrogen rich. Furthermore, some antioxidants, such as glutathione, contain nitrogen and restriction of their production could reduce the cellular capacity to respond to oxidative stress. In the current study the Fv/Fm of *T. pseudonana* cultures decreased rapidly as growth became nitrogen limited, which indicates a reduction in photosynthetic efficiency. Finally DMSP might also be acting in an overflow role; nitrate reduction and assimilation requires energy, carbon and reducing equivalents and therefore reduced nitrate availability can cause these components to accumulate. Since sulphate is not limiting in the ocean its assimilation and production of DMSP might act as a sink for this excess energy, carbon and reducing equivalents, which would otherwise increase cellular levels of oxidative stress (Stefels 2000).

3.3.5. Concluding Remarks

Intracellular DMSP concentration increases with increased salinity, increased light intensity and nitrogen limitation in *T. pseudonana*, however no effect of sulphur deprivation on DMSP synthesis was seen. These data support the multifunctional role of DMSP in the cell, as a potential compatible solute, an antioxidant and an overflow metabolite. In the natural environment *T. pseudonana* is a bloom forming species and is likely to be exposed to high light intensities and nitrogen limitation. The findings presented here highlight the potential for these environmental conditions to affect DMSP production in this species and provides evidence that diatoms could contribute more to global DMSP production than originally suggested by experiments with actively growing, nutrient replete, batch cultures (Keller et al. 1989).

We cannot fully understand the impact of environmental conditions on the regulation of DMSP production without a detailed knowledge of the cellular processes underpinning its synthesis. We now have three conditions that increase the concentration of DMSP in *T. pseudonana* cells. These can be used to compare cells with up-regulated DMSP production to control cells with reference to protein accumulation and levels of gene expression. The conditions described are quite different (osmotic adjustment, oxidative stress and nutrient limitation) and each will have a specific set of genes and proteins adapting the cell to that specific stress. Therefore I hypothesised that any changes that take place under all three treatments are involved in DMSP production.

Chapter 4. Insights into the Regulation of DMSP Synthesis through APR Activity, Proteomics and Gene Expression Analyses.

4.1. Introduction

Despite the environmental importance of DMSP and the availability of genome sequences for DMSP producing phytoplankton, the genes and enzymes involved in its production have yet to be identified and very little is known about the regulation of its synthesis. DMSP is generated from the methionine (Greene 1962) and by using ^{35}S-labelling Gage et al. (1997) revealed the steps converting this amino acid to DMSP in the green macroalga *U. intestinalis*. Methionine first undergoes transamination to MTOB and then reduction to MTHB, before *S*-methylation to DMSHB and finally oxidative decarboxylation to DMSP (Gage et al. 1997). The activities of putative substrate specific enzymes for the first three steps of this pathway have been measured in this species (Summers et al. 1998). These authors also found activity in three additional chlorophyte seaweeds that contain DMSP, but not in three species without detectable DMSP.

As discussed in Chapter 1.3.2, multiple cellular roles have been proposed for DMSP, including as an osmolyte (Dickson et al. 1980), antioxidant defence (Sunda et al. 2002) and as an 'overflow metabolite' in the dissipation of excess energy, carbon and reducing equivalents when growth and photosynthesis are unbalanced (Stefels 2000). In Chapter 3 I demonstrated that intracellular levels of DMSP increase in *T. pseudonana* under nitrogen starvation, increased salinity and increased

light intensity and here these growth conditions were used to investigate the regulation of DMSP production at a cellular level.

In higher plants the production of sulphur metabolites is regulated by the assimilation of sulphate and, more specifically, the activity of the enzyme APR. I therefore measured changes in the expression levels of genes involved in sulphur assimilation in *T. pseudonana* under nitrogen starvation, increased salinity and increased light intensity, along with the activity of APR. I also used these growth conditions to compare the proteomes of *T. pseudonana* with up-regulated DMSP synthesis to control cultures using 2-dimensional gel electrophoresis. As the final gene product, measuring protein abundance of enzymes is a good insight into the functioning of a pathway, since there are many levels of regulation in protein synthesis. The overall hypothesis of this study was that enzymes related to DMSP synthesis would be found amongst proteins that increase or decreased in abundance across all three treatments.

4.2. Methods

4.2.1. Culturing

Experimental growth conditions of axenic cultures of *T. pseudonana* were comparable to those shown to increase intracellular DMSP concentration in Chapter 3, although the culture volume was increased to 3 L, grown in triplicate 5 L Duran bottles, to achieve the biomass required. At a time point where the previous experiments demonstrated increased intracellular DMSP levels, cultures were collected by filtration of multiple 250 ml aliquots onto, 47 mm diameter nucleopore membranes with a 1 µm pore size (Whatman) at a pressure of 35 KPa. Filters were immediately snap frozen in liquid nitrogen and stored at -80 ^{o}C. In all experiments cell number, volume and Fv/Fm were measured in the cultures daily (see Chapter 2.1 for methods) and intracellular DMSP concentration was measured at points during the experiment to confirm that it was increased as seen in Chapter 3.

4.2.2. Salinity

T. pseudonana cells previously acclimated to a salinity of 10 for a minimum of four subcultures were grown in triplicate to ca. 1 x 10^6 cells ml^{-1}. At this point half of the culture was removed and replaced with media with either a salinity of 10, to maintain the salinity, or 60, with all salt concentrations increased, to achieve a final salinity of 35. In Chapter 3 (Figure 3.6) I found that 48 h after cultures were adjusted to a salinity of 35 the intracellular DMSP concentration was 3.8 mM, whereas the concentration in cells maintained at a salinity of 10 was below the level of detection at this point. I therefore sampled the experiment 48 h after the salinity change for transcript and proteome comparison.

4.2.3. Light Intensity

T. pseudonana cells acclimated to a low light intensity of 50 µmol photons m^{-2} s^{-1} for a minimum of four subcultures were grown in triplicate to ca. 5 x 10^5 cells ml^{-1}. At this point cultures were either maintained at a light intensity of 50 µmol photons m^{-2} s^{-1} or exposed to a high light intensity of 1000 µmol photons m^{-2} s^{-1}. Based on my findings in Chapter 3 (Figure 3.7), I sampled the cultures for further analysis 48 h after the change in light intensity as the intracellular DMSP concentration of cultures adjusted to the high light intensity had been 2.3-fold higher than cultures maintained at a low light intensity at this point.

4.2.4. Nitrogen Starvation

Triplicate *T. pseudonana* cultures were started with initial concentrations of either 550 µM or 30 µM nitrate. In Chapter 3 (Figure 3.8) I demonstrated that the intracellular DMSP concentration of cultures with 30 µM nitrate was 11.2 mM as they became yield limited on day 4 at 1 x 10^6 cells ml^{-1} and their Fv/Fm decreased relative to the cultures with 550 µM nitrate control cultures which had an intracellular DMSP concentration of 3.4 at this point. Therefore, the samples were taken on day 4.

4.2.5. Sample Analysis

Each experiment was conducted with triplicate control and treated cultures. For each culture proteins were extracted from 2 filters per culture (representing 250 ml culture each) and separated by 2-dimensional gel electrophoresis (as described in Chapter 2.3). It should be noted that the gel of one biological replicate grown at a salinity of 10 was unsuccessful and was not included in this comparison. The proteomic comparison of this treatment is therefore based on two biological replicates, whereas all others are in biological triplicate. All gels included in this study were aligned using Progenesis SameSpots analysis software (v4.1; Nonlinear Dynamics Ltd), the gels were highly reproducible and aligned very well. For each treatment the protein abundance of spots were compared between the gels of the control and treated cultures by fold change and t-test.

RNA was extracted from another replicate filter from each culture to compare the transcript levels of genes involved in sulphur assimilation from each culture by qRT-PCR (as described in Chapter 2.4). Subsequently, the experiments were repeated with 1 L cultures to measure the enzyme activity of APR over a time series (as described in chapter 2.5).

4.3. Results and Discussion

4.3.1. APR Activity

DMSP is a product of sulphur metabolism and the assimilation of this nutrient may therefore be limiting to its synthesis. APR is an important point of regulation in the pathway of sulphur assimilation in higher plants (Kopriva et al. 2008) and has been shown to be regulated in a demand driven manner by the thiols glutathione and cysteine (Bick et al. 2001; Vauclare et al. 2002), amino compounds (Neuenschwander et al. 1991; Koprivova et al. 2000), carbohydrates (Kopriva et al. 1999; Kopriva et al. 2002) and hormones (Harada et al. 2000; Ohkama et al. 2002). To test whether APR might also have a regulatory role in the biosynthesis of DMSP in *T. pseudonana* I measured the activity of this enzyme under nitrogen starvation, increased salinity and increased light intensity

(Figure 4.1); three growth conditions shown to increase intracellular DMSP concentration in this species.

The APR activities measured in the nitrogen replete cultures, which were grown under standard conditions (described in Chapter 2.1), were between 66 and 209 nmol min^{-1} mg^{-1} protein depending on growth stage of the culture. This is comparable to the APR activity reported for the diatoms *T. weissflogii* and *T. oceanica* which range from 80 to 200 nmol min^{-1} mg^{-1} protein (Gao et al. 2000). Under nitrogen starvation APR activity was found to be 2.8-fold higher (t-test; $P < 0.001$; Figure 4.1 D) than in nitrogen replete cultures on day 2, the first time point measured, when an increase in intracellular DMSP had already been seen (Figure 4.1 G). However, whilst DMSP concentration of the nitrogen starved cells continued to increase throughout the experiment the APR activity gradually decreased to the level of the nitrogen replete cultures. In *T. pseudonana* cultures adjusted from a salinity of 10 to 35 the activity of APR had an initial 1.7-fold increase after 24 hr, although this was not found to be significant, possibly due to the variability of the measurements (Figure 4.1 E). Again this increase was not maintained and the activity decreased to the level of the cultures that were kept at a salinity of 10, despite the intracellular DMSP concentration of cultures adjusted to a salinity of 35 increasing from below the level of detection to over 20 mM during this time period (Figure 4.1 H). For *T. pseudonana* cultures exposed to a high light intensity of 1000 µmol m^{-2} s^{-1} the data were quite noisy and there was no apparent difference in APR activity compared to those kept at a low light intensity of 50 µmol m^{-2} s^{-1} (Figure 4.1 F), whilst again there was a clear increase in intracellular DMSP concentration (Figure 4.1 I). It is also noteworthy that the intracellular DMSP concentration of cultures acclimated to a salinity of 10 was considerably lower than in the nitrogen replete cultures, which were grown under standard conditions (Chapter 2.1) at a salinity of 31, however the APR activities of the former were only marginally reduced. In addition, I also measured the activity of APR under reduced sulphate availability (in samples taken from growth experiment described in Chapter 3.2.2) and little difference was seen between cultures grown with 5 mM and 25 mM sulphate (Figure 4.2).

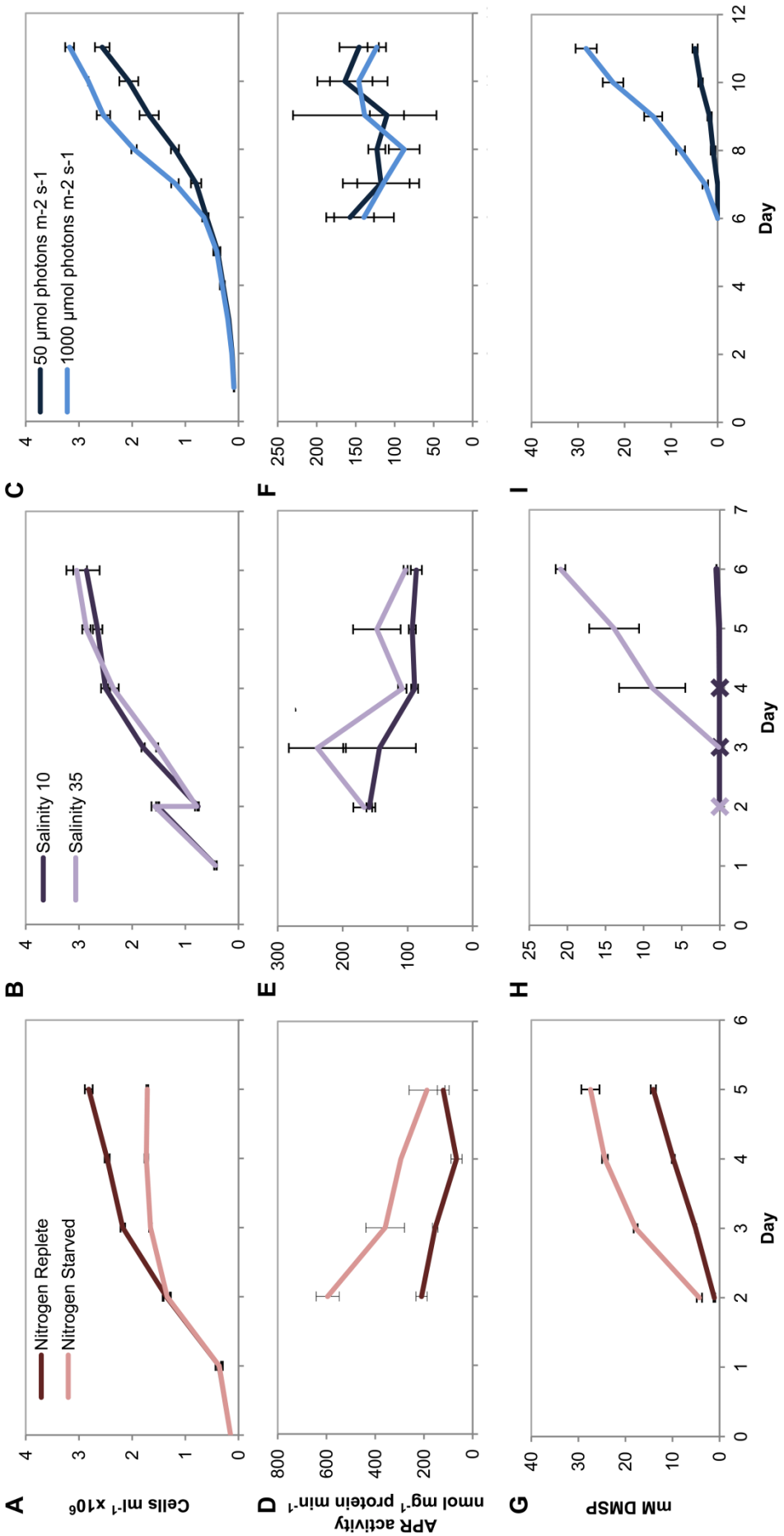

Figure. 4.1. The effect of nitrogen starvation (red), increased salinity (purple) and increased light intensity (blue) on APR activity, as measured by the production of [^{35}S]sulphide , (D-F) in *Thalassiosira pseudonana*, also showing the cell numbers of cultures throughout the experiments (A-C) and the intracellular concentration of DMSP (G-I). Results are shown as means ± standard deviation from 3 independent cultures

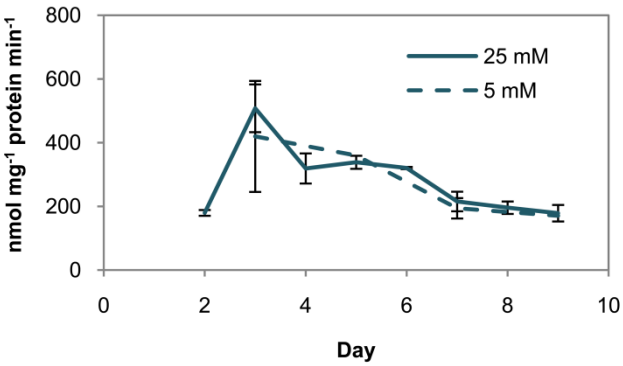

Figure 4.2. The effect of reduced sulphate availability on the APR activity of *Thalassiosira pseudonana* , quantified by the production of [^{35}S]sulphide, measured in samples taken from the growth experiment described in Chapter 3.2.2.

Gao et al. (2000) also found that APR activity decreased through the growth curve despite a progressive increase in DMSP content per cell under nitrogen limitation in the chlorophyte microalga *T. subcordiformis*. My results suggest that increased sulphur assimilation, might be required initially to increase DMSP synthesis in *T. pseudonana*, but later in the batch culture growth sulphur for DMSP synthesis might be made available by other cell processes. The lack of change in APR activity with increased light intensity suggests that increased APR activity is not critical for increased DMSP biosynthesis and that the regulation of diatom sulphur metabolism might be quite different to that of higher plants. Gao et al. (2000) also reported that the APR activity of *Heterocapsa triquetra*, at only 0.5 to 5 µmol m^{-2} s^{-1}, is considerably lower than that found for diatoms in that study and here. However, as a dinoflagellate this species possesses a high intracellular DMSP concentration at approximately 300 mM (Caruana 2010), compared to a maximum of 15 to 20 mM for *T. pseudonana*. This provides further evidence that increased APR activity is not required for increased DMSP synthesis, but might also suggest that there is a divergence in the regulation of sulphur metabolism between these two groups.

4.3.2. Expression of Genes involved in Sulphur Assimilation

To investigate whether other enzymes might regulate DMSP production in *T. pseudonana* I measured changes in the transcript levels of genes associated with the assimilation of sulphate to cysteine (reviewed in Chapter 1.3.3) under nitrogen starvation, increased salinity and increased light intensity. Intracellular DMSP concentration was analysed and confirmed to increase at the time points chosen to compare the transcript and protein abundance (Figure 4.3). On comparison of the DMSP measurements between Chapter 3, and the two studies described here (Figure 4.1 and 4.3) there was some variation in the intracellular concentrations measured. However, the DMSP concentration of *T. pseudonana* increases through the growth cycle in batch culture and quite large changes can be seen from day to day, if the samples were taken at a slightly different cell density the DMSP could be quite different. In addition a higher light intensity was used as a 'high light treatment' in Chapter 4 compared to Chapter 3, and a marginally higher salinity difference was used in Chapter 3, which might account for the higher DMSP measured here.

Of genes involved in sulphur assimilation (table 4.1) surprisingly little coordination was found in the transcript level response to the three treatments, including the two isoforms of APR (Figure 4.4). Transcript levels of APR1 increased under nitrogen starvation, but not with increased salinity or light intensity, whereas APR2 transcript levels increased with increased salinity, but not with the other two treatments. This suggests that different APR isoforms may be responsible for the initial increase in APR activity seen with nitrogen starvation and increased salinity. The lack of change in APR transcripts under increased light intensity corresponds with the lack of change in APR activity under this treatment. Indeed, APR is mainly under transcriptional regulation in higher plants (Takahashi et al. 2011).

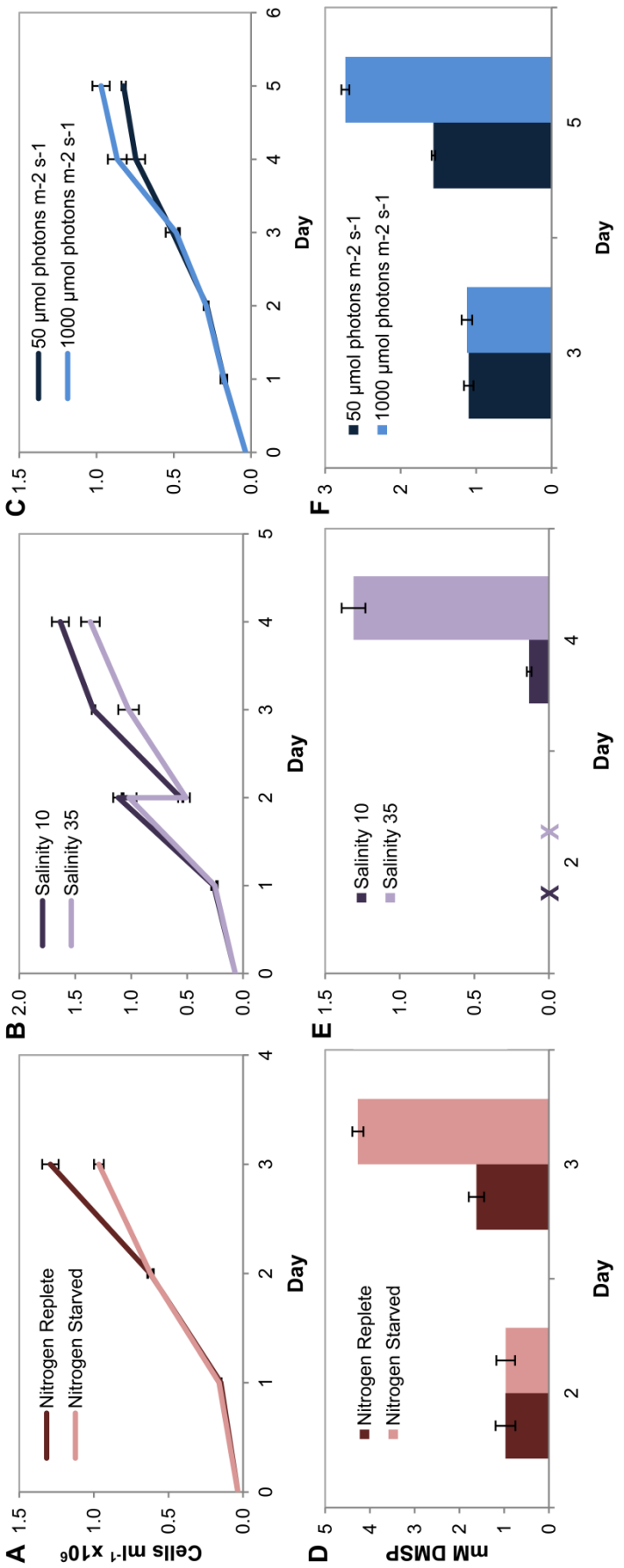

Figure 4.3. A-C. growth and D-F. intracellular DMSP concentration of *Thalassiosira pseudonana* under nitrogen starvation (red), increased salinity (purple) and increased light intensity (blue) in experiments where cells were harvested for quantification of transcript and protein abundance. Intracellular DMSP concentrations below the level of detection are marked x and results are shown as means ± standard deviation from 3 independent cultures .

Table 4.1 Abbreviation for the enzymes discussed in Chapter 4 with regards to transcript and protein abundance. Numbers represent different isoforms

Enzyme	Abbreviation
Sulphate transporter 1	Trans1
Sulphate transporter 2	Trans3
ATP sulphurylase 1	ATPS1
ATP sulphurylase 2	ATPS2
ATPS reductase 1	APR1
ATPS reductase 1	APR2
OAS thiollyase 1	OASTL1
OAS thiollyase 2	OASTL2
OAS thiollyase 3	OASTL3
Serine acetyltransferase 1	SAT1
Serine acetyltransferase 2	SAT2
Serine acetyltransferase 3	SAT3
Sulphite reductase	SiR

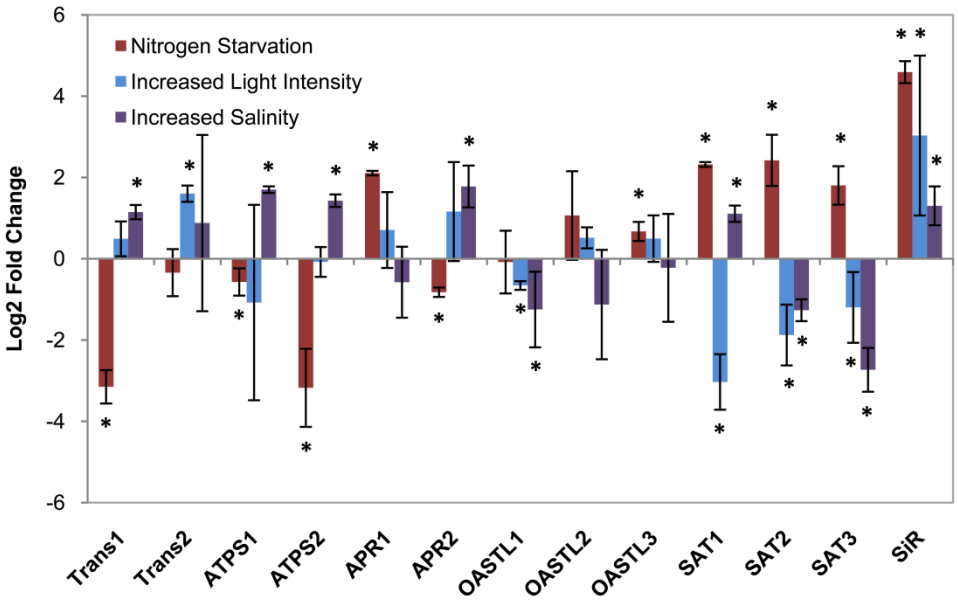

Figure 4.4. The relative fold change in the transcript levels of genes involved in sulphur assimilation in *Thalassiosira pseudonana* exposed to nitrogen starvation, increased salinity and increased light intensity quantified by qRT-PCR. Results are shown as means ± standard deviation from 3 independent cultures. Asterisks show t-test, $P < 0.05$.

Interestingly, the transcript levels of all three SAT genes increased 5-, 5.7-, and 3.6-fold (t-test, $P < 0.05$) in *T. pseudonana* under nitrogen starvation. In plants SAT is another enzyme often associated with the regulation of sulphur assimilation through the production of OAS, as modulation of SAT expression affects the concentration of cysteine and GSH (Harms et al. 2000; Haas et al. 2008). Thus it is possible that under nitrogen starvation OAS synthesis might be limiting for cysteine and consequently DMSP production in *T. pseudonana*.

The only gene up-regulated under all three growth conditions was SiR and this may therefore be an important point of regulation in diatom sulphur assimilation, as opposed to APR. APR activity in the diatoms is about two orders of magnitude higher than in plants and therefore it might be too high to effectively control the flux through sulphate assimilation. The control thus might move to another component of the pathway which could be limiting for cysteine synthesis. Alternatively, the general lack of coordination in this pathway, in addition to the different responses of APR activity, across these treatments could suggest that sulphur assimilation is not limiting to DMSP production. To add complexity to the regulation of sulphur assimilation and DMSP synthesis, at a number of steps in the pathway there is more than one isoform that catalyses the reaction, and these might have different kinetic properties and be localised to different compartments. The different regulation of isoforms seen here is interesting and could warrant further investigation in the future.

4.3.3. Identification of Proteins involved in DMSP synthesis

In a broader approach to identify enzymes involved in DMSP biosynthesis I compared changes in the proteomes of *T. pseudonana* cultures in response to nitrogen starvation, increased salinity and increased light intensity (as described in section 4.2.5). The separation of protein extracts by 2-dimensional gel electrophoresis yielded 3310 distinguishable protein spots (an example gel is shown in Figure 6.2). Initially I considered spots that changed by greater than 1.5-fold in relative abundance with $P < 0.005$ (determined by t-test) under any of the three treatments and this highlighted 263 spots. For the salinity and light treatments the 10 spots with the greatest fold change were picked from the gel, and for the nitrogen starvation treatment all spots that changed

were picked (the response of the diatom proteome to nitrogen starvation is discussed further in Chapter 6). I had hypothesised that any protein found to change in abundance under all three treatments would be involved in DMSP biosynthesis, however I found that most of the changes were treatment specific, with very few protein spots changing in abundance under multiple treatments and none changing under all three (Figure 4.5). I, therefore, increased the P-value cut-off to $P < 0.05$ (determined by t-test) and searched for spots changing in the same direction under all three treatments to maximise the chance of finding proteins related to DMSP biosynthesis; this resulted in a further 4 spots. In total the MALDI-TOF MS analysis of the tryptic digests of all selected spots resulted in identification of 87 proteins that changed in relative abundance under one or more treatment (appendix table 1). A number of changes in the *T. pseudonana* proteome that might be related to sulphur metabolism were detected, but these were quite specific to individual treatments (Figure 4.6; table 4.2). It is important to note that the absence of a protein among the analysed spots in the study does not prove its stable abundance.

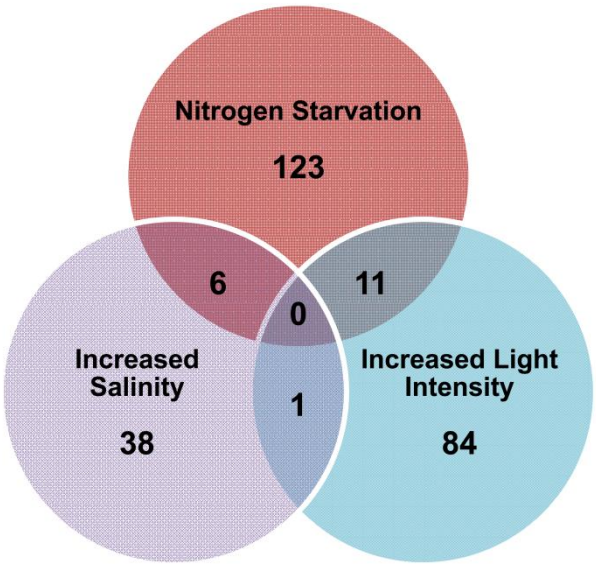

Figure 4.5. Number of protein spots identified by 2-dimensional gel electrophoresis, changing in relative abundance by more than 1.5-fold (t-test, $P < 0.005$) in *Thalassiosira pseudonana* under nitrogen starvation, increased salinity and increased light intensity.

Proteins involved in the active methyl cycle, which salvages methionine from methyl transferase reactions, increased in abundance with increased salinity. An S-adenosylmethionine (SAM) synthetase (ProtID 21815), which catalyses the formation of SAM from methionine was found to increase by 2.9-fold in abundance. SAM is used as a methyl donor in a wide variety of methyltransferase reactions and a 3.6-fold increase in the abundance of a SAM-dependent methyltransferase (ProtID 20797) was measured. Enzymes of this family have a diverse range of functions, they are involved in modification of DNA, RNA, histones and other proteins, in replication, repair and epigenetic modification (Loenen 2006) and they also have a role in the synthesis of various metabolites. The SAM-dependent methyl transferase identified (ProtID 20797) has similarities to a sarcosine/dimethylglycine methyltransferase (BlastP E= 3×10^{-32}) which provides an alternative route for GBT synthesis through the methylation of glycine. Induction of GBT synthesis is well connected to increased salinity as it is also an osmolyte. This metabolic route of GBT synthesis is distinct from the pathway of choline oxidation of higher plants and it has been identified in a number of halotolerant bacteria and cyanobacteria (Nyyssölä et al. 2000; Waditee et al. 2003), and also in the red alga *Galdieria sulphuraria* (McCoy et al. 2009). To my knowledge, this is the first evidence of its presence in a diatom. A reciprocal relationship that is dependent on nitrogen availability has been found between cellular DMSP and GBT content in continuous cultures of *T. pseudonana* (Keller et al. 1999) and accordingly the SAM-dependent methyltransferase identified in this study decreased by 2.1-fold in protein abundance under nitrogen starvation.

Table 4.2. Proteins that are related to sulphur assimilation and may influence DMSP synthesis in *Thalassiosira pseudonana* identified as changing under nitrogen starvation (N), increased salinity (S) and increased light intensity (L). Red numbers indicate an increase and green a decrease in fold change by more than 1.5-fold. Blue highlights $P < 0.005$. Protein name is based on UniProtKB unless otherwise stated and Protein IDs are from the Joint Genome Institute *T. pseudonana* genome version 3 (http://genome.jgi-psf.org/Thaps3/Thaps3.home.html).

Protein ID	Protein Name	Fold Change			t-test (P)		
		N	S	L	N	S	L
260934	Branched-chain-amino-acid aminotransferase[6]	6.4	1.3	-1.2	0.0001	0.1580	0.1778
270365	Sulphite reductase[mbc]	1.6	1.2	1.1	0.0016	0.1578	0.2229
20797	S-adenosylmethionine (SAM)-dependent Methyltransferase[mbc]	-1.7	3.6	1.2	0.0153	0.0017	0.1000
		-3.0	3.6	1.3	0.0136	0.0027	0.0535
21815	S-adenosylmethionine synthetase	-1.4	2.9	1.1	0.0122	0.0001	0.1684
644	Adenosine kinase	1.1	2.5	1.2	0.1847	0.0000	0.0129
27273	Methylenetetrahydrofolate reductase	1.0	2.0	1.5	0.4366	0.0031	0.0020
28496	Adenosylhomocysteinase	-1.7	2.6	1.3	0.0022	0.0023	0.0243
25402	Fucoxanthin chl a/c light-harvesting protein	-1.0	1.2	-3.6	0.3946	0.3275	0.0001
22747	Fucoxanthin chlorophyll a/c light-harvesting protein	-1.0	1.0	-3.5	0.4740	0.4651	0.0002
bd1048	Photosystem I iron-sulphur centre[MB]	1.0	-1.2	-2.6	0.2815	0.0132	0.0004
30385	Fucoxanthin chlorophyll a/c protein-LI818 clad	-1.2	-1.2	-2.5	0.1386	0.1856	0.0002
24080	Fucoxanthin chl a/c light-harvesting protein	-1.1	1.2	-2.4	0.2963	0.3389	0.0024
38583	Fucoxanthin chlorophyll a/c protein	1.0	-1.4	-2.4	0.4380	0.0006	0.0001
268546	Phosphoenolpyruvate carboxylase[6]	2.5	1.7	1.4	0.0010	0.0726	0.0120
		2.0	1.5	1.4	0.0140	0.0903	0.0088
		1.8	1.3	1.4	0.0021	0.0698	0.0017
		1.6[z]	1.7[z]	1.5[z]	0.0027	0.0040	0.0259

[m] Manual Annotation. [b] Supported by BlastP ($E<3x10^{-32}$). [c] Supported by conserved domains identified through Pfam. [6]Also discussed in Chapter 6. [z]Combined with another protein making fold change imprecise.

The S-adenosylhomocysteine produced by methyltransferase activity can be recycled to homocysteine through the action of adenosylhomocysteinase; this enzyme (ProtID 28496) was also found to increase by 2.6-fold in abundance with increased salinity. Adenosine is the second product of this reaction and, correspondingly, an adenosine kinase (ProtID 644), which catalyses the reversible phosphorylation of adenosine to adenosine monophosphate, increased 2.5-fold with increased salinity. This enzyme might remove adenosine, thereby promoting the activity of homocysteinase. Together the enzymes of the active methyl cycle might influence the free methionine pool in the cell and thereby its availability for DMSP synthesis under increased salinity.

The abundance of methylenetetrahydrofolate reductase (ProtID 27273) was found to increase 2- and 1.5-fold under increased salinity and light intensity respectively. This enzyme reduces 5,10-methylenetetrafolate to 5-methyltetrahydropteroyltri-L-glutamate, which donates its methyl group in synthesis of methionine from homocysteine. It has been demonstrated in the bacterium *Streptomyces lividans* that the disruption of the methylenetetrahydrofolate reductase gene leads to methionine auxotrophy (Blanco et al. 1998). The increase in methylenetetrahydrofolate reductase protein abundance indicates that this might be a limiting point in methionine synthesis and therefore DMSP production in *T. pseudonana*. However, under nitrogen starvation methylenetetrahydrofolate reductase was unchanged suggesting that a different mechanism might affect the availability of components for DMSP synthesis under this treatment.

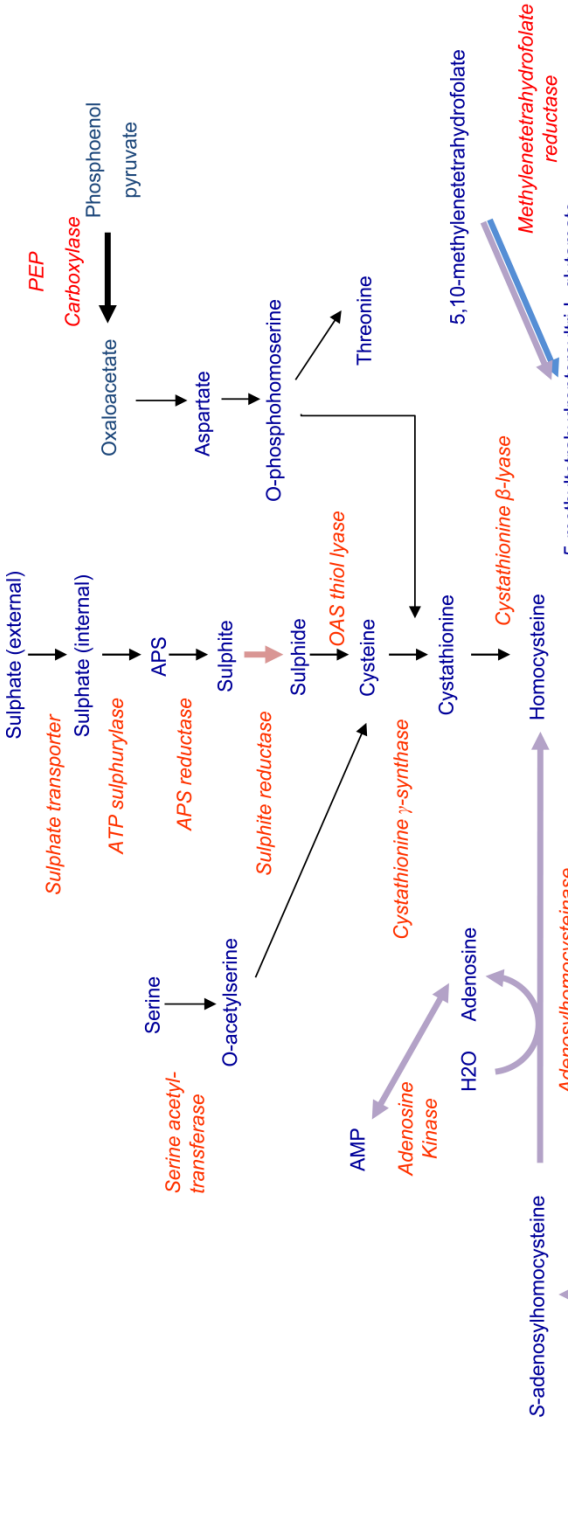

Figure 4.6. Pathway of sulphur assimilation and DMSP synthesis proposed for diatoms, showing changes in relative protein abundance , determined by 2-dimensional gel electrophoresis of *Thalassiosira pseudonana* under conditions known to increase intracellular DMSP concentration in this species. Bold arrows show proteins that increased in relative abundance, where red represents nitrogen starvation, purple represents increased salinity, blue represents increased light intensity and a bold black arrow shows that the protein abundance increased under all three treatments.

In *T. pseudonana* grown under increased light intensity five light harvesting proteins (ProtIDs 25402, 22747, 30385, 24080, 38583) and one photosystem I centre (ProtID bd1563) decreased in abundance relative to the control, which implies that photosynthetic proteins are selectively degraded. Photosystem I and II proteins are reported to be degraded under excess light and this is thought to be mediated by ROS and proteolytic activity (Hui et al. 2000; Yamamoto 2001; Zolla and Rinalducci 2002; Rajagopal et al. 2005). The degradation of photosynthetic proteins could increase the availability of amino acids such as cysteine and methionine for DMSP synthesis. Under nitrogen starvation a decrease in cellular protein level was measured and there is also evidence of increased protein catabolism (discussed further in Chapter 6.3.5), which would influence the amino acid pools in the same way.

The only enzyme found to increase in abundance by more than 1.5-fold under all three treatments that increased the intracellular DMSP concentration of *T. pseudonana* was a phosphoenolpyruvate carboxylase (PEPC; ProtID 268546), an enzyme that is best known for its involvement in C4 photosynthesis. The genomes of *T. pseudonana* and *P. tricornatum* were found to contain genes to operate this pathway suggesting that diatoms might possess C4 photosynthesis (Armbrust et al. 2004; Bowler et al. 2008). However a ^{14}C-labelling study showed considerable labelling of C4 and C3 products in *T. weissflogii*, but exclusively C3 products in *T. pseudonana* (Roberts et al. 2007). The presence of C4 enzymes in C3 plants higher plants is not unusual and C4 enzymes are known to be involved in various stress responses including, increased salinity, nutrient deficiency, and aluminium and ozone exposure, mainly through the synthesis of the TCA component malate (Doubnerová and Ryšlavá 2011). However, oxaloacetate, produced by PEPC, is also used in the synthesis of aspartate, which is a precursor of methionine. OPH, an intermediate between aspartate and methionine is the substrate of both CgS, forming cystathionine, and TS, forming threonine, and the balance of these processes is an important point of regulation in methionine synthesis in higher plants (Hesse et al. 2004). It is plausible that increased PEPC activity is a response to increased demand for aspartate and DMSP synthesis.

Finally, the protein with the greatest increase in abundance identified in this study was a branched chain aminotransferase (ProtID 260934) that increased 6.4-fold under nitrogen starvation, however it was not found to change under increased salinity or light intensity. This might be a candidate for the first step of DMSP biosynthesis of MTOB from methionine by transamination. However, further research would be required to confirm this such as substrate specificity testing and also demonstrating that over expression or silencing of the gene has an effect on DMSP synthesis. If this enzyme were found to catalyse the transamination of DMSP to MTOB this would raise questions as to why it did not increase in under increased salinity or increased light intensity.

4.3.4. What does this tell us about the regulation of DMSP production?

The lack of coordination in transcript level throughout the pathway of sulphur assimilation in these experiments could suggest that sulphur is not limiting to DMSP production in *T. pseudonana*, as it is for sulphur compounds in higher plants. This would not be entirely surprising since marine algae evolved in a very different sulphur environment to terrestrial plants (Ratti et al. 2011). The ocean is a sulphur reservoir where this nutrient is unlikely to limit productivity, whereas in terrestrial habitats sulphur availability does limit growth. The APR activities measured in *T. pseudonana* here, and in other algal species (Gao et al. 2000), are more than two orders of magnitude higher than in plants. Gao et al. (2000) suggest that these algae species have a high capacity to assimilate sulphate and may build up an intracellular stores that are used in DMSP production rather than newly assimilated sulphate.

There are, indeed, some patterns in the transcript and protein responses to the treatments that could highlight potential points of regulation other than sulphate assimilation. Interestingly, a number of these changes occurred in the branches bringing carbon and nitrogen skeletons to the central pathway of sulphur assimilation. The increased transcript levels of SAT under nitrogen starvation, increased methyltetrahydrofolate reductase protein abundance under increased salinity and light intensity, and increase PEPC protein abundance under all three growth conditions, perhaps suggests that carbon and nitrogen skeletons limit DMSP synthesis rather than sulphur. Only transcript levels

of SiR were increased under all three growth conditions suggesting that, if sulphur assimilation is regulated, this enzyme might be a key controlling point in diatoms rather than APR as in higher plants.

Perhaps most interesting is the lack of coordination in the response of the pathways to these growth conditions, each of which leads to an increase in the cellular concentration of DMSP. It is thought that DMSP has multiple functions within the cell, and indeed, in the experiments here I might consider it to be used as an osmolyte, antioxidant and perhaps as an overflow metabolite. I propose that different regulatory mechanisms, each of which leads to an increase in the methionine pool, might relate to its different roles in the cell under the different conditions. Under increased salinity the production of glycine betaine, by the methylation of glycine, might affect the methionine pool through the active methyl cycle; of which many of the enzymes were seen to increase in abundance. The increase in the abundance of methylenetetrahydrofolate reductase under increased salinity and light intensity is likely to increase 5-methyltetrahydropteroyltri-L-glutamate supply for methionine biosynthesis, thereby increasing the availability of this amino acid. Methionine availability could be increased under increased light intensity and nitrogen starvation by protein degradation. Perhaps there is not an individual limiting step or ‘on-switch’, instead under different conditions different components are limiting. This might depend on the carbon and nitrogen status of the cell, each of which will be different under these conditions.

Chapter 5. Diurnal Regulation of Sulphur Metabolism in *Thalassiosira pseudonana*

5.1. Introduction

Sulphur metabolism and photosynthesis are closely linked by the need to reduce sulphate to sulphide for incorporation into organic compounds. In all photosynthetic organisms this takes place in the plastid, with the exception of *Euglena gracilis* which locates enzymes for the reductive assimilation of sulphur in the mitochondria (Brunold and Schiff 1976; Patron et al. 2008). The reduction of sulphate to sulphide consumes approximately twice as much energy as the reduction of nitrate to ammonium, consuming 732 kJ mol^{-1} compared to 347 kJ mol^{-1} (Leustek and Saito 1999), therefore making it an important sink for energy and reducing equivalents. As with nitrogen, sulphur deficiency negatively impacts on photosynthesis in both plants and green algae (Gilbert et al. 1997; Wykoff et al. 1998). In plants sulphur assimilation is known to be tightly regulated at the steps of sulphate uptake and reduction and the activity and mRNA levels of APR, the key enzyme of this pathway, undergo a diurnal cycle and are strongly regulated by light (Kopriva et al. 1999).

Stefels (2000), however, points out that although sulphate reduction is tightly linked to cell processes by its requirement for energy and reductants, it is not necessarily 'dependent' on light and uptake of sulphate in the dark has been reported in the green alga *Dunaliella tertiolecta* (Cuhel et al. 1984). In plants sulphate reduction can occur in the plastids of roots and other heterotrophic tissues, although to a lesser extent than is found in the leaves (Hell 1997). In *A. thaliana* root APR activities are approximately 50 % lower compared to the shoots (Kopriva et al. 1999). Hell et al.

(1997) suggests that while the reduction of sulphate in the light is linked to photosynthesis by ferredoxin dependent sulphite reductase, NADPH, produced by the oxidative pentose phosphate cycle, most probably provides the reducing power for the reduction in the dark. Yeast with impaired glucose-6-phosphate dehydrogenase, the first enzyme of the pentose phosphate cycle, were found to be unable to grow on sulphate and require an organic sulphur source (Thomas et al. 1991). Therefore, the physiological state of the cell is potentially important for determining its capacity to reduce sulphate in the dark (Stefels 2000).

The link between sulphur metabolism and light is not limited to reductive assimilation. Sulpholipids are an important component of photosynthetic membranes (Benning 1998). In addition, the sulphur metabolite glutathione is essential as redox buffer and antioxidant, the latter being a function that has also been proposed for DMSP (Sunda et al. 2002). Antioxidant compounds scavenge reactive oxygen species that are by-products of photosynthesis. The alternate role proposed for DMSP as an 'overflow' sink for reducing equivalents when growth is unbalanced would also link sulphur metabolism to photosynthesis (Stefels 2000). Simó et al. (2002) found a close coupling between DMSP biosynthesis and primary production in natural assemblages and calculated that DMSP was not produced in the dark. Moreover, D. Gage (in Simó et al. 2002) suggests that the enzymes of DMSP synthesis are closely linked to photosynthesis in *E. huxleyi* and that the final stages of DMSP production might occur in the chloroplast. However, dark synthesis of DMSP has been observed in *U. lactuca* (Dickson et al. 1982) and *E. huxleyi* (Bucciarelli et al. 2007).

Based on the relationship between sulphur metabolism and light it is interesting to investigate whether diurnal patterns of variation of sulphur metabolism and DMSP production also occur in the diatom *T. pseudonana*, however there has been limited research into this basic question to date. A small number of studies on the diurnal regulation of algal sulphur metabolism have been conducted, however these have focused on specific details and a complete picture has yet to be formed. Dupont et al. (2004) measured the intracellular concentration of the thiols cysteine and

glutathione in *T. pseudonana* and *E. huxleyi*, but did not measure DMSP concentration. On the other hand, Bucciarelli et al. (2007) measured diurnal patterns of DMSP concentration in *E. huxleyi*. However, based on the large difference in intracellular DMSP concentrations between coccolithophores and diatoms, it is likely that there will be differences in its cellular role and therefore its regulation between these species. Here I have measured the concentrations of both DMSP and the thiols, cysteine and glutathione, in *T. pseudonana* through 29 h of a light:dark cycle along with APR activity. I will draw comparisons between these measurements and a parallel study on the coccolithophore *E. huxleyi*, which was conducted by Michal Bochenek (University of East Anglia and John Innes Centre, personal communication).

5.2. Methods

T. pseudonana were cultured as described in Chapter 2.1 in 1.5 L to approximately 1 x 10^6 cells ml^{-1}. Cell number and cell volume were measured every 2-3 hours over a 29 hour period, with the first samples taken at 9.00, at the onset of the light period. Samples for thiols, DMSP and APR activities were taken at these points. Descriptions of collection techniques and analysis are described in Chapter 2.7, 2.2 and 2.5. During dark sampling, care was taken to avoid exposure of the cells to light; cultures were covered in black material and minimal light was used in the room whilst sampling took place.

5.3. Results and Discussion

5.3.1. Growth Measurements

To gain insight into the regulation of sulphur metabolism in *T. pseudonana* we measured cell growth and aspects of sulphur metabolism throughout a diurnal cycle. During the light period no increase in *T. pseudonana* cell number was seen, whilst a 1.2-fold increased was observed during the dark period suggesting that the cells are dividing at night (Figure 5.1 A). This increase in cell number over the sampling period was not as great as would have been expected in cultures at this growth stage (See Figure 3.4 in Chapter 3 for an example) and it is possible that the growth rate

was affected by the high frequency of sampling during this experiment. To avoid this disturbance, in future studies the algae could be grown in a series of small cultures, three of which would be removed for each time point.

The volume per cell appears to remain stable throughout the diurnal cycle (Figure 5.1 B). Species of phytoplankton from other groups, such as the coccolithophore *E. huxleyi* are reported to gradually increase their size per cell, followed by a decrease in cell size as they divide (Bucciarelli et al. 2007). However, diatom cell size is restricted by their silica frustule encasing.

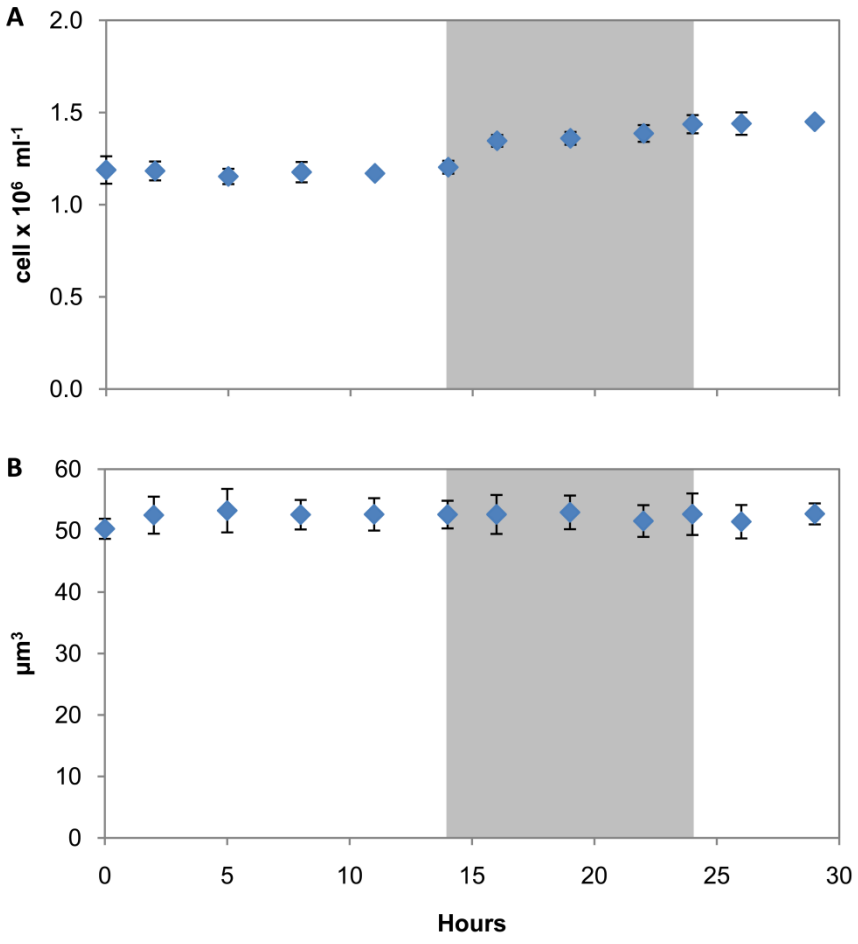

Figure 5.1. A. cell number and B. cell volume of *Thalassiosira pseudonana* through a diurnal cycle. Shaded area indicates dark period. Results are shown as means ± standard deviation from 3 independent cultures.

5.3.2. Thiols

Thiols such as cysteine and glutathione are characterised by their sulfhydryl group, which is involved in cellular redox reactions. In the present study levels of cysteine, remained low and stable in *T. pseudonana* throughout the diurnal cycle, ranging from 0.58 to 0.79 mM (Figure 5.2 A), this trend is in agreement with the findings of Dupont et al. (2004) for this species. Cysteine is central to sulphur metabolism, being the first organic compound formed by reductive assimilation, used in the synthesis of protein, methionine and glutathione and as donor of reduced sulphur for most other sulphur-containing compounds. In protein structure cysteine has a role in forming tertiary and quaternary structures through the formation of disulphide bonds between sulfhydryl groups. These can be broken by oxidation, thereby allowing redox regulation of protein activity. This strong reducing potential means that cellular levels of free cysteine are highly regulated as described in Chapter 1.3.3.2 to maintain cellular redox potential.

I also measured cellular glutathione levels in *T. pseudonana*, since it is a major sink for sulphur and has multiple roles in the cell. In agreement with the findings of Dupont et al. (2004) levels of glutathione in *T. pseudonana* exhibited clear diurnal variation, increasing during the light and decreasing during the dark ranging from 2.07 to 3.82 mM (Figure 5.2 B). This pattern has also been found in the needles of spruce trees (Schupp and Rennenberg 1988) and fits with the proposed antioxidant function of glutathione. The reducing power of glutathione can be transferred directly to ROS produced by photosynthesis or to dehydroascorbate, to regenerate ascorbate in the glutathione-ascorbate cycle, which is the primary cellular ROS scavenging mechanism. Once oxidised two glutathione molecules form the stable glutathione disulphide, therefore high levels of free glutathione can be maintained in the cell. Reduced glutathione is regenerated by the enzyme glutathione reductase. Through its control of the redox state of the cell it has been proposed that glutathione, might be involved in regulating responses to light environment. Bartoli et al. (2009) found that exposure of the bean plant *Phaseolus vulgaris* to a high ratio of red:far red, as experienced by plants in full light, resulted in higher glutathione levels than in plants exposed to a low ratio of red:far red, which replicates shaded conditions. A genetic link between glutathione and

photoreceptor signalling has also been identified in plants. An *A. thaliana* phytochrome A mutant (ars4) was found to have up to 80 % higher levels of thiols than wild type plants under arsenic and buthionine sulphoximine (BSO) exposure (Sung et al. 2007). In addition, recently a transcription factor Long Hypocotyl5, which is involved in regulation of several thousand genes by light in *A. thaliana*, controls also sulphate assimilation and glutathione synthesis (Lee et al. 2011). These antioxidant and redox-signalling functions link glutathione levels to photosynthesis and are likely to account for the diurnal pattern seen in *T. pseudonana* here. Glutathione levels have also been linked to growth and development (Foyer and Noctor 2011). It would be interesting to consider whether the diurnal variations seen in glutathione levels might be linked to cell division.

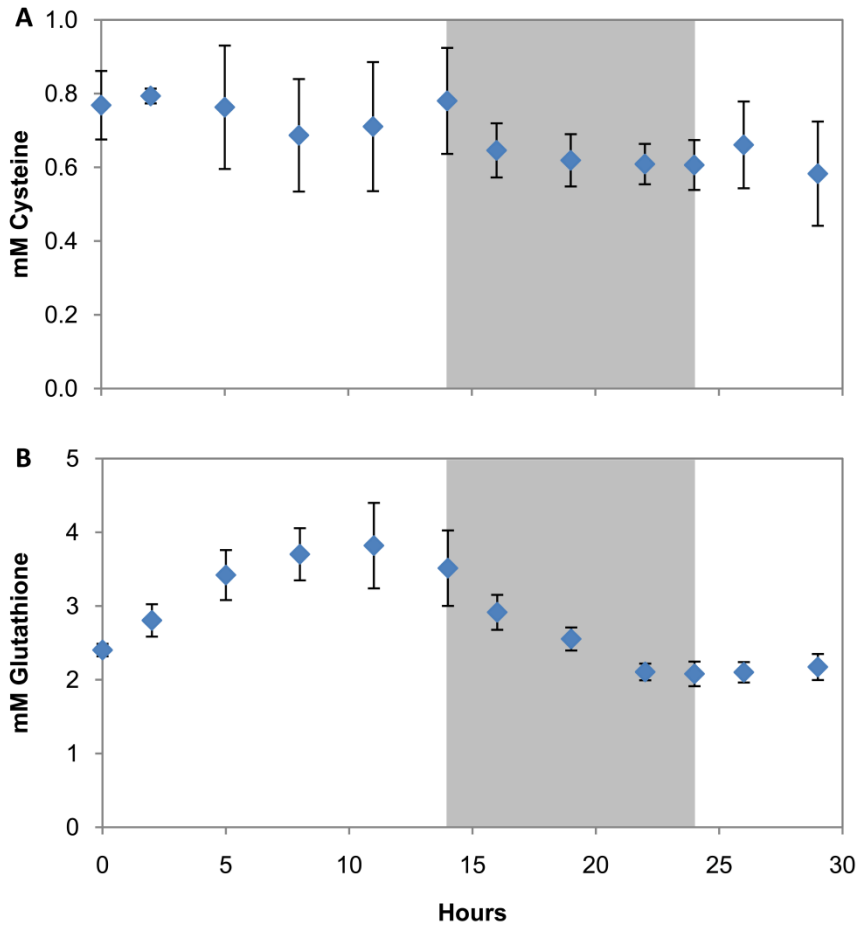

Figure 5.2. Intracellular concentration of A. cysteine and B. glutathione, quantified by HPLC analysis, in *Thalassiosira pseudonana* through a diurnal cycle. Shaded area indicates dark period. Results are shown as means ± standard deviation from 3 independent cultures.

The level of cysteine measured in *T. pseudonana* was slightly higher than reported for other organisms. Park and Imlay (2003) describe normal levels of cysteine in *E. coli* to be 0.1 to 0.2 mM and cysteine concentration in higher plants is generally 10- to 50-fold lower than glutathione (Noctor et al. 2011). In *T. pseudonana* cysteine levels were only approximately 5-fold lower than glutathione. This might be related to the additional demand on the cysteine pool due to DMSP biosynthesis, which is supported by the 1 to 2 mM cysteine levels measured in *E. huxleyi* (Michal Bochenek, University of East Anglia and John Innes Centre, personal communication) and even higher than those in *T. pseudonana*. *E. huxleyi* has a 50- fold higher intracellular DMSP concentration than *T. pseudonana* increasing thus the demand on the cysteine pool in this species. Dupont et al. (2004) reported cellular levels of cysteine in *T. pseudonana* to be approximately 10-fold lower than reported in the current study, which might be due to experimental difference. However they do describe their measurements as close to the detection limit, which could also account for the discrepancy.

The concentration of glutathione measured in *T. pseudonana* is similar to other organisms: concentrations of 2 to 4 mM were reported for *E. coli* (Park and Imlay 2003) and 1 to 5 mM for higher plants (Noctor et al. 2011). The concentration of glutathione measured in *E. huxleyi* was 4 to 7 mM (Michal Bochenek, University of East Anglia and John Innes Centre, personal communication) which is higher than that measured in *T. pseudonana*. A major difference between these species is the presence of a vacuole in the diatom. In *E. huxleyi* glutathione might act as a stable store for reduced sulphur, which is another proposed role for this compound in higher plants, so that it is available for more rapid synthesis of DMSP when required.

5.3.3. DMSP

Until now the diurnal variation of DMSP in diatoms had not been addressed. Here the intracellular DMSP concentration of *T. pseudonana* increased by 1.54-fold (t-test, $P = 0.0002$) through the light period and then remained constant during the dark phase (Figure 5.3 A). At the onset of the second light phase intracellular levels of DMSP appear to continue to increase. It is known that

intracellular DMSP levels increase through the growth curve of *T. pseudonana* (see Figure 3.4 in Chapter 3) and the increase seen during the light phase is quite comparable to that seen over 24 h. This pattern of increasing intracellular DMSP concentration in the light and lack of change during the dark suggests that cellular DMSP levels are somehow related to photosynthesis, which supports the proposed roles of antioxidant (Sunda et al. 2002) and overflow mechanism (Stefels 2000). Alternatively, this diurnal variation could suggest that reduced sulphur is limiting to DMSP synthesis in the dark or possibly that enzymes between methionine and DMSP are 'light-dependent'. The maintenance of DMSP levels during the dark is quite interesting, since levels of the known antioxidant glutathione decreased during this time.

In *E. huxleyi* DMSP per cell also varied diurnally, increasing in the light and decreasing in the dark (Michal Bochenek, University of East Anglia and John Innes Centre, personal communication, Bucciarelli et al. 2007). However, when normalised to cell volume, which has its own diurnal cycle in this species, the intracellular concentration of DMSP in the cell is stable throughout diurnal cycle. It is well known that coccolithophores maintain much higher cellular DMSP concentrations than diatoms, in the present study 200 to 250 mM was measured in *E. huxleyi* (Michal Bochenek, University of East Anglia and John Innes Centre, personal communication) compared to 4.67 to 7.4 mM in *T. pseudonana*. This high stable intracellular DMSP concentration seen in *E. huxleyi* compared to the lower and what appears to be light-induced DMSP levels in *T. pseudonana* suggests that this compound might have a different role in these two species. In coccolithophores these characteristics would fit a role as an osmolyte, whereas in diatoms the diurnal cycle suggests an antioxidant or overflow function.

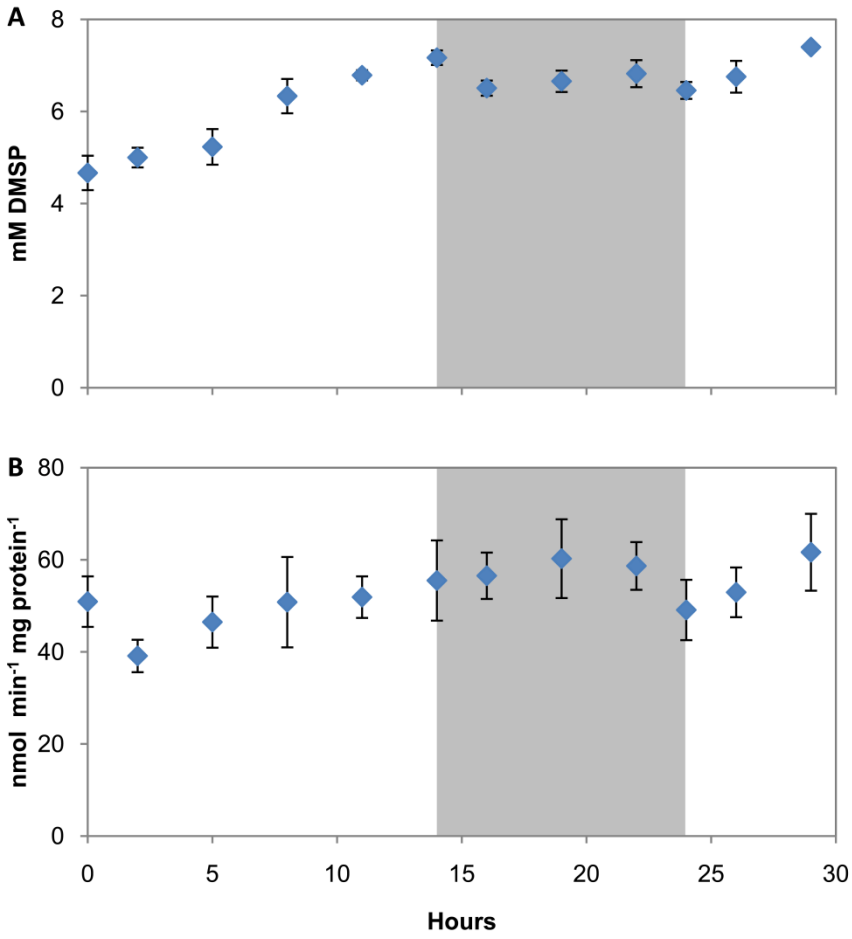

Figure 5.3. A. Intracellular DMSP concentration and B. APR activity, quantified by the production of [^{35}S]sulphide, of *Thalassiosira pseudonana* through a diurnal cycle. Shaded area indicates dark period. Results are shown as means ± standard deviation from 3 independent cultures.

5.3.4. APR

There is very limited knowledge of APR regulation in marine algae and no reports on its diurnal activity despite its key role in the regulation of sulphur metabolism in higher plants. In *T. pseudonana* I found no variation in APR activity through the diurnal cycle (Figure 5.3 B). The variation between biological replicates might hide any small pattern in activity, however, this would still not be comparable to the diurnal variation in APR activity and expression seen in higher plants. Kopriva et al. (1999) found that APR activity and mRNA levels in *A. thaliana* shoots varied approximately 2-fold over the diurnal cycle, peaking in the light phase and reaching a minimum in

the dark. APR activity is also strongly repressed on the transfer of *L. minor* from light to dark (Neuenschwander et al. 1991). This difference in the diurnal regulation of diatom and higher plant APR activity further supports the suggestion that the regulation of sulphur assimilation in diatoms is quite different to plants and that APR activity is not limiting to this pathway in *T. pseudonana*.

5.3.5. Concluding Remarks

The knowledge on regulation of sulphur-containing compounds in marine algae is fragmented and scattered with conflicting results obtained with a large variety of species. Here I have presented a comprehensive study of a single species allowing direct comparison of diurnal regulation of diverse components of sulphur metabolism. This has shown that like higher plants the levels of cysteine in the cell are kept relatively low and constant throughout the cycle, while glutathione levels are higher and exhibit diurnal regulation, increasing in the light and decreasing in the dark. In the first study on the diurnal pattern of DMSP production in a diatom, I found that this compound increased in concentration in the light and remained stable in the dark, linking its function and/or synthesis to photosynthesis. In higher plants the assimilatory enzyme APR is known to be induced by light, however I found no change in the activity of APR in *T. pseudonana* throughout this experiment and in addition to the findings of Chapter 4, this further suggests that the regulation of sulphur assimilation in diatoms might be quite different to higher plants.

Chapter 6. The Response of Diatom Central Carbon Metabolism to Nitrogen Starvation is Different to that of Green Algae and Higher Plants

This chapter has been published in Plant Physiology. Minor alterations have been made to fit with the thesis (Hockin et al. 2012). Co-authors are Gill Malin, Stanislav Kopriva, Fran Mulholland and Thomas Mock, who provided supervision and advice on this work.

6.1. Introduction

Nitrogen is an essential nutrient for all organisms and is required for the biosynthesis of macromolecules, such as proteins, nucleic acids and chlorophyll. The availability of nitrogen in the ocean varies dramatically on spatial and temporal scales due to physical and biological processes. As for terrestrial plants, nitrogen is a major limiting nutrient for primary production in the ocean, with consequences for marine food webs (Falkowski 1997).

Diatoms, characterised by their silica frustules, are a key group of the eukaryotic phytoplankton and are found throughout the world's oceans from polar to tropical latitudes. This group is particularly successful in upwelling environments, where they are able to rapidly respond to nitrate influx and out-compete other marine phytoplankton while this nutrient and silicate are abundant (Estrada and Blasco 1979). As much as 20 % of global net primary productivity can be accounted for by diatoms, which is more than of all terrestrial rainforests combined (Nelson et al. 1995; Field et al. 1998), and the sheer magnitude of their productivity in upwelling regions provides the basis

of short, energy-efficient food webs that support large scale coastal fisheries (Mann 1993). Diatoms are also important contributors to biological carbon pump that draws carbon down into the deep ocean through the settling of cells.

Diatoms belong to the heterokont algae, which arose from a secondary endosymbiotic event when a photosynthetic eukaryote, thought to be a red alga, became associated with a heterotrophic eukaryote (Falkowski et al. 2004a). The chloroplast that was formed differs from that of primary endosymbionts, such as plants and green algae, by the presence of four membrane layers (Gibbs 1981). The pathway of nitrate assimilation in diatoms is comparable to that of other eukaryotic photoautotrophs (Armbrust et al. 2004; Bowler et al. 2008) and there is evidence that some elements are of endosymbiont origin (Bowler et al. 2010).

Nitrate is taken up into the diatom cell, where it is first reduced to nitrite by a cytosolic NADH-dependent nitrate reductase (NR) (Gao et al. 1993; Berges and Harrison 1995; Allen et al. 2005). Nitrite is then transported into the chloroplast and further reduced to ammonium by a cyanobacterial-like ferredoxin-dependent nitrite reductase (Fd-NiR) (Milligan and Harrison 2000; Bowler et al. 2010). The joint action of glutamine synthetase (GS) and glutamate synthase (GOGAT) is thought to be the main route of ammonium assimilation into amino acids and other nitrogenous compounds (Dortch et al. 1979; Clayton and Ahmed 1986). Diatoms possess a plastid localised glutamine synthetase II (GSII) that is of red algal origin (Robertson et al. 1999; Robertson and Tartar 2006; Siaut et al. 2007) and thought to be responsible for the assimilation of ammonium produced by nitrate reduction. Transcript levels of *glnII* (encoding GSII) are higher in diatom cells assimilating nitrate than in those assimilating ammonium directly (Takabayashi et al. 2005). Diatoms also appear to have an NAD(P)H-dependent (NAD(P)H-GOGAT) and a plastid localised ferredoxin-dependent (Fd-GOGAT) form of glutamate synthase (Clayton and Ahmed 1986; Zadykowicz and Robertson 2005), however our knowledge on this enzyme is limited. The activity of the GS/GOGAT cycle requires input of carbon skeletons in the form of 2-oxoglutarate, while oxaloacetate is also important in the production of amino acids. These are both intermediates of the

tricarboxylic acid (TCA) cycle and provide an important link between nitrogen assimilation and carbon metabolism.

A number of bacterial genes have been identified in diatom genomes (Armbrust et al. 2004; Bowler et al. 2008) and these are thought to have been acquired by horizontal transfer (Allen et al. 2006). They include a cytosolic NAD(P)H-dependent nitrite reductase (NAD(P)H-NiR) which is homologous to nirB of bacteria and fungi, along with a mitochondrial glutamine synthetase III (GSIII) (Robertson and Alberte 1996; Armbrust et al. 2004; Allen et al. 2006; Siaut et al. 2007). Neither of these enzymes has been found in green algae or plants. Genome projects have also revealed that diatoms possess a full urea cycle (Armbrust et al. 2004; Bowler et al. 2008), which had not been found previously in eukaryotes outside the Metazoans. This pathway is thought to be involved in mobilising nitrogen and carbon produced by cell processes back into central metabolism (Allen et al. 2006). The presence of further bacterial-like genes in the diatom genome, such as an ornithine cyclodeaminase, which catalyses the conversion of ornithine to proline in arginine degradation, might expand the function of the urea cycle (Bowler et al. 2010).

Diatoms have an evolutionary history, which is distinct from plants and green algae and this has brought together a unique combination of genes, providing the potential for novel biochemical processes in this group. Although genome and proteome studies offer clues as to the success of diatoms (Armbrust et al. 2004; Bowler et al. 2008; Nunn et al. 2009), further investigation is now required to understand the adaptive responses of diatoms to dynamic environmental conditions such as nutrient availability.

Here we compare the proteome of the diatom *T. pseudonana* (CCMP 1335) at the onset of nitrogen starvation to that of nitrogen replete cells with the aim of gaining insight into the global regulation of metabolic pathways in response to nitrogen starvation. We assess our dataset alongside the results of a whole genome tiling-array analysis of *T. pseudonana* (CCMP 1335) in which the response to a comparable nitrogen starved condition was measured in a study of biosilification

(Mock et al. 2008). This enables us to obtain a more detailed picture of the processes affected by nitrogen starvation in diatoms, and also gain insight into the levels of their regulation. In addition, through comparison of our findings to higher plants, green algae and cyanobacteria, we demonstrate that the distinct evolutionary history of the diatoms has resulted in a fundamentally different metabolic response to nitrogen starvation compared to other eukaryotic photoautotrophs studied to date.

6.2. Methods

Preliminary tests showed that when *T. pseudonana* cultures with an initial concentration of 550 µM nitrate were still in logarithmic growth cultures started with 30 µM nitrate were yield-limited at ca. $1x10^6$ cell ml^{-1}. Hence, triplicate cultures were started with initial concentrations of 550 µM nitrate (standard ESAW) or 30 µM nitrate. Samples were taken as low nitrate cultures reached the onset of nitrogen starvation (around $1x10^6$ cell ml^{-1}) to measure amino acids and cellular nitrate and to access changes in relative protein abundance by 2-dimensional gel electrophoresis (methods for which are detailed in Chapter 2).

6.3. Results and Discussion

6.3.1. Physiological Effects of Nitrogen Deprivation

The onset of nitrogen starvation in *T. pseudonana* cultures grown with an initial nitrate concentration of 30 µM was identified by comparing daily cell counts and Fv/Fm values to nitrogen replete cultures grown with an initial nitrate concentration of 550 µM (Chapter 3, figure 3.8). Cultures grown with 30 µM nitrate were yield-limited by nitrogen availability at a maximum density of ca. 1×10^6 cell ml^{-1} on day 4 of the experiment, whereas cultures with 550 µM nitrate continued to grow to ca. 3×10^6 cell ml^{-1}. From day 3 to 5 the growth rate of low nitrate cultures was 0.21 compared to a growth rate of 0.51 in the nitrogen replete control cultures. The efficiency of photosystem II (Fv/Fm) of the low nitrate cultures decreased as growth became yield-limited.

Fv/Fm was 0.57 in low nitrate cultures on day 4 compared to 0.63 in the nitrogen replete cultures and continued to decline, relative to that of nitrogen replete cultures, throughout the experiment.

Intracellular levels of nitrogenous molecules, such as free nitrate, amino acids and protein give a good indication of the nitrogen status of the cell. As the growth of the low nitrate cultures became yield-limited (day 4), levels of free nitrate and free amino acids were 3-fold lower than in the nitrogen replete control cultures (Figure 6.1) and protein content was 2.2-fold lower. For the purpose of this study this point is considered to be the onset of nitrogen starvation.

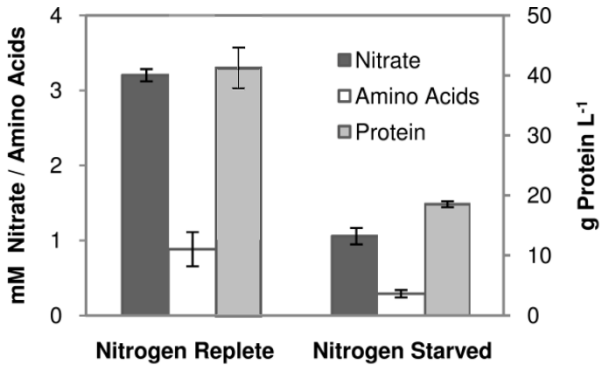

Figure 6.1. Intracellular concentration of free nitrate, amino acids, and protein in nitrogen replete (550 µM nitrate) and nitrogen starved (30 µM nitrate*) Thalassiosira pseudonana* cultures at the onset of nitrogen starvation. Results are shown as means of 3 biological replicates ± standard deviation.

6.3.2. Proteome Comparison

Proteins are the biochemically active components that define the flux through metabolic pathways. Therefore, monitoring changes in their abundance provides good insight into how the cell is adapting to a specific condition. Here the proteomes of *T. pseudonana* cultures at the onset of nitrogen starvation were compared to those of nitrogen replete cultures using 2-dimensional gel electrophoresis (Figure 6.2).

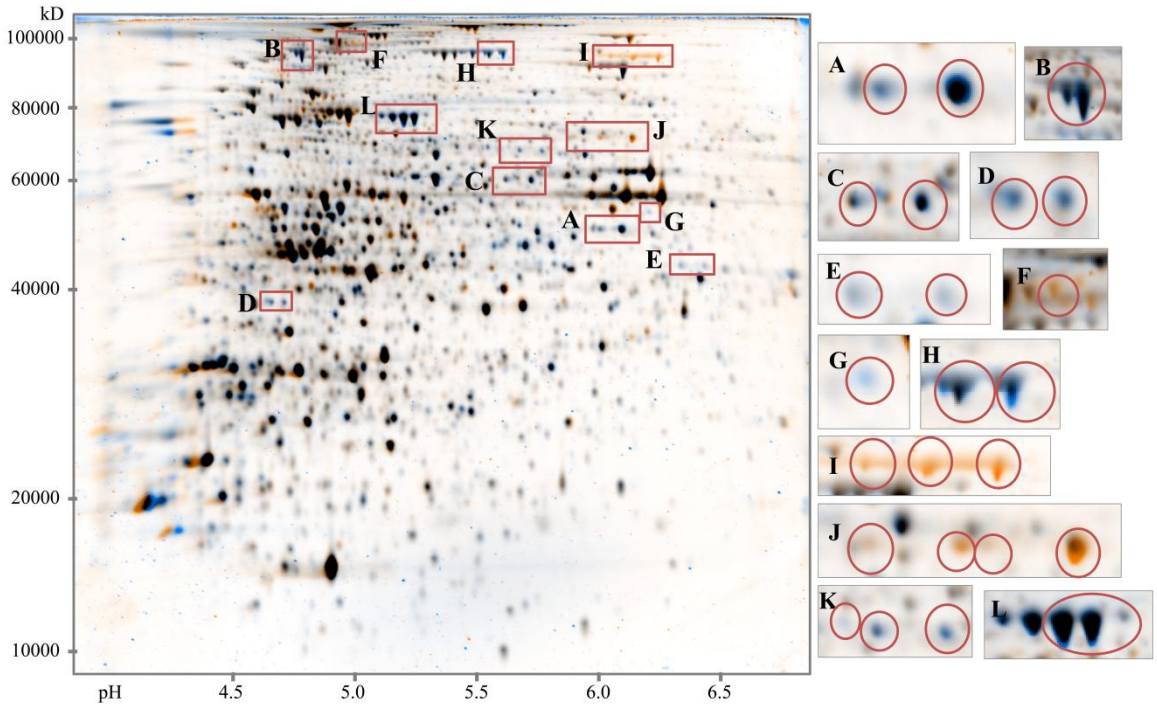

Figure 6.2. Effect of nitrogen starvation on the proteome of *Thalassiosira pseudonana*. Soluble proteins were isolated from *T. pseudonana* cultures grown in nitrogen replete (550 µM nitrate) and nitrogen starved (30 µM nitrate) conditions and resolved by 2-D electrophoresis. Gels of three biological replicates were used for quantitative analysis and for this illustration representative gels from each treatment were overlaid. Equal protein abundance is represented by black spots, blue spots represent proteins more abundant in N starved cells while orange represents proteins more abundant in N replete cells. Examples of proteins of interest (A-L) are expanded. A. Citrate synthase (ProtID 11411). B. Aconitase hydratase (ProtID 268965). C. Isocitrate dehydrogenase (ProtID 21640). D. Pyruvate dehydrogenase (ProtID 8778). E. Pyruvate dehydrogenase (ProtID 268374). F. NADPH-dependent nitrite reductase (ProtID 26941). G. Branched-chain aminotransferase (ProtID 260934). H. Phosphoenolpyruvate carboxylase (ProtID 268546). I. Nitrate reductase (ProtID 25299). J. Ferredoxin-dependent nitrite reductase (ProtID 262125). K. NAD(P)H-dependent glutamate synthase (ProtID 269160). L. Type III glutamine synthetase (ProtID 270138).

Following filtering to remove speckling and background 3310 distinct protein spots were detected and taken for further analysis, of which 140 spots had a greater than 1.5-fold increase or decrease in relative abundance between the two treatments ($P<0.005$, based on t-test). These were picked from the gel and their MALDI-TOF MS analysis after trypsin digestion resulted in the identification of 65 proteins, of which 42 were increased and 23 decreased at the onset of nitrogen starvation (listed in appendix table 1). It should be noted that the lack of identification of a specific

protein does not prove its stable abundance under the growth conditions tested and there are a number of reasons why a regulated protein might not have been identified. For example 2-dimensional gels are not optimised for membrane bound proteins and very low abundance proteins might also not be detected. Also if the protein mass or isoelectric point (pI) were outside the range of the gel the protein would not be seen. While a broader pH range was tested (data not shown), we found that pH 4-7 gave the best spot separation and the maximum number of spots detected (Figure 6.2).

6.3.3. Functional Characterisation of Proteins

We were interested in the biological significance of changes in relative protein abundance associated with the onset of nitrogen starvation and proteins were therefore grouped according to the KEGG (Kyoto Encyclopaedia of Genes and Genomes) categorisation (Figure 6.3). Proteins involved in nitrogen and protein metabolism decreased in abundance along with those of photosynthesis and chlorophyll biosynthesis. Carbohydrate and amino acid metabolism were highly represented in both the increasing and decreasing groups of proteins, making these processes potentially important in the adaptation of the cells to nitrogen starvation.

In an independent study on diatom silicon processing Mock et al. (2008) compared the transcriptomes of the same *T. pseudonana* isolate grown under comparable, nitrogen starved and control, growth conditions by whole-genome tiling array. By assigning the same KEGG categorisation as described above to differentially regulated transcripts (fold change > 2, $P < 0.05$) we demonstrate that the functional categories represented by differentially regulated transcripts (Mock et al. 2008) are similar to those of the proteins described in the present study (Figure 6.3).

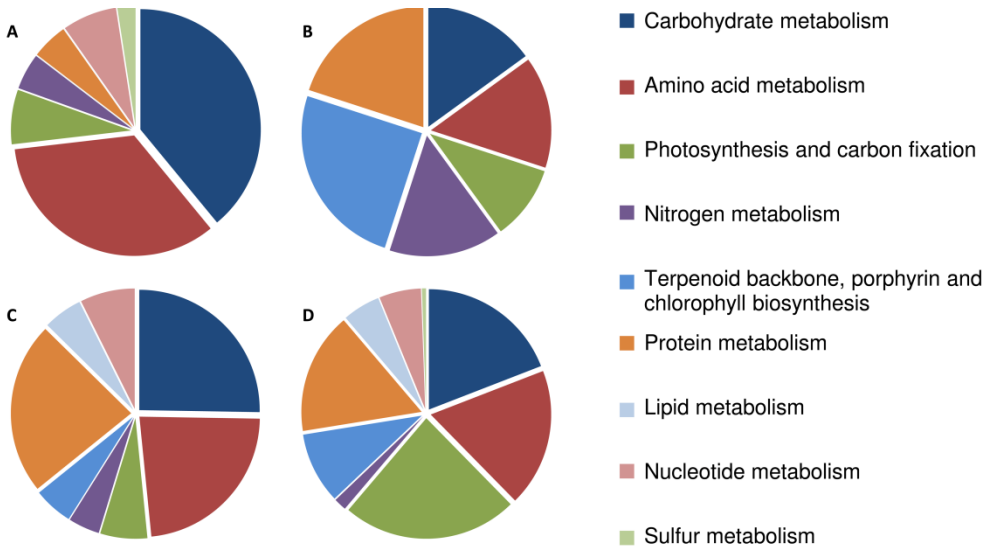

Figure 6.3. Categories of genes and proteins altered in expression between nitrogen starved and replete *Thalassiosira pseudonana* cells. Categorisation is based on KEGG, some categories were split to subcategories to illustrate points of specific interest, whereas categories that were under represented were merged with related groups. A. Proteins increased in abundance under nitrogen starvation. Of 42 proteins increasing in abundance 32 could be assigned a function, of which 4 are not represented by this categorisation. B. Proteins decreased in abundance under nitrogen starvation. From 23 proteins decreased in abundance, 18 could be assigned a function. C. Transcripts more highly expressed in nitrogen starved cells (Mock et al. 2008). Of 305 transcripts that increased in abundance 101 could be assigned a function, of which 23 are not represented. D. Transcripts decreased in expression in nitrogen starved cells. 362 transcripts decreased in abundance and 167 were assigned a function, of which 27 are not represented.

6.3.4. Nitrogen Assimilation

Proteins involved in the reduction of nitrate and nitrite to ammonium, such as NR (ProtID 25299), NADPH-NiR (ProtID 26941) and Fd-NiR (ProtID 262125) decreased by 2.5- to 9.5-fold in abundance in *T. pseudonana* at the onset of nitrogen starvation (Figure 6.4; table 6.1). Mock et al. (2008), however, detected no change in the transcript levels of genes encoding these proteins under comparable growth conditions, indicating post-transcriptional regulation of protein accumulation. Indeed, NR is known to be under multiple levels of regulation in diatoms as in other photosynthetic eukaryotes (Parker and Armbrust 2005). Using GFP fused promoter and terminator elements, it has been demonstrated that the transcription of *nia* (encoding NR) is maintained under nitrogen limited

conditions in the diatom *C. fusiformis*, but that nitrate is required for its translation (Poulsen and Kroger 2005). The decreased abundances of Fd- and NAD(P)H-NiR and the lack of change in transcript levels of the corresponding genes implies that they might be under similar regulation.

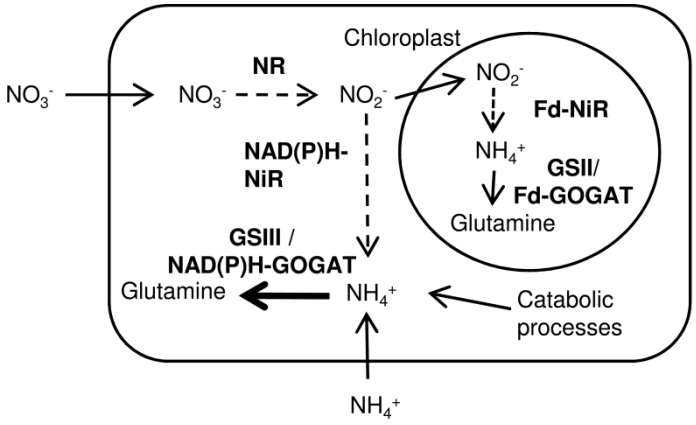

Figure 6.4. Representation of the changes in the abundance of proteins associated with nitrogen assimilation in *Thalassiosira pseudonana*, brought on by the onset of nitrogen starvation. Increases are shown by bold arrows and decreases by dashed arrows.

Despite a decrease in the abundance of proteins for nitrate and nitrite reduction, members of the GS/GOGAT cycle increased in abundance. We measured a 1.6- and 2.2-fold increase in GSIII (ProtID 270138) and NAD(P)H-GOGAT (ProtID 269160) abundance respectively. GSIII is not thought to contribute to the assimilation of ammonium derived from nitrate reduction since *glnN* (encoding GSIII) does not follow the diurnal expression pattern of genes involved in nitrate assimilation (NR, Fd-NiR and GSII) in the diatom *S. costatum* (Brown et al. 2009). Interestingly, GSIII is also induced in the cyanobacterium *Synechococcus* during the early stages of nitrogen deprivation (Sauer et al. 2000). In addition, Mock et al. (2008) measured increased transcript levels of two NAD(P)H-GOGAT genes (ProtIDs 29861 and 269160) along with a ferredoxin-dependent form of this enzyme (ProtID 269900). Increased capacity for ammonium assimilation thus appears to be important in the response of *T. pseudonana* to nitrogen starvation.

Table 6.1. Proteins involved in nitrogen, protein and amino acid metabolism with a greater than 1.5 fold change (P<0.05) in *Thalassiosira pseudonana* at the onset of nitrogen starvation, compared to nitrogen replete cultures. Values are based on three biological replicates. Protein name is based on UniProtKB unless otherwise stated and Protein IDs are from the Joint Genome Institute *T. pseudonana* genome version 3 (http://genome.jgi-psf.org/Thaps3/Thaps3.home.html).

Protein ID	Protein Name	Fold Change	p	Microarray Log2
Nitrogen Assimilation				
25299	Nitrate reductase[mbc]	-10.72 -9.69 -8.81	0.00001 0.00002 0.00005	ND
26941	NADPH nitrite reductase	-3.01	0.00012	ND
262125	Nitrite reductase-ferredoxin dependent	-3.67 -3.04 -1.95 -1.71	0.00010 0.00001 0.00095 0.00108	ND
269160	Glutamate Synthase	2.93 1.80 1.74	0.00124 0.00310 0.00031	1.71
270138	Glutamine synthetase type III [mbc]	1.63 1.61 1.51	0.00090 0.00233 0.00063	ND
Amino Acid Metabolism				
260934	Branched-chain-amino-acid aminotransferase	6.39	0.00008	3.08
28544	Dihydrodipicolinate reductase[mbc]	1.62	0.00211	1.48
25130	D-isomer specific 2-hydroxyacid dehydrogenase[mbc]	-1.73	0.00214	ND
23175	Acetolactate synthase[mb]	-1.97	0.00478	ND
22208	Class V aminotransferase[mbc]	1.86	0.00203	- 2.56
bd1806[l]	DegT/DnrJ/EryC1/StrS aminotransferase[mbc]	1.67 -2.26	0.00156 0.00001	ND
Protein Metabolism				
21235	S1 ribosomal protein[mc]	-2.01	0.00054	ND
15259	S1 ribosomal protein	-3.36 -2.93	0.00002 0.00137	ND
31912	Peptidyl-prolyl cis-trans isomerase	1.65	0.00463	ND
13254	RNA helicase	-2.28	0.00115	ND
269148	Translation factor tu domain 2	-1.94 -1.66	0.00266 0.00500	ND
15093	Serine carboxypeptidase	2.03	0.00093	1.1
Urea Cycle and Arginine Metabolism				
270136	N-acetylornithine aminotransferase	2.37	0.00006	1.77
21290	N-acetyl-gamma-glutamyl-phosphate reductase	1.74	0.00048	ND
30193	Urease	1.62[z]	0.00271	ND

[m] Manual Annotation. [b] Supported by BlastP ($E<1x10^{-50}$). [c] Supported by conserved domains identified through Pfam. [l] Location: bd_10x65:12123-13902. [z] Combined with another protein, making fold change imprecise.

There has been limited research into diatom GOGAT isoforms, but it seems possible that NAD(P)H-GOGAT and GSIII might act together in the assimilation of ammonium produced by cellular processes, such as protein catabolism under this growth condition.

Diatoms possess a complete urea cycle, which may allow more efficient use of alternative nitrogen sources taken up and produced by cellular processes. The increased abundance of a urease (ProtID 30193) seen in the present study, could enable the cell to use urea as a nitrogen source in a reaction that yields ammonium. However, this protein spot coincided with another protein in the gel making it impossible to calculate an accurate fold-change. Mock et al. (2008) also found decreased transcript levels of a carbamoyl phosphate synthase (ProtID 40323), which directs ammonium into the urea cycle (Mock et al. 2008). A urea transporter (ProtID 24250) and an amino acid transporter (ProtID 262236) also increased in transcript level, suggesting that *T. pseudonana* increases its capacity to take up these alternative forms of nitrogen when nitrate availability is limited. Any source of intra- or extracellular nitrogen must first be converted to ammonium before assimilation to amino acids and other nitrogenous compounds. This may explain why although nitrate assimilation decreases at the onset of nitrogen starvation, ammonium assimilation remains important.

6.3.5. Protein and Amino Acid Metabolism

There is evidence for the remobilisation and redistribution of intracellular nitrogen in *T. pseudonana* at the onset of nitrogen starvation. The cellular protein content of *T. pseudonana* decreased and correspondingly, the abundance of two ribosomal proteins (ProtIDs 21235 and 15259) and a translation factor (ProtID 269148) decreased by 1.8- to 3.1-fold in abundance, suggesting that protein biosynthesis was decreased. Mock et al. (2008) found that the transcript levels of a number of aminoacyl-tRNA synthetases, which bind specific amino acids to be added to the polypeptide chain by the ribosome, decreased under nitrogen starvation in this species. Protein degradation may also be increased given that a serine carboxypeptidase (ProtID 15093) increased 2-fold in protein abundance, and transcript levels for this gene and a further three proteases

(ProtIDs 16390, 17687 and 38360) also increased (Mock et al. 2008). On the other hand, four other proteases (ProtIDs 29314, 866, 1738 and 31930) decreased in transcript level (Mock et al. 2008); this may be a response to the reduced protein content of the cell or alternatively differential expression of proteases, with different substrate specificities, may play a regulatory role in the response of *T. pseudonana* to nitrogen starvation.

While the total free amino acid content of *T. pseudonana* decreased at the onset of nitrogen starvation the abundance of individual amino acids showed different responses to this growth condition (Figure 6.5). The steady-state levels of many amino acids decreased; notably the most abundant members such as glutamate, histidine, aspartate and serine decreased by 2.9- to 22.8-fold, contributing substantially to the decrease of total amino acids seen. On the other hand, leucine, cysteine, isoleucine and valine increased by 2.1- to 5.4-fold.

Correspondingly, the proteomics and transcriptomics analyses provide evidence for increased amino acid catabolism; the most highly increased protein in the current study was a branched chain aminotransferase (ProtID 260934) which changed 6.4-fold. This enzyme catalyses the first step in the degradation of the amino acids valine, leucine and isoleucine. Transcript levels of this gene and one other branched chain aminotransferase (ProtID 20816) also increased (Mock et al. 2008). Valine, leucine and isoleucine degradation proceeds via a number of oxidation steps, ultimately yielding the TCA cycle intermediates acetyl- or succinyl CoA. The transcript levels of an alpha-keto acid dehydrogenase complex (ProtIDs 795, 32067 and 36291), and a short-chain acyl-CoA dehydrogenase (ProtID 269127) that catalyse steps of this pathway, also increased (Mock et al. 2008). The increased intracellular valine, leucine and isoleucine levels in *T. pseudonana* at the onset of nitrogen starvation could be responsible for triggering the up-regulation of genes encoding enzymes catalysing their degradation.

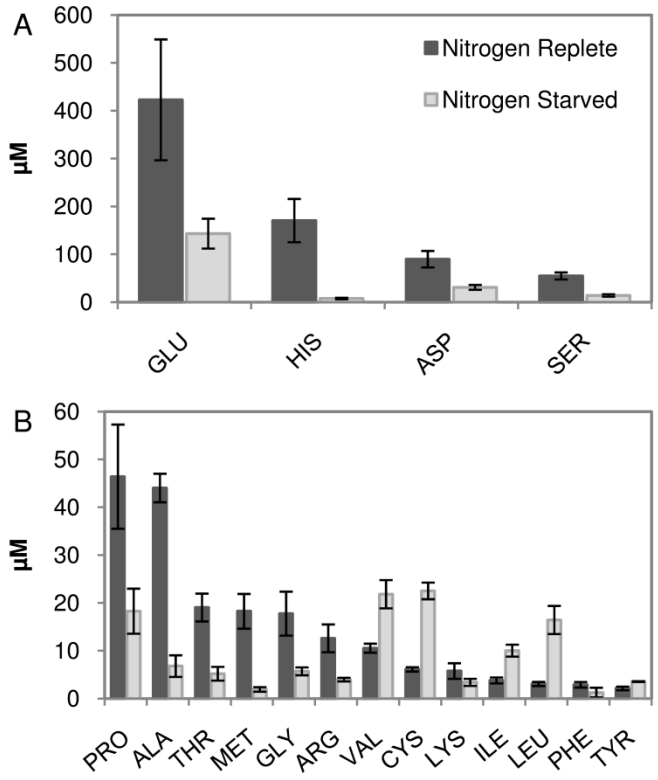

Figure 6.5. Intracellular concentration of individual amino acids in nitrogen replete (550 µM nitrate) and nitrogen starved (30 µM nitrate) *Thalassiosira pseudonana* cells. A. The most abundant and B. the least abundant amino acids were determined by HPLC. Results are shown as means of 3 biological replicates ± standard deviation.

A class V aminotransferase (ProtID 22208), which may be involved in amino acid degradation, increased 1.9-fold in protein abundance. However, the transcript level of this gene decreased, as did a number of others involved in amino acid catabolism, including genes involved in glycine, serine and threonine metabolism and degradation (Mock et al. 2008). The cellular content of these amino acids decreased 3- to 4-fold at the onset of nitrogen starvation and may have reached such a level that transcription of genes involved in their degradation had ceased. The degradation of proteins and amino acids produces ammonium, which might be reassimilated by GS/GOGAT enzymes, as discussed above. Various carbon skeletons, many of which are also TCA cycle intermediates are also produced by this process (Figure 6.6).

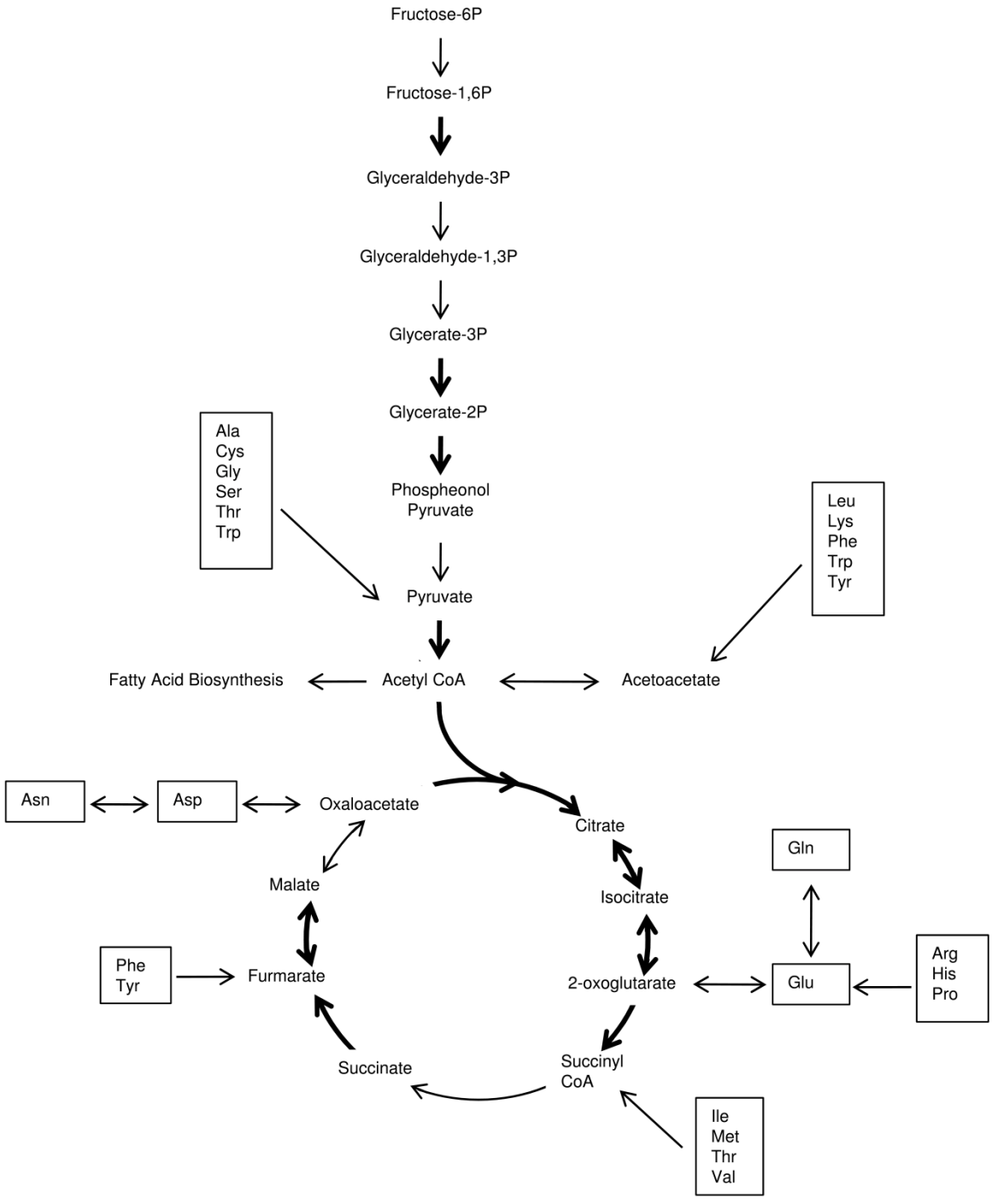

Figure 6.6. Representation of the changes in the abundance of proteins associated with carbon metabolism in *Thalassiosira pseudonana* at the onset of nitrogen starvation. Increases are shown by bold arrows and no decreases were seen. Boxes show where carbon skeletons from amino acid degradation feed into the pathway.

It is noteworthy that intracellular levels of the amino acid proline decreased 2.5-fold in *T. pseudonana* at the onset of nitrogen starvation, since this is a major osmolyte in some marine diatoms (Dickson and Kirst 1987). As discussed in Chapter 4, we measured a 2.6-fold increase in intracellular DMSP, from 1.6 mM in nitrogen replete *T. pseudonana* cultures to 4.3 mM in cultures at the onset of nitrogen starvation. In addition to being the precursor of the environmentally important volatile sulphur compound, dimethylsulphide, DMSP is a compatible solute that does not contain nitrogen and Andreae (1986) suggested that it might replace nitrogen-containing osmolytes under nitrogen deprivation. Keller et al. (1999) also found that DMSP increased in *T. pseudonana* under nitrogen limited conditions, whilst the nitrogenous osmolytes including glycine betaine and amino acids were depleted. The proteins involved in the DMSP biosynthesis pathway have yet to be identified, although it is thought that the first step involves the transamination of methionine, to yield the 2-oxo acid 4-methylthio-2-oxobutyrate (MTOB) (Gage et al. 1997). As discussed above, we identified a branched chain aminotransferase (ProtID 260934) as the most highly increased protein at the onset of nitrogen starvation and this may therefore be a candidate for the enzyme catalysing this step.

6.3.6. Photosynthesis

The down-regulation of photosynthesis is a universal response to nitrogen starvation among photosynthetic eukaryotes and accordingly we measured a reduction in the efficiency of photosystem II (Fv/Fm) in *T. pseudonana* under this growth condition. Carbon and nitrogen metabolism are closely linked, since the assimilation of nitrate to amino acids and nitrogenous compounds is an energy consuming process that requires reducing equivalents and carbon skeletons. Reduced nitrate assimilation causes excess of these components to accumulate, and the resultant metabolic imbalance leads to increased oxidative stress (Logan et al. 1999). Furthermore, photosynthetic carbon fixation is a nitrogen demanding process and nitrogen starvation could therefore disrupt the flow of electrons though the photosynthetic apparatus, causing increased production of reactive oxygen species (ROS) and thus oxidative stress.

Table 6.2. Proteins involved in photosynthesis and carbon metabolism that had a greater than 1.5 fold change ($P < 0.05$) in *T. pseudonana* at the onset of nitrogen starvation, compared to nitrogen replete cultures. Values are based on three biological replicates Protein name is based on UniProtKB unless otherwise stated and Protein IDs are from the Joint Genome Institute *Thalassiosira pseudonana* genome version 3 (http://genome.jgi-psf.org/Thaps3/Thaps3.home.html).

Protein ID	Protein Name	Fold Change	t-test (P)	Microarray Log2
Chlorophyll Biosynthesis				
258111	Glutamate-1-semialdehyde aminotransferase[mb]	-1.61	0.00469	ND
270378	Magnesium-protoporphyrin IX methyltransferase[mbc]	-2.69	0.00013	ND
270312	1-deoxy-D-xylulose-5-phosphate synthase[mbc]	-2.14	0.00043	ND
29228	1-hydroxy-2-methyl-2-(E)-butenyl-4-diphosphate synthase[mbc]	-1.98	0.00050	ND
10234	Geranyl-geranyl reductase[mb]	-2.33 -1.92	0.00059 0.00248	-3.98
Antioxidant				
40713	Superoxide dismutase	1.89	0.00307	ND
38428	Mitochondrial alternative oxidase	2.24	0.00106	ND
Glycolysis and Gluconeogenesis				
40391	Enolase	1.52	0.00249	1.83
27850	Phosphoglycerate mutase	1.83	0.00241	2.99
270288	Fructose-bisphosphate aldolase[mbc]	1.83 1.80 1.72	0.00056 0.00356 0.00188	ND
31636	Aldose-1-epimerase	-2.37	0.00106	-1.57
26678	Transketolase	1.63	0.00254	ND
21175	Transketolase	-1.55	0.00450	-5.62
22301	Phosphomannomutase	1.68	0.00040	ND
Pyruvate Metabolism				
268546	Phosphoenolpyruvate carboxylase	2.53 2.52 1.79 1.62[z]	0.00104 0.00013 0.00206 0.00271	ND
268374	Pyruvate dehydrogenase	2.27 1.78	0.00218 0.00077	2.49
8778	Pyruvate dehydrogenase	2.09 1.76	0.00013 0.00004	2.99
268280	Dihydrolipoamide s-acetyltransferase	1.95	0.00064	ND
TCA Cycle				
11411	Citrate synthase	2.24 1.76	0.00429 0.00037	2.09
268965	Aconitase hydratase 2	1.70 1.62	0.00069 0.00089	1.96
1456	Isocitrate Dehydrogenase	1.62	0.00354	-1.38
21640	Isocitrate dehydrogenase[mbc]	1.66 1.53	0.00015 0.00418	1.73
42475	Succinate dehydrogenase flavoprotein subunit	1.89 1.79	0.00417 0.00196	ND
22464	Furmarate hydratase	2.49	0.00014	ND

[m] Manual Annotation. [b] Supported by BlastP ($E<1x10^{-50}$). [c] Supported by conserved domains identified through Pfam. [z] Combined with another protein, making fold change imprecise.

Chlorophyll is a nitrogenous macromolecule and reducing its synthesis reduces the nitrogen demand of the cells and also diminishes the light capturing capacity and ROS production. Therefore it is not surprising that five proteins involved in the synthesis of chlorophyll and its precursors decreased by 1.5- to 2.5-fold in abundance under nitrogen starvation; including a geranyl geranyl reductase (ProtID 10234), which has been shown to catalyse a critical step in chlorophyll synthesis in vascular plants (Tanaka et al. 1999). Transcript levels of six genes involved in chlorophyll biosynthesis (ProtIDs 32201, 26573, 32431, 5077, 262279 and 31012) were also found to decrease (Mock et al. 2008) and reduced chlorophyll content (Mock and Kroon 2002) and chlorophyll degradation (D. Franklin, personal communication) have previously been measured in *T. pseudonana* under nitrogen starvation.

In agreement with increased oxidative stress, a superoxide dismutase (ProtID 40713) and a mitochondrial alternative oxidase (ProtID 38428) both increased approximately 2.2-fold. The increase of intracellular levels of DMSP in *T. pseudonana* under nitrogen starvation might also be linked to oxidative stress. In addition to its role as a compatible solute DMSP is thought to be part of a cellular antioxidant system (Sunda et al. 2002) and its synthesis might dissipate excess energy, carbon and reducing equivalents under nutrient limited conditions (Stefels 2000).

6.3.7. Carbon Metabolism

Reduced demand for carbon skeletons in nitrogen assimilation along with the production of carbon skeletons from catabolic processes, as described above, are expected to impact on central carbon metabolism. In fact, in the proteome comparison we see evidence for increased glycolytic activity in *T. pseudonana* at the onset of nitrogen starvation that would direct carbon from intracellular carbohydrate stores to central carbon metabolism. The abundance of a phosphoglycerate mutase (ProtID 27850), enolase (ProtID 40391) and fructose-1,6-bisphosphate aldolase (ProtID 270288) increased by 1.5- to 2.9-fold (Figure 6.6). Although these enzymes can also catalyse the reverse reactions of gluconeogenesis, transcript levels of a phosphofructokinase (ProtID 31232) and two pyruvate kinase genes (ProtIDs 22345 and 40393) also increased, while one pyruvate kinase

(ProtID 4875) decreased (Mock et al. 2008). These enzymes are specific to glycolysis, indicating that this is the direction of carbon flow.

Pyruvate, the product of glycolysis, can be converted to acetyl CoA through the activity of the multi-enzyme complex pyruvate dehydrogenase. In our study the protein abundance of three subunits of this complex (ProtIDs 268374, 8778 and 268280) increased by around 2.0-fold. This enzyme is also unidirectional, further supporting an increase in glycolytic activity. Acetyl CoA is used in fatty acid biosynthesis and as a carbon input to the TCA cycle, which is a source of energy and reducing equivalents, but also provides carbon skeletons for nitrogen assimilation and the biosynthesis of compounds, including fatty acids. In this proteomics study many of the proteins of the TCA cycle increased by 1.6- to 2.5-fold in abundance (Figure 6.6), suggesting that the carbon from glycolysis might be channelled through acetyl CoA and then into this pathway.

6.3.8. Regulation

Regulating the balance between carbon and nitrogen metabolism is crucial, particularly under changing nitrogen availability, and there are a range of regulatory elements known to be involved in coordinating this response. The signal transduction protein PII is conserved among bacteria, Archaea and higher plants and binds to central regulators and enzymes involved in nitrogen metabolism (Commichau et al. 2006). PII senses levels of the TCA cycle intermediate 2-oxoglutarate along with glutamine and ATP and thereby integrates the carbon, nitrogen and energy status of the cell (Commichau et al. 2006). In higher plants PII regulates key enzymes for arginine biosynthesis (Ferrario-Méry et al. 2006) and in bacteria it also interacts with the high affinity ammonium permease AmtB (Javelle and Merrick 2005), the glutamine synthetase regulator GlnE (Arcondeguy et al. 2001) and the global transcription factor of nitrogen control NtcA (Aldehni et al. 2003). Interestingly, the sequence of the N-acetyl-gamma-glutamyl-phosphate reductase (ProtID 21290) identified in this study appears to contain a PII domain, suggesting that diatoms also have this form of regulation.

The transcript levels of a number of other regulatory elements were altered in *T. pseudonana* at the onset of nitrogen starvation (Mock et al. 2008). These include a NarL family histidine kinase (ProtID 24704), which increased in abundance, and also an alkaline phosphatase (ProtID 20880) and a phosphate transport system substrate binding protein (ProtID 262506), which both decreased in transcript level. These are all required for a two-component signal transduction pathway and might therefore act together in regulating the cell response to nitrogen starvation.

6.3.9. Inter-Species Comparison

This novel combined analysis of the proteome and transcriptome of *T. pseudonana* at the onset on nitrogen starvation has revealed that nitrate assimilation is reduced, which would reduce demand for energy, reducing equivalents and carbon skeletons, and in response photosynthetic carbon fixation is decreased. In higher plants and green algae photosynthetic carbon fixation is also reduced in response to nitrogen deprivation and excess carbon is generally stored in molecular pools that contain little or no nitrogen. In higher plants this is usually in the form of starch (Diaz et al. 2005; Wingler et al. 2006) and Peng et al. (2007) described increased transcript levels of two genes involved in starch biosynthesis in *A. thaliana* under nitrogen starvation. In the fresh water green alga *C. reinhardtii*, on the other hand, excess carbon is reportedly directed to fatty acid biosynthesis (Wang et al. 2009; Moellering and Benning 2010), and Miller et al. (2010) found increased expression of genes involved in lipid biosynthesis in *C. reinhardtii* when nitrogen was not available. The increase in glycolytic proteins and their transcripts in *T. pseudonana* seems opposed to the patterns described in higher plants and green algae; while they are increasing carbon stores, *T. pseudonana* appears to be remobilising them.

Figure 6.7 (next page). A comparison of changes in transcript levels associated with nitrogen deprivation in A. *Thalassiosira pseudonana* (Mock et al. 2008), B. *Chlamydomonas reinhardtii* (Miller et al. 2010), C. *Arabidopsis thaliana* (Peng et al. 2007), and D. *Prochlorococcus marinus* (Tolonen et al. 2006). Each box represents an isoform and multiple rows show that there is more than one enzyme responsible for a specific step. See Appendix table 2 A to D for EC numbers and accession numbers. Red shows that transcript increased, green shows a decrease and blue shows stable transcript level.

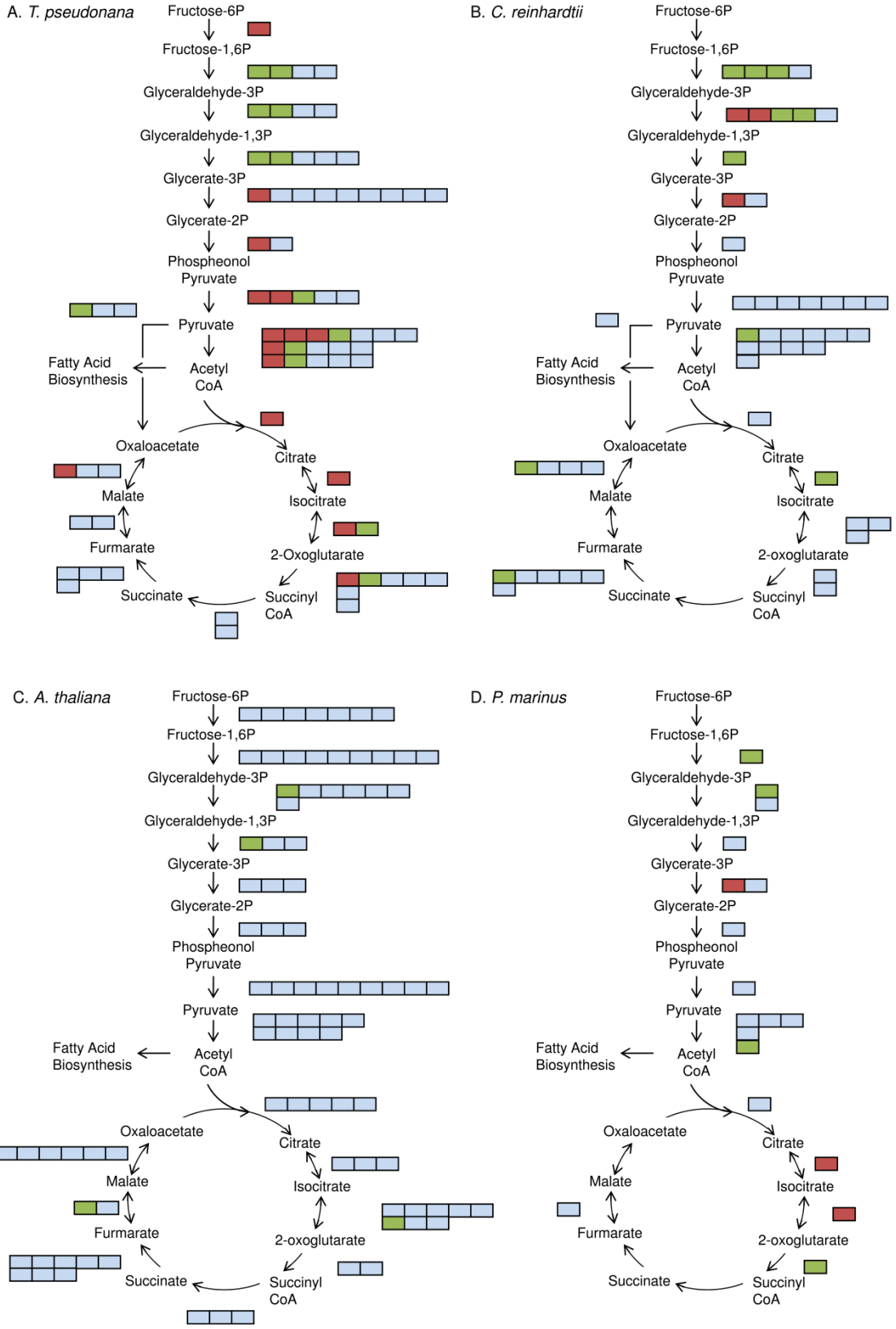
A. T. pseudonana
Fructose-6P
Fructose-1,6P
Glyceraldehyde-3P
Glyceraldehyde-1,3P
Glycerate-3P
Glycerate-2P
Phospheonol Pyruvate
Pyruvate
Fatty Acid Biosynthesis
Acetyl CoA
Oxaloacetate
Citrate
Malate
Isocitrate
Furmarate
2-Oxoglutarate
Succinate
Succinyl CoA
B. C. reinhardtii
Fructose-6P
Fructose-1,6P
Glyceraldehyde-3P
Glyceraldehyde-1,3P
Glycerate-3P
Glycerate-2P
Phospheonol Pyruvate
Pyruvate
Fatty Acid Biosynthesis
Acetyl CoA
Oxaloacetate
Citrate
Malate
Isocitrate
Furmarate
2-oxoglutarate
Succinate
Succinyl CoA
C. A. thaliana
Fructose-6P
Fructose-1,6P
Glyceraldehyde-3P
Glyceraldehyde-1,3P
Glycerate-3P
Glycerate-2P
Phospheonol Pyruvate
Pyruvate
Fatty Acid Biosynthesis
Acetyl CoA
Oxaloacetate
Citrate
Malate
Isocitrate
Furmarate
2-oxoglutarate
Succinate
Succinyl CoA
D. P. marinus
Fructose-6P
Fructose-1,6P
Glyceraldehyde-3P
Glyceraldehyde-1,3P
Glycerate-3P
Glycerate-2P
Phospheonol Pyruvate
Pyruvate
Fatty Acid Biosynthesis
Acetyl CoA
Oxaloacetate
Citrate
Malate
Isocitrate
Furmarate
2-oxoglutarate
Succinate
Succinyl CoA

In addition, in both *A. thaliana* (Peng et al. 2007) and *C. reinhardtii* (Miller et al. 2010) transcript levels of genes associated with the TCA cycle either decreased in abundance or remained unchanged in response to nitrogen deprivation (Figure 6.7; table S2). This is very different to *T. pseudonana*, where the abundance of proteins and transcripts (Mock et al. 2008) associated with the TCA cycle increased at the onset of nitrogen starvation (Figure 6.6 and Figure 6.7).

If photosynthetic carbon fixation is decreased in *T. pseudonana* due to reduced demand for carbon skeletons, reducing equivalents and energy, why are glycolysis and the TCA cycle, which are a source of these components, up-regulated? Interestingly a similar expression pattern, with increased levels of TCA cycle transcripts, is seen in the marine cyanobacterium *P. marinus* subsp. pastoris (strain CCMP1986, previously MED4) under nitrogen limited conditions (Figure 6.7) (Tolonen et al. 2006). These authors propose that under nitrogen limited conditions the breakdown of intracellular stores is a more efficient source of carbon for the reassimilation of nitrogen than photosynthesis. As discussed above, photosynthesis is a nitrogen demanding process, which can also increase oxidative stress. This hypothesis fits with the proposed protein and amino acid catabolism and increased GS/GOGAT enzymes for ammonium assimilation seen in the current study. In common with cyanobacteria, diatoms possess a complete urea cycle (Armbrust et al. 2004), which has the potential to increase the efficiency of nitrogen reassimilation from catabolic processes (Allen et al. 2006) thereby leading to a higher demand for carbon skeletons than in organisms that lack a urea cycle. Allen et al. (2011) illustrated a close link between the urea and TCA cycles through the metabolite analysis of nitrogen-limited *P. tricornutum* by using RNA interference-mediated knockdown of carbamoyl phosphate synthase and resupplying with nitrogen. Changes in both protein abundance (table 1) and transcript levels of enzymes associated with the urea cycle were seen in *T. pseudonana* at the onset of nitrogen starvation.

There are reports of increased lipid and fatty acid production in diatoms and many other microalgae under nitrogen starved conditions (Collyer and Fogg 1955; Mock and Kroon 2002; Palmucci et al. 2011). Although we found no changes in the abundance of proteins associated with this pathway

and there were few changes in transcript levels (Mock et al. 2008), these studies provide an alternative hypothesis to explain responses to nitrogen starvation seen here. Indeed the protein and transcript data discussed here were collected in the early stages of nitrogen starvation and it is possible that fatty acid biosynthesis increases at a later stage in the response. The changes in protein abundance observed do suggest increased synthesis of acetyl CoA, which is a precursor for fatty acid biosynthesis.

But why break down carbohydrates while building fatty acid stores? Palmucci et al. (2011) have shown that the diatoms *P. tricornutum* and *T. weissflogii* reduce carbohydrate stores whilst increasing levels of fatty acids under nitrogen starvation. They propose that fatty acids are more energy and reductant demanding than carbohydrates and that moving between these carbon stores increases the intracellular sink for these components. No change in either carbon store was found in *T. pseudonana*, but also no change in protein content (Palmucci et al. 2011). This suggests that nitrogen levels were not low enough to instigate a response to nitrogen starvation, and given a more severe starvation treatment, as used here, changes in carbon storage might occur.

If acetyl CoA is directed into fatty acid biosynthesis, how can the increase TCA enzymes be explained? It should be noted that most enzymes of the TCA cycle are not unidirectional and, under certain circumstances, can catalyse the reverse reaction. In their review Sweetlove et al. (2010) propose that the flux of the TCA cycle is highly adaptable and is likely to reflect the physiological and metabolic demands of the cell. They discuss that in higher plants the 'conventional' cyclic flux of TCA, which produces reducing equivalents for ATP synthesis, is thought only to be active in the dark. In illuminated leaves of *Spinacia oleracea* the TCA cycle forms two branches, converting acetyl CoA to 2-oxoglutarate, for nitrogen assimilation, and oxaloacetate for aspartate biosynthesis (Hanning and Heldt 1993). Furthermore in *Brassica napus* seeds cultured with the amino acids alanine and glutamine as a nitrogen source, the carbon skeletons produced by their catabolism enter the TCA cycle and this directs the carbon in both the forward and, to a lesser extent, the reverse reactions to form citrate, which is then converted to acetyl CoA and used in fatty acid elongation

(Schwender et al. 2006; Junker et al. 2007). The suggested catabolism of amino acids in *T. pseudonana* under nitrogen starvation would yield various TCA intermediates that could feed into the TCA cycle in this way (Figure 6.6) and be directed to fatty acid biosynthesis.

6.3.10. Concluding Remarks

Changes in the abundance of proteins identified in the current study, especially the increase in glycolytic and TCA cycle enzymes, suggest that the central carbon metabolism response of *T. pseudonana* to nitrogen starvation might differ considerably from that seen in other eukaryotic photoautotrophs studied to date. These pathways could be involved in providing carbon skeletons, for nitrogen reassimilation, or in the diversion of excess carbon into fatty acid biosynthesis. It is possible that both processes might have a place, with the TCA cycle acting as a hub, balancing the demand for specific carbon skeletons with the input of excess carbon from catabolic process in the cell. The similarity between the TCA cycle responses of *T. pseudonana* and the cyanobacteria *P. marinus*, both of which possess a urea cycle, suggests that the presence of this pathway might be closely related to the response of the TCA cycle seen here. The relationship between central carbon metabolism and the catabolic processes of the cell could play an important role in the success of diatoms in the ocean, where nitrogen availability is highly dynamic. Given the potential for manipulation of nitrogen and carbon metabolism these findings also have relevance for algal and plant biofuels and crop nutrition research.

Chapter 7. General Discussion

In this thesis I have presented one of the first studies on how changing growth conditions affect the proteome of the model diatom *T. pseudonana* and I have compared my findings to data for a wide variety of photosynthetic organisms, illustrated by figure 7.1. Diatoms are quite distant from the extant plants, chlorophytes, haptophyte algae, and cyanobacterium used in the discussion of my finding and I have demonstrated that accordingly the responses of *T. pseudonana* do not always follow expectations based on studies with other photosynthetic eukaryotes. In some aspects the diatom response was actually more similar to that of a cyanobacterium. In this discussion I will summarise my main findings and put forward ideas for future research.

7.1. Summary of Findings

Since DMSP has an important role in the global sulphur cycle and in climate regulation, in this study I have investigated sulphur metabolism and synthesis of this compound in the sequenced centric diatom *T. pseudonana*. An important objective of these experiments was to unify previous findings obtained with a range of different phytoplankton species and growth conditions for a single model and to develop a defined set of reproducible laboratory conditions. I found that the intracellular DMSP concentration in *T. pseudonana* increased with increased light intensity, increased salinity and nitrogen starvation. While similar results have been described before for various eukaryotic phytoplankton species, the increase in intracellular DMSP in a single species in response to three different conditions, oxidative stress, osmotic adjustment and nutrient limitation, highlights the multifunctional role of this compound. It also suggests that *T. pseudonana* and other diatoms might contribute more to DMSP production under the dynamic environmental conditions

found in the oceans than has been previously suggested by measurements conducted on actively growing nutrient-replete cultures (e.g. Keller et al. 1989).

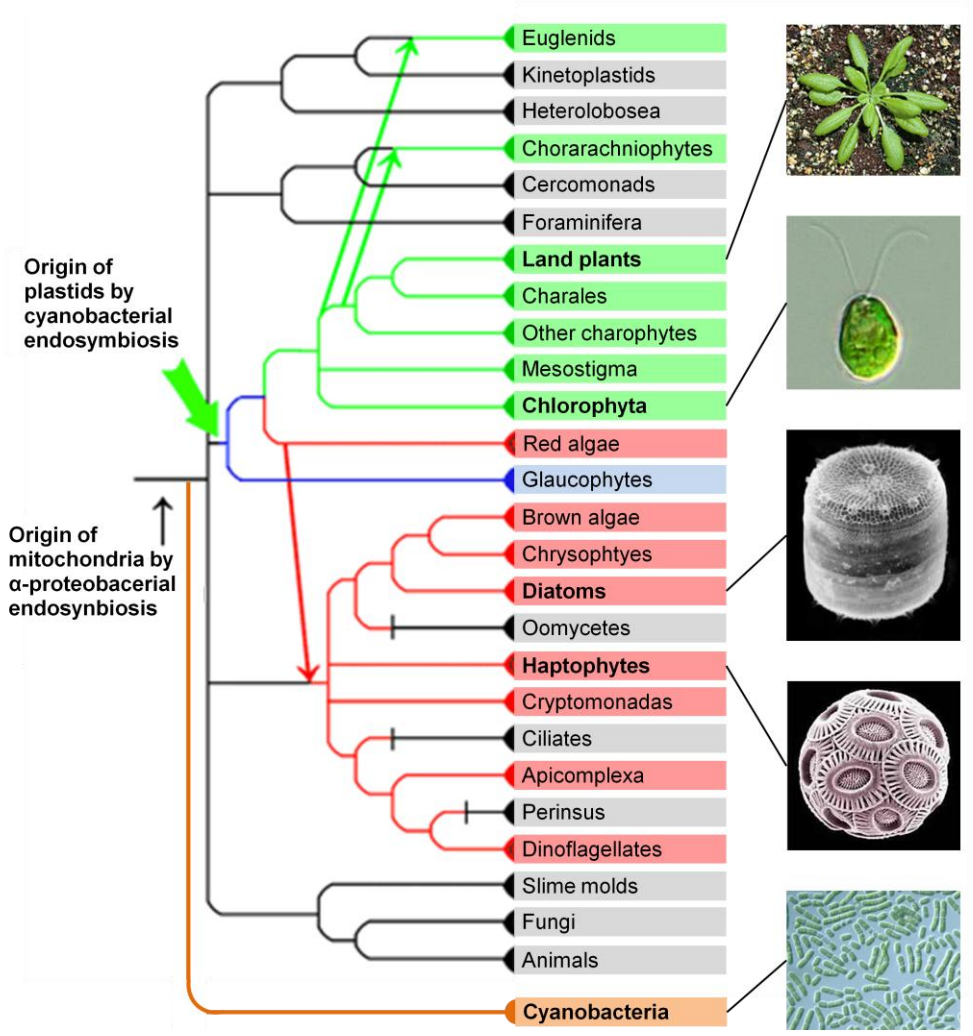

Figure 7.1. A phylogenetic tree showing the relationships of the major groups of extant eukaryotes and also cyanobacteria to represent the diversity of organisms discussed in this study; modified from Palmer et al. (2004). Arrows indicate endosymbiotic events. Green and red represent the appropriate plastid lineages. Eukaryotic heterotrophs are shown in grey and cyanobacteria are shown in orange. Groups used for comparison in the present study are in bold type. The branch lengths have no implications with respect to time.

APR is a key enzyme in the regulation of sulphur metabolism and the synthesis of sulphur containing metabolites, such as GSH, in higher plants (Vauclare et al. 2002; Scheerer et al. 2010). However, the activity of this enzyme did not increase with increasing DMSP concentration under increased light intensity, increased salinity and nitrogen starvation, suggesting that it does not have a role in the regulation of DMSP production in *T. pseudonana*. The activity of APR measured in this diatom is more than two orders of magnitude higher than is found in plants and it does seem unlikely that an enzyme with such high activity would have a controlling role in the pathway.

The transcript levels of genes involved in *T. pseudonana* sulphur assimilation showed little coordination in their response to the three treatments that increased intracellular DMSP concentration. The only gene up-regulated under all conditions was SiR, making it a candidate point for the regulation of the sulphur assimilatory pathway in this species as opposed to APR which fulfils this role in higher plants. Corresponding to the lack of transcriptional regulation, no proteins involved in the uptake, reduction or assimilation of sulphate increased in abundance in *T. pseudonana* under increased salinity, increased light intensity or nitrogen starvation. Generally, most of the changes in protein and transcript abundance seen were treatment specific. The only protein which increased in abundance under all three treatments was PEPC, which catalyses the production of oxaloacetate, a compound that can feed into methionine synthesis through aspartate, thus potentially linking it to DMSP synthesis.

Among the treatment specific changes in protein and transcript abundance were enzymes that link carbon and nitrogen metabolism with the sulphate assimilatory pathway. Transcripts of all three SAT isoforms increased in abundance under nitrogen starvation; SAT catalyses the production of OAS for cysteine synthesis. Proteins of the active methyl cycle, which recycles methionine from methyltransferase reactions, increased in abundance with increased salinity. The abundance of a methylenetetrahydrofolate reductase protein, which produces the cofactor 5-methyltetrahydropteroyltri-L-glutamate required for the synthesis of methionine from homocysteine, increased under both increased salinity and increased light intensity. It is also

noteworthy that under nitrogen starvation there was evidence of increased protein catabolism and under increased light intensity many light harvesting proteins decreased in abundance, suggesting that they might be selectively degraded. Increased protein catabolism might result in increased availability of free amino acids including cysteine and methionine.

Based on these findings I propose that sulphur is not limiting in the production of DMSP in *T. pseudonana* and that instead the availability of carbon and nitrogen are important for the control of DMSP accumulation. Correspondingly, reduced sulphate availability did not affect intracellular DMSP concentration or growth in this species. Furthermore, intracellular DMSP concentration showed diurnal variation, increasing during the light and remaining constant in the dark. This might be related to changes in the cellular carbon pools associated with photosynthesis, although it is also possible that the circadian clock or redox potential of the cell might also be responsible for this pattern.

Koprivova et al. (2000) and Kopriva et al. (2002) have demonstrated the regulatory interactions of nitrogen and carbon metabolism with the assimilation of sulphate in higher plants. These studies showed that deprivation of either of these essential nutrients resulted in reduced APR activity and mRNA levels and reduced rates of sulphate assimilation. The addition of OAS, which provides nitrogen and carbon for cysteine synthesis, to nitrogen or carbon deficient plants restored sulphate uptake and APR activity (Koprivova et al. 2000; Kopriva et al. 2002). However, in higher plants sulphur is often limiting for sulphate assimilation, therefore the regulation of enzymes directly involved in sulphate uptake and reduction have important roles to play. Increased sulphur assimilation is required for the synthesis of sulphur containing metabolites, such as GSH, in higher plants and this is generally regulated by the activity of APR (Bick et al. 2001). On the other hand in the marine environment sulphur is never limiting and perhaps it is not surprising that the regulation of sulphur assimilation in *T. pseudonana* is different to that described for higher plants.
An interesting connection between DMSP synthesis, carbon and nitrogen metabolism, that as far as I am aware remains unexplored, is the proposed requirement of the enzyme that catalyses the

transamination of methionine to MTOB in marine algae for 2-oxoglutarate (Summers et al. 1998). This TCA metabolite is required for the synthesis of glutamate in nitrogen assimilation and in bacteria it regulates the activity of the signal transduction molecule PII (Commichau et al. 2006). When nitrogen uptake rates are high, 2-oxoglutarate could be limiting to DMSP synthesis.

Under growth conditions that increased the intracellular DMSP concentration of *T. pseudonana* many of the processes described above were specific to individual treatments and, with the exception of SiR and PEPC, there was little coordination in transcript or protein abundance in parallel with the observed DMSP accumulation. However, the responses to each of the three treatments does have the potential to increase the availability of methionine either through its synthesis, protein degradation or recycling from cell processes. Therefore, I suggest that there might not be a single limiting step or 'on-off switch' for DMSP synthesis, but instead a range of cell processes might be involved in regulating the availability of methionine which can be used in DMSP synthesis. Kirst (1996) proposed that methionine availability might regulate DMSP synthesis since many stress conditions that increase levels of DMSP in algal cells are also associated with protein degradation. Simó (2001) suggests that DMSP production might prevent the accumulation of cysteine and methionine, thereby avoiding inhibitory feedback mechanisms and allowing the continuation of metabolic pathways. This hypothesis would also fit with Stefels (2000) proposed role for DMSP as an overflow metabolite. The specificity of the processes described, each of which might increase methionine availability in the cell, to the different growth conditions tested might reflect the multiple functions that DMSP has in the cell.

A branched-chain aminotransferase (ProtID 260934) was found to increase by 6.4-fold in protein abundance in *T. pseudonana* under nitrogen starvation. This could be a candidate for the first step from methionine to MTOB in DMSP synthesis, however substrate specificity must be confirmed and the effect of silencing of this gene on DMSP accumulation should be tested. A question that must be addressed is why no enzymes involved in the synthesis of DMSP from methionine were identified among those changing in abundance under all of the growth conditions that increased

intracellular DMSP levels as I had hypothesised? If the enzymes are membrane bound they would not have been identified because 2-dimensional gels are not optimised for these proteins; this is because the detergents that are require to solubilise membrane proteins, such as SDS, cannot be used in the first dimension as they introduce a negative charge that disrupts the pI separation. Also, if the mass or pI of proteins is outside the limits of the gel they would again not be found. Alternatively, the activity of enzymes between methionine and DMSP might not be limiting and instead substrate availability could regulate DMSP production. In this case the proteins concerned would not be expected to change in abundance. Actually, such regulation would be in agreement with the proposed function of DMSP as an overflow system (Stefels 2000). The proteins might also be under post-translational regulation, in which case an increase in abundance would not necessarily be required for increased activity. Another possibility is that processes other than DMSP synthesis are responsible for the observed increase in intracellular DMSP concentration, such as decreased DMSP lysis or leakage from the cell. Measuring dissolved DMSP in the medium and intracellular and dissolved DMS would help towards eliminating this hypothesis. Flux experiments using labelled substrates would also help to determine whether the rate of DMSP production is increased. Stefels et al. (2009) has developed a method in which either the addition of deuterium (D_2O) or ^{13}C (added as $NaH^{13}CO_3$) is used to quantify the rate of DMSP synthesis in vivo. Finally, the existence of an alternative pathway for DMSP synthesis in diatoms, which may act alongside the route described by Gage et al. (1997), cannot be ruled out. Gage et al. (1997) did identify the intermediate DMSHB in the diatom *M. nummuloides* and I have also detected DMSHB in preliminary experiments with *T. pseudonana* (data not shown), which suggests that DMSP synthesis in this group does follow the expected algal pathway. However, these measurements were carried out under optimal conditions and there is a possibility that another pathway might contribute to the increased in intracellular DMSP concentration seen under one or more of the three treatments tested. Although this is quite speculative, throughout this thesis I have discussed the diverse metabolic pathways that have been brought together in diatom evolution and how these pathways can act together in unexpected ways. Could one of these novel processes produce an

alternative precursor of DMSP, such as SMM, which is used in the plant pathway of DMSP synthesis?

Nitrogen is often limiting in marine environments and the metabolism of nitrogen by marine phytoplankton is important in determining how much carbon is fixed in the ocean; therefore I investigated the response of *T. pseudonana* metabolism to nitrogen starvation further. This was done by identifying all of the proteins that changed in abundance under this treatment (fold change > 1.5; t-test, $P < 0.005$). These were then compared to the transcriptome response of *T. pseudonana* (Mock et al. 2008) and also a plant, a green alga and a cyanobacterium to this growth condition. I found that with nitrogen depletion nitrate and nitrite reductases were reduced, but the abundance of proteins involved in the assimilation of ammonium increased. Rather unexpectedly, enzymes of the TCA cycle and glycolysis increased in abundance despite a decreased photosynthetic efficiency. This is quite different to the response of other photosynthetic eukaryotes and is likely to be related to the presence of the urea cycle in diatoms. I hypothesised that carbohydrate stores are either being used in the reassimilation of nitrogen from catabolic processes, or that these carbon stores are being redistributed to form fatty acids, which are a superior sink for carbon, reducing equivalents and energy. This work highlights that even if the genes of a pathway are present in the diatom genome, the interaction with pathways not found together in any other eukaryotic organism can result in an entirely different regulation than expected. It is possible that this may also be true for sulphur assimilation and DMSP synthesis.

7.2. Future Work

Many of the hypotheses put forward in this discussion could be addressed by conducting flux experiments with either ^{35}S- or ^{13}C-labelled substrates. The benefit of this approach is that the rate of uptake and incorporation into different metabolites can be measured. It is also possible to screen for all labelled metabolites to identify alternative pathways and to measure the ratio of labelling between metabolite pools. This approach was used by Kopriva et al. (2002) to measure ^{35}S-labelled

sulphate assimilation and distribution of ^{35}S in metabolites in *L. minor* under a CO_2 free atmosphere and to assess whether the addition sucrose or OAS affected these parameters. Vauclare et al. (2002) also used ^{35}S-labelled sulphate to demonstrate that feeding cysteine or glutathione to *A. thaliana* reduced sulphate uptake, APR activity and the flux of labelled sulphur into cysteine. Gage et al. (1997) fed *U. intestinalis* with ^{35}S-labelled methionine to identify intermediates in the pathway of DMSP synthesis in this species.

In a similar way, one could feed *T. pseudonana* cultures with ^{35}S-labelled sulphate, measure the uptake and flux through the assimilatory pathway and the relative incorporation of sulphur to DMSP and other sulphur metabolites under increased salinity, increased light intensity and nitrogen starvation. Feeding with carbon and nitrogen substrates, such as OAS, OPH and methionine, could also be tested to see whether these affect uptake and incorporation. This approach could also be used to confirm whether sulphate uptake and/or DMSP synthesis occur in the dark and comparing this to dark cultures with added sucrose, OAS or OPH would establish whether carbon availability is responsible for the diurnal variation in intracellular DMSP concentration seen. Feeding sucrose in the dark has been used in plants to investigate how carbon availability regulates NR (Cheng et al. 1992). *A. thaliana* have also been fed with sucrose to test the effect on APR regulation (Kopriva et al. 1999) and OAS has been fed to *L. minor* to test whether this carbon input is limiting to cysteine synthesis (Neuenschwander et al. 1991). Finally by comparing the flux of sulphur-35 though the assimilatory pathway in cultures with reduced sulphate availability to a control culture it would be possible to determine whether stored (un-labelled) sulphate is being used to maintain growth and DMSP synthesis. However, while these experiments are feasible with plants and freshwater algae, the high sulphate content in sea water essentially precludes the use of ^{35}S-labelling, since very high amounts of radioactivity would have to be used to overcome the isotope dilution. An alternative approach could be to use ^{34}S-labelling, which is not radioactive, although this isotope is not as easily available and is more expensive. There is also an issue of the preferential use of lighter isotopes, which would have to be investigated. Of course ^{35}S-labelled methionine could be used to specifically investigate the steps from methionine to DMSP, but this would not improve our

understanding of the broader regulation of the pathway. A labelling approach could also be used to determine the fate of carbon in *T. pseudonana* under nitrogen starvation.

In addition, the over-expression of proteins in the pathway of sulphate assimilation, such as ATPS, APR and SiR, and also those in branching pathways highlighted in this study, such as SAT, methylenetetrahdrofolate reductase and PEPC, could provide information on which steps are limiting to DMSP synthesis. In higher plants Martin et al. (2005) demonstrated that the over expression of APR resulted in increased levels of sulphur metabolites, whereas the over expression of ATPS had little effect (Hatzfeld et al. 1998). Gakiere et al. (2002) also used this approach to demonstrate that CgS has a regulatory role in methionine synthesis whereas CbL does not.

The isoforms of genes involved in sulphur assimilation had a differential response of to the growth conditions tested in this study and it would be interesting to investigate the contribution of individual isoforms to the pathway further. This could be done by using RNA interference methods, as used by Allen et al. (2011) for the diatom *P. tricornatum*, to silence the expression of individual isoforms and then analyse the effects on sulphur metabolites including DMSP.

7.3. Long-Term Perspectives

The research in this thesis has highlighted the importance of studying interaction between sulphur, nitrogen and carbon metabolism. Due to the 'chimeric' nature of the diatom genome (Armbrust et al. 2004; Bowler et al. 2008) it is likely that metabolic pathways of this group could interact in quite unexpected ways and must therefore be investigated as a network rather in isolation. A key finding of this work has been the differential regulation of the diatom TCA cycle under nitrogen starvation, compared to other photosynthetic organisms. This is thought to be due to its interaction with the urea cycle. It is also possible that the connection between DMSP synthesis, which is not found in most higher plants, and TCA metabolites could impact on the regulation of carbon metabolism in diatoms and other marine algae. I propose that further research into diatom carbon

metabolism is now required, since much of our understanding is currently based on findings of the genome projects (Armbrust et al. 2004; Bowler et al. 2008) and assumptions based on what we know for higher plants and green algae, rather than on experimental work with diatoms (Kroth et al. 2008). The interaction of carbon and nutrient metabolism is also of interest with regards to biofuel production and there may also be far reaching applications in crop research. In the future it might be possible to introduce algal pathways to plants with the aim on improving nutrient use efficiency.

There is also great future potential for this research with regards to environmental science. If key genes involved in the regulation of DMSP production can be identified they could be used to develop molecular markers to test hypotheses concerning environmental conditions in the field. Molecular markers could also provide more precise geographical and temporal information on DMSP production for predictive climate models; they would provide a measure of the productivity of the pathway rather than intracellular concentration alone. Finally it might be possible to design the probes (or primers) in such a way to determine group, or even species, specific contribution to DMSP production in the field and under different conditions; this would greatly increase the complexity of climate models. This approach is already being used to investigate nitrogen assimilation (Allen et al. 2005). Once the enzymes for DMSP synthesis are identified for one species of phytoplankton this will open the way to the rapid screening of other species and their responses to different environmental conditions.

References

Aldehni MF, Sauer J, Spielhaupter C, Schmid R, Forchhammer K (2003) Signal transduction protein P-II is required for NtcA-regulated gene expression during nitrogen deprivation in the cyanobacterium *Synechococcus elongatus* strain PCC 7942. *J. Bacteriol.* **185**: 2582-2591.

Allen AE, Dupont CL, Obornik M, Horak A, Nunes-Nesi A, McCrow JP, Zheng H, Johnson DA, Hu HH, Fernie AR, Bowler C (2011) Evolution and metabolic significance of the urea cycle in photosynthetic diatoms. *Nature* **473**: 203-207.

Allen AE, Vardi A, Bowler C (2006) An ecological and evolutionary context for integrated nitrogen metabolism and related signaling pathways in marine diatoms. *Curr. Opin. Plant Biol.* **9**: 264-273.

Allen AE, Ward BB, Song BK (2005) Characterization of diatom (Bacillariophyceae) nitrate reductase genes and their detection in marine phytoplankton communities. *J. Phycol.* **41**: 95-104.

Andreae MO (1986) The ocean as a source of atmospheric sulfur compounds In P Buat-Menard, eds, The Role of Air-Sea Exchange in Geochemical Cycling. Reidel, Dordrecht, pp 331-362.

Arcondeguy T, Jack R, Merrick M (2001) PII signal transduction proteins, pivotal players in microbial nitrogen control. *Microbiol. Mol. Biol. Rev.* **65**: 80-105.

Armbrust EV (2009) The life of diatoms in the world's oceans. *Nature* **459**: 185-192.

Armbrust EV, Berges JA, Bowler C, Green BR, Martinez D, Putnam NH, Zhou SG, Allen AE, Apt KE, Bechner M, Brzezinski MA, Chaal BK, Chiovitti A, Davis AK, Demarest MS, Detter JC, Glavina T, Goodstein D, Hadi MZ, Hellsten U, Hildebrand M, Jenkins BD, Jurka J, Kapitonov VV, Kroger N, Lau WWY, Lane TW, Larimer FW, Lippmeier JC, Lucas S, Medina M, Montsant A, Obornik M, Parker MS, Palenik B, Pazour GJ, Richardson PM, Rynearson TA, Saito MA, Schwartz DC, Thamatrakoln K, Valentin K, Vardi A, Wilkerson FP, Rokhsar DS (2004) The genome of the diatom *Thalassiosira pseudonana*: Ecology, evolution, and metabolism. *Science* **306**: 79-86.

Bartlem D, Lambein I, Okamoto T, Itaya A, Uda Y, Kijima F, Tamaki Y, Nambara E, Naito S (2000) Mutation in the threonine synthase gene results in an over-accumulation of soluble methionine in Arabidopsis. *Plant Physiol.* **123**: 101-110.

Bartoli CG, Tambussi EA, Diego F, Foyer CH (2009) Control of ascorbic acid synthesis and accumulation and glutathione by the incident light red/far red ratio in *Phaseolus vulgaris* leaves. *FEBS Lett.* **583**: 118-122.

Bennett RN, Wallsgrove RM (1994) Secondary metabolites in plant defence-mechanisms. *New Phytologist* **127**: 617-633.

Benning C (1998) Biosynthesis and function of the sulfolipid sulfoquinovosyl diacylglycerol. *Annu. Rev. Plant Physiol. Plant Mol. Biol.* **49**: 53-75.

Berges JA, Harrison PJ (1995) Nitrate reductase-activity quantitatively predicts the rate of nitrate incorporation under steady-state light limitation - A revised assay and characterization of the enzyme in 3 species of marine-phytoplankton. *Limnol. Oceanogr.* **40**: 82-93.

Berman T, Chava S (1999) Algal growth on organic compounds as nitrogen sources. *J. Plankton Res.* **21**: 1423-1437.

Bhattacharya D, Medlin L (1995) The phylogeny of plastids - A review based on comparisons of small-subunit ribosomal-RNA coding regions. *J. Phycol.* **31**: 489-498.

Bick JA, Setterdahl AT, Knaff DB, Chen YC, Pitcher LH, Zilinskas BA, Leustek T (2001) Regulation of the plant-type 5 '-adenylyl sulfate reductase by oxidative stress. *Biochemistry* **40**: 9040-9048.

Blanco J, Coque JJR, Martin JF (1998) The folate branch of the methionine biosynthesis pathway in *Streptomyces lividans*: Disruption of the 5,10-methylenetetrahydrofolate reductase gene leads to methionine auxotrophy. *J. Bacteriol.* **180**: 1586-1591.

Bode A, Botas JA, Fernandez E (1997) Nitrate storage by phytoplankton in a coastal upwelling environment. *Mar. Biol.* **129**: 399-406.

Bowler C, Allen AE, Badger JH, Grimwood J, Jabbari K, Kuo A, Maheswari U, Martens C, Maumus F, Otillar RP, Rayko E, Salamov A, Vandepoele K, Beszteri B, Gruber A, Heijde M, Katinka M, Mock T, Valentin K, Verret F, Berges JA, Brownlee C, Cadoret JP, Chiovitti A, Choi CJ, Coesel S, De Martino A, Detter JC, Durkin C, Falciatore A, Fournet J, Haruta M, Huysman MJJ, Jenkins BD, Jiroutova K, Jorgensen RE, Joubert Y, Kaplan A, Kroger N, Kroth PG, La Roche J, Lindquist E, Lommer M, Martin-Jezequel V, Lopez PJ, Lucas S, Mangogna M, McGinnis K, Medlin LK, Montsant A, Oudot-Le Secq MP, Napoli C, Obornik M, Parker MS, Petit JL, Porcel BM, Poulsen N, Robison M, Rychlewski L, Rynearson TA, Schmutz J, Shapiro H, Siaut M, Stanley M, Sussman MR, Taylor AR, Vardi A, von Dassow P, Vyverman W, Willis A, Wyrwicz LS, Rokhsar DS, Weissenbach J, Armbrust EV,

Green BR, Van De Peer Y, Grigoriev IV (2008) The *Phaeodactylum* genome reveals the evolutionary history of diatom genomes. *Nature* **456**: 239-244.

Bowler C, Vardi A, Allen AE (2010) Oceanographic and biogeochemical insights from diatom genomes. *Annual Review of Marine Science* **2**: 333-365.

Bradford MM (1976) Rapid and sensitive method for quantitation of microgram quantities of protein utilizing principle of protein-dye binding. *Anal. Biochem.* **72**: 248-254.

Brown KL, Twing KI, Robertson DL (2009) Unraveling the regulation of nitrogen assimilation in the marine diatom *Thalassiosira pseudonana* (Bacillariophyceae): Diurnal variations in transcript levels for five genes involved in nitrogen assimilation. *J. Phycol.* **45**: 413-426.

Bruland KW, Rue EL, Smith GJ, DiTullio GR (2005) Iron, macronutrients and diatom blooms in the Peru upwelling regime: brown and blue waters of Peru. *Mar. Chem.* **93**: 81-103.

Brunner M, Kocsy G, Ruegsegger A, Schmutz D, Brunold C (1995) Effect of chilling on assimilatory sulfate reduction and glutathione synthesis in maize. *J. Plant Physiol.* **146**: 743-747.

Brunold C, Schiff JA (1976) Studies of sulfate utilization by algae: 15. Enzymes of assimilatory sulfate reduction in *Euglena* and their cellular localization. *Plant Physiol.* **57**: 430-436.

Bucciarelli E, Sunda WG (2003) Influence of CO_2, nitrate, phosphate, and silicate limitation on intracellular dimethylsulfoniopropionate in batch cultures of the coastal diatom *Thalassiosira pseudonana*. *Limnology and Oceanography* **48**: 2256-2265.

Bucciarelli E, Sunda WG, Belviso S, Sarthou G (2007) Effect of the diel cycle on production of dimethylsulfoniopropionate in batch cultures of *Emiliania huxleyi*. *Aquat. Microb. Ecol.* **48**: 73-81.

Buchner P, Takahashi H, Hawkesford MJ (2004) Plant sulphate transporters: co-ordination of uptake, intracellular and long-distance transport. *J. Exp. Bot.* **55**: 1765-1773.

Butow B, Wynne D, Sukenik A, Hadas O, Tel-Or E (1998) The synergistic effect of carbon concentration and high temperature on lipid peroxidation in *Peridinium gatunense*. *Journal of Plankton Research* **20**: 355-369.

Butterfield NJ (2001) Paleobiology of the late Mesoproterozoic (ca. 1200 Ma) Hunting Formation, Somerset Island, arctic Canada. *Precambrian Res.* **111**: 235-256.

Carpenter EJ, Janson S (2000) Intracellular cyanobacterial symbionts in the marine diatom *Climacodium frauenfeldianum* (Bacillariophyceae). *J. Phycol.* **36**: 540-544.

Caruana A (2010) *DMS and DMSP production by marine dinoflagellates*. School of Environmental Science, University of East Anglia, UK. **PhD Thesis**.

Charlson RJ, Lovelock JE, Andreae MO, Warren SG (1987) Oceanic phytoplankton, atmospheric sulphur, cloud albedo and climate. *Nature* **326**: 655-661.

Chen HC, Melis A (2004) Localization and function of SulP, a nuclear-encoded chloroplast sulfate permease in *Chlamydomonas reinhardtii*. *Planta* **220**: 198-210.

Chen HC, Newton AJ, Melis A (2005) Role of *SulP*, a nuclear-encoded chloroplast sulfate permease, in sulfate transport and H_2 evolution in *Chlamydomonas reinhardtii*. *Photosynthesis Research* **84**: 289-296.

Chen HC, Yokthongwattana K, Newton AJ, Melis A (2003) *SulP*, a nuclear gene encoding a putative chloroplast-targeted sulfate permease in *Chlamydomonas reinhardtii*. *Planta* **218**: 98-106.

Chiba Y, Ishikawa M, Kijima F, Tyson RH, Kim J, Yamamoto A, Nambara E, Leustek T, Wallsgrove RM, Naito S (1999) Evidence for autoregulation of cystathionine γ-synthase mRNA stability in *Arabidopsis*. *Science* **286**: 1371-1374.

Clayton JR, Ahmed SI (1986) Detection of glutamate synthase (GOGAT) activity in phytoplankton - Evaluation of cofactors and assay optimization. *Mar. Ecol. Prog. Ser.* **32**: 115-122.

Collyer DM, Fogg GE (1955) Studies on fat accumulation by algae. *J. Exp. Bot.* **6**: 256-275.

Commichau FM, Forchhammer K, Stulke J (2006) Regulatory links between carbon and nitrogen metabolism. *Curr. Opin. Microbiol.* **9**: 167-172.

Contreras L, Ritter A, Dennett G, Boehmwald F, Guitton N, Pineau C, Moenne A, Potin P, Correa JA (2008) Two-dimensional gel electrophoresis analysis of brown algal protein extracts. *J. Phycol.* **44**: 1315-1321.

Croft MT, Lawrence AD, Raux-Deery E, Warren MJ, Smith AG (2005) Algae acquire vitamin B-12 through a symbiotic relationship with bacteria. *Nature* **438**: 90-93.

Cuhel RL, Ortner PB, Lean DRS (1984) Night synthesis of protein by algae. *Limnol. Oceanogr.* **29**: 731-744.

Curien G, Dumas R, Ravanel S, Douce R (1996) Characterization of an *Arabidopsis thaliana* cDNA encoding an S-adenosylmethionine-sensitive threonine synthase - Threonine synthase from higher plants. *FEBS Lett.* **390**: 85-90.

Davidian J-C, Kopriva S (2010) Regulation of Sulfate Uptake and Assimilation-the Same or Not the Same? *Molecular Plant* **3**: 314-325.

Diaz C, Purdy S, Christ A, Morot-Gaudry JF, Wingler A, Masclaux-Daubresse CL (2005) Characterization of markers to determine the extent and variability of leaf senescence in *Arabidopsis*. A metabolic profiling approach. *Plant Physiol.* **138**: 898-908.

Dickson DMJ, Kirst GO (1986) The role of β-dimethylsulphoniopropionate, glycine betaine and homarine in the osmoacclimation of *Platymonas subcordiformis*. *Planta* **167**: 536-543.

Dickson DMJ, Kirst GO (1987) Osmotic adjustment in marine eukaryotic algae: The role of inorganic ions, quarternary ammonium, tertiary sulphonium and carbohydrate solutes- I Diatoms and Rhodophyte. *New Phytol.* **106**: 645-655.

Dickson DMJ, Wyn Jones RG, Davenport J (1980) Steady state osmotic adaption in *Ulva lactuca*. *Planta* **150**: 158-165.

Dickson DMJ, Wyn Jones RG, Davenport J (1982) Osmotic adaptation in *Ulva lactuca* under fluctuating salinity regimes. *Planta* **155**: 409-415.

Dortch Q, Ahmed SI, Packard T (1979) Nitrate reductase and glutamate dehydrogenase activities in *Skeletonema costatum* as measures of nitrogen assimilation rates *J. Plankton Res.* **1**: 169-186.

Doubnerová V, Ryšlavá H (2011) What can enzymes of C_4 photosynthesis do for C_3 plants under stress? *Plant Sci.* **180**: 575-583.

Douglas S, Zauner S, Fraunholz M, Beaton M, Penny S, Deng LT, Wu XN, Reith M, Cavalier-Smith T, Maier UG (2001) The highly reduced genome of an enslaved algal nucleus. *Nature* **410**: 1091-1096.

Droux M (2003) Plant serine acetyltransferase: New insights for regulation of sulphur metabolism in plant cells. *Plant Physiol. Biochem.* **41**: 619-627.

Droux M, Ruffet ML, Douce R, Job D (1998) Interactions between serine acetyltransferase and *O*-acetylserine (thiol) lyase in higher plants. *255*.

Dupont CL, Goepfert TJ, Lo P, Wei LP, Ahnerz BA (2004) Diurnal cycling of glutathione in marine phytoplankton: Field and culture studies. *Limnol. Oceanogr.* **49**: 991-996.

Edwards DM, Reed RH, J.A. C, Foster R, Stewart WDP (1987) Organic Solute accumulation in osmotically stressed *Enteromorpha intestinalis*. *Marine Biology* **95**: 583-592.

Eppley RW, Rogers JN, McCarthy JJ (1969) Half-saturation constants for uptake of nitrate and ammonium by marine phytoplankton. *Limnol. Oceanogr.* **14**: 912-&.

Estrada M, Blasco D (1979) 2 phases of the phytoplankton community in the Baja California upwelling. *Limnol. Oceanogr.* **24**: 1065-1080.

Evans C, Kadner SV, Darroch LJ, Wilson WH, Liss PS, Malin G (2007) The relative significance of viral lysis and microzooplankton grazing as pathways of dimethylsulfoniopropionate (DMSP) cleavage: An *Emiliania huxleyi* culture study. *Limnol. Oceanogr.* **52**: 1036-1045.

Falkowski PG (1997) Evolution of the nitrogen cycle and its influence on the biological sequestration of CO_2 in the ocean. *Nature* **387**: 272-275.

Falkowski PG, Barber RT, Smetacek V (1998) Biogeochemical controls and feedbacks on ocean primary production. *Science* **281**: 200-206.

Falkowski PG, Katz ME, Knoll AH, Quigg A, Raven JA, Schofield O, Taylor FJR (2004a) The evolution of modern eukaryotic phytoplankton. *Science* **305**: 354-360.

Falkowski PG, Schofield O, Katz ME, Van de Schootbrugge B, Knoll AH (2004b) Why is the land green and the ocean red? In HR Thierstein, JR Young, eds, Coccolithophores: from molecular processes to global impact. Springer-Verlag Heidelberg, pp 429-453.

Ferguson RL, Collier A, Meeter DA (1976) Growth response of *Thalassiosira pseudonana* clone 3H to illumination temperature and nitrogen source. *Chesapeake Science* **17**: 148-158.

Ferrario-Méry S, Besin E, Pichon O, Meyer C, Hodges M (2006) The regulatory PII protein controls arginine biosynthesis in *Arabidopsis*. *FEBS Lett.* **580**: 2015-2020.

Field CB, Behrenfeld MJ, Randerson JT, Falkowski P (1998) Primary production of the biosphere: Integrating terrestrial and oceanic components. *Science* **281**: 237-240.

Foyer CH, Harbinson J (1994) Oxygen metabolism and the regulation of photosynthetic electron transport. In CH Foyer, eds, Causes of Photooxidative Stress and Amelioration of Defense Systems in Plants. CRC Press, Boca Raton FL., pp 1-42.

Foyer CH, Noctor G (2011) Ascorbate and glutathione: The heart of the redox hub. *Plant Physiol.* **155**: 2-18.

Gage DA, Rhodes D, Nolte KD, Hicks WA, Leustek T, Cooper AJL, Hanson AD (1997) A new route for synthesis of dimethylsulphoniopropionate in marine algae. *Nature* **387**: 891-894.

Gakiere B, Denis L, Droux M, Job D (2002) Over-expression of cystathionine gamma-synthase in *Arabidopsis thaliana* leads to increased levels of methionine and S-methylmethionine. *Plant Physiol. Biochem.* **40**: 119-126.

Galili G, Höfgen R (2002) Metabolic engineering of amino acids and storage proteins in plants. *Metab. Eng.* **4**: 3-11.

Galloway JN, Townsend AR, Erisman JW, Bekunda M, Cai Z, Freney JR, Martinelli LA, Seitzinger SP, Sutton MA (2008) Transformation of the nitrogen cycle: Recent trends, questions, and potential solutions. *Science* **320**: 889-892.

Gao Y, Schofield OME, Leustek T (2000) Characterization of sulfate assimilation in marine algae focusing on the enzyme 5'-adenylylsulfate reductase. *Plant Physiol.* **123**: 1087-1096.

Gao Y, Smith GJ, Alberte RS (1993) Nitrate reductase from the marine diatom *Skeletonema costatum* - Biochemical and immunological characterization. *Plant Physiol.* **103**: 1437-1445.

Gibbs SP (1981) The chloroplasts of some algal groups may have evolved from endosymbiotic eukaryotic algae. *Ann. N. Y. Acad. Sci.* **361**: 193-208.

Gilbert SM, Clarkson DT, Cambridge M, Lambers H, Hawkesford MJ (1997) SO_4^{2-} deprivation has an early effect on the content of ribulose-1,5-bisphosphate carboxylase/oxygenase and photosynthesis in young leaves of wheat. *Plant Physiol.* **115**: 1231-1239.

Giordano M, Chen YB, Koblizek M, Falkowski PG (2005) Regulation of nitrate reductase in *Chlamydomonas reinhardtii* by the redox state of the plastoquinone pool. *Eur. J. Phycol.* **40**: 345-352.

Giovanelli J (1990) Regulatory aspects of cysteine and methionine biosynthesis. In H Rennenberg, C Brunold, LJ De Kok, I Stulen, eds, Sulfur Nutrition and Sulfur Assimilation in Higher Plants: Fundamental Environmental and Agricultural Aspects. SPB Academic Publishing, The Hague, pp 33–48.

Giovanelli S, Mudd H, Dakto AH (1980) Homocysteine biosynthesis in plants. In D Cavallini, eds, Natural sulfur compounds: Novel biochemical and structural aspects. Plenum. **30**, pp 8 l-90.

Gonzalez JC, Banerjee RV, Huang S, Sumner JS, Matthews RG (1992) Comparison of cobalamin-independent and cobalamin-dependent methionine synthases from Escherichia coli - 2 solutions to the same chemical problem. *Biochemistry* **31**: 6045-6056.

Govindjee, G. Papageorgiou G, Rabinowitch E (1973) Chlorophyll fluorescence and photosynthesis. In GG Guilbault, eds, Practical Fluorescence Theory, Methods, and Techniques. Marcel Dekker Inc, New York, pp 543-575.

Green L, Laudenbach D, Grossman A (1989) A region of cyanobacterial genome required for sulfate transport. *Proceedings of the National Academy of Science USA* **86**: 1949-1953.

Greene RC (1962) Biosynthesis of dimethyl-β-propiothetin. *J. Biol. Chem.* **237**: 2251-2254.

Gröne T, Kirst GO (1991) Aspects of dimethylsulfoniopropionate effects on enzymes isolated from the marine phytoplankter *Tetraselmis subcordiformis* (Stein) *Journal of Plant Physiology* **138**: 85-91.

Gröne T, Kirst GO (1992) The effect of nitrogen deficiency, methionine and inhibitors of methionine metabolism on the DMSP contents of *Tetraselmis subcordiformis* (Stein). *Marine Biology* **112**: 497-503.

Haas FH, Heeg C, Queiroz R, Bauer A, Wirtz M, Hell R (2008) Mitochondrial serine acetyltransferase functions as a pacemaker of cysteine synthesis in plant cells. *Plant Physiol.* **148**: 1055-1067.

Hanning I, Heldt HW (1993) On the function of mitochondrial metabolism during photosynthesis in Spinach (*Spinacia-oleracea L*) leaves - partitioning between respiration and export of redox equivalents and precursors for nitrate assimilation products. *Plant Physiol.* **103**: 1147-1154.

Hanson AD, Rivoal J, Paquet L, Gage DA (1994) Biosynthesis of 3-dimethylsulfoniopropionate in *Wollastonia biflora* (L.) DC. *Plant Physiology* **105**: 103-110.

Harada E, Kusano T, Sano H (2000) Differential expression of genes encoding enzymes involved in sulfur assimilation pathways in response to wounding and jasmonate in *Arabidopsis thaliana*. *J. Plant Physiol.* **156**: 272-276.

Harada H, Vila-Costa M, Cebrian J, Kiene RP (2009) Effects of UV radiation and nitrate limitation on the production of biogenic sulfur compounds by marine phytoplankton. *Aquat. Bot.* **90**: 37-42.

Harms K, von Ballmoos P, Brunold C, Hofgen R, Hesse H (2000) Expression of a bacterial serine acetyltransferase in transgenic potato plants leads to increased levels of cysteine and glutathione. *Plant J.* **22**: 335-343.

Harrison PJ, Berges JA (2005) Marine culture medium. In RA Andersen, eds, Algal Culturing Techniques. Academic Press, San Diego, pp 21-33.

Hatzfeld Y, Cathala N, Grignon C, Davidian J-C (1998) Effect of ATP Sulfurylase Overexpression in Bright Yellow 2 Tobacco Cells. *Plant Physiol.* **116**: 1307-1313.

Hell R (1997) Molecular physiology of plant sulfur metabolism. *Planta* **202**: 138-148.

Hesse H, Kreft O, Maimann S, Zeh M, Hoefgen R (2004) Current understanding of the regulation of methionine biosynthesis in plants. *J. Exp. Bot.* **55**: 1799-1808.

Hildebrand M (2005) Cloning and functional characterization of ammonium transporters from the marine diatom *Cylindrotheca fusiformis* (Bacillariophyceae). *J. Phycol.* **41**: 105-113.

Hildebrand M, Dahlin K (2000) Nitrate transporter genes from the diatom *Cylindrotheca fusiformis* (Bacillariophyceae): mRNA levels controlled by nitrogen source and the cell cycle. *J. Phycol.* **36**: 702-713.

Hockin NL, Mock T, Mulholland F, Kopriva S, Malin G (2012) The Response of Diatom Central Carbon Metabolism to Nitrogen Starvation Is Different from That of Green Algae and Higher Plants. *Plant Physiol.* **158**: 299-312.

Hui Y, Jie W, Carpentier R (2000) Degradation of the Photosystem I Complex During Photoinhibition. *Photochem. Photobiol.* **72**: 508-512.

Inaba K, Fujiwara T, Hayashi H, Chino M, Komeda Y, Naito S (1994) Isolation of an *Arabidopsis thaliana* mutant, *mto*1, that overaccumulates soluble methionine. *Plant Physiol.* **105**: 1465-1465.

Jakob B, Heber U (1996) Photoproduction and detoxification of hydroxyl radicals in chloroplasts and leaves and relation to photoinactivation of photosystems I and II. *Plant and Cell Physiology* **37**.

James F, Paquet L, Sparace SA, Gage DA, Hanson AD (1995) Evidence implicating dimethylsulfoniopropionaldehyde as an intermediate in dimethylsulfoniopropionate biosynthesis. *Plant Physiology* **108**: 1439-1448.

Javelle A, Merrick M (2005) Complex formation between AmtB and GlnK: an ancestral role in prokaryotic nitrogen control. *Biochem. Soc. Trans.* **33**: 170-172.

Jochem FJ, Smith GJ, Gao Y, Zimmerman RC, Cabello-Pasini A, Kohrs DG, Alberte RS (2000) Cytometric quantification of nitrate reductase by immunolabeling in the marine diatom *Skeletonema costatum*. *Cytometry* **39**: 173-178.

Jost R, Berkowitz O, Wirtz M, Hopkins L, Hawkesford M, Hell R (2000) Genomic and functional characterization of the *oas* gene family encoding *O*-acetylserine (thiol) lyase, enzymes catalyzing the final step in cysteine biosynthesis in *Arabidopsis thaliana*. *Gene* **253**: 237-247.

Junker BH, Lonien J, Heady LE, Rogers A, Schwender J (2007) Parallel determination of enzyme activities and *in vivo* fluxes in *Brassica napus* embryos grown on organic or inorganic nitrogen source. *Phytochemistry* **68**: 2232-2242.

Kadota H, Ishida Y (1968) Effect of salts on enzymatical production of dimethyl sulfide from *Gyrodinium cohnii*. *Bulletin of the Japanese Society of Scientific Fisheries* **34**: 512-518.

Karsten U, Kuck K, Vogt C, Kirst GO (1996) Dimethylsulfoniopropionate production in phototrophic organisms and its physiological function as a cryoprotectant. In RP Kiene, PT Visscher, MD Keller, GO Kirst, eds, Biological and Environmental Chemistry of DMSP and Related Sulfonium Compounds. Plenum, New York, pp 143-153.

Karsten U, Weincke C, Kirst GO (1992) Dimethylsulphoniopropionate (DMSP) accumulation in green macroalgae from polar to temperate regions: interactive effects of light versus salinity and light versus temperature. *Polar Biology* **12**: 603-607.

Karsten U, Wiencke C, Kirst GO (1991) Growth pattern and β-dimethylsulphoniopropionate (DMSP) content of green macroalgae at different irradiances. *Marine Biology* **108**: 151-155.

Katz ME, Wright JD, Miller KG, Cramer BS, Fennel K, Falkowski PG (2005) Biological overprint of the geological carbon cycle. *Mar. Geol.* **217**: 323-338.

Keller MD, Bellows WK, Guillard RRL (1989) Dimethyl sulfide production in marine phytoplankton. In ES Saltzman, WJ Cooper, eds, Biogenic Sulfur in the Environment. American Chemical Society, Washington, DC, pp 167-182.

Keller MD, Kiene RP, Matrai PA, Bellows WK (1999) Production of glycine betaine and dimethylsulfoniopropionate in marine phytoplankton. II. N-limited chemostat cultures. *Mar. Biol.* **135**: 249-257.

Keller MD, Korjeff-Bellows W (1996) Physiological aspects of the production of dimethylsulfoniopropionate (DMSP) by marine phytoplankton. In RP Kiene, eds, Biological and Environmental Chemistry of DMSP and Related Sulfonium Compounds. Plenum Press, New York, pp 131-142.

Kettle AJ, Andreae MO (2000) Flux of dimethylsulfide from the oceans: a comparison of updated data seas and flux models. *Journal of Geophysical Research-Atmospheres* **105**: 26793-26808.

Kiene RP, Linn LJ, Bruton JA (2000) New and important roles for DMSP in marine microbial communities. *J. Sea Res.* **43**: 209-224.

Kim J, Lee M, Chalam R, Martin MN, Leustek T, Boerjan W (2002) Constitutive overexpression of cystathionine gamma-synthase in Arabidopsis leads to accumulation of soluble methionine and S-methylmethionine. *Plant Physiol.* **128**: 95-107.

Kirst GO (1996) Osmotic adjustment in phytoplankton and macroalgae: The use of dimethylsulfoniopropionate (DMSP). In RP Kiene, PT Visscher, MD Keller, GO Kirst,

eds, Biological and Environmental Chemistry of Dmsp and Related Sulfonium Compounds. pp 121-129.

Kocsis MG, Hanson AD (2000) Biochemical evidence for two novel enzymes in the biosynthesis of 3-dimethylsulfoniopropionate in *Spartina alterniflora*. *Plant Physiology* **123**: 1153-1161.

Kocsis MG, Nolte KD, Rhodes D, Shen TL, Gage DA, Hanson AD (1998) Dimethylsulfoniopropionate biosynthesis in *Spartina alterniflora*. *Plant Physiology* **117**: 273-281.

Kooistra WH, Gersonde R, Medlin LK, Mann DG (2007) The origin and evolution of the diatoms: Their adaptation to a planktonic existence. In P Falkowski, AH Knoll, eds, Evolution of primary producers in the sea. Academic Press, Inc.

Kopriva S, Fritzemeier K, Wiedemann G, Reski R (2007) The putative moss 3 '-phosphoadenosine-5 '-phosphosulfate reductase is a novel form of adenosine-5 '-phosphosulfate reductase without an iron-sulfur cluster. *J. Biol. Chem.* **282**: 22930-22938.

Kopriva S, Muheim R, Koprivova A, Trachsel N, Catalano C, Suter M, Brunold C (1999) Light regulation of assimilatory sulphate reduction in *Arabidopsis thaliana*. *Plant J.* **20**: 37-44.

Kopriva S, Patron N, Keeling P, Leustek T (2008) Phylogenetic analysis of sulfate assimilation and cysteine biosynthesis in phototrophic organisms. In R Hell, C Dahl, D Knaff, T Leustek, eds, Sulfur Metabolism in Phototrophic Organisms. Springer, Dordrecht. **27**, pp 31-58.

Kopriva S, Suter M, von Ballmoos P, Hesse H, Krahenbuhl U, Rennenberg H, Brunold C (2002) Interaction of sulfate assimilation with carbon and nitrogen metabolism in *Lemna minor*. *Plant Physiol.* **130**: 1406-1413.

Koprivova A, North KA, Kopriva S (2008) Complex signaling network in regulation of adenosine 5'-phosphosulfate reductase by salt stress in *Arabidopsis* roots. *Plant Physiol.* **146**: 1408-1420.

Koprivova A, Suter M, Op den Camp R, Brunold C, Kopriva S (2000) Regulation of sulfate assimilation by nitrogen in Arabidopsis. *Plant Physiol.* **122**: 737-746.

Kroth PG, Chiovitti A, Gruber A, Martin-Jezequel V, Mock T, Parker MS, Stanley MS, Kaplan A, Caron L, Weber T, Maheswari U, Armbrust EV, Bowler C (2008) A Model for Carbohydrate Metabolism in the Diatom *Phaeodactylum tricornutum* Deduced from Comparative Whole Genome Analysis. *Plos One* **3**.

Kudela RM, Dugdale RC (2000) Nutrient regulation of phytoplankton productivity in Monterey Bay, California. *Deep-Sea Research Part Ii-Topical Studies in Oceanography* **47**: 1023-1053.

LaRoche J, Breitbarth E (2005) Importance of the diazotrophs as a source of new nitrogen in the ocean. *J. Sea Res.* **53**: 67-91.

Lass B, Ullricheberius CI (1984) Evidence for proton sulfate cotransport and its kinetics in *Lemma gibba* G1. *Planta* **161**: 53-60.

Laudenbach DE, Grossman AR (1991) Characterization and mutagenesis of sulfur-regulated genes in a cyanobacterium: Evidence for function in sulfate transport. *J. Bacteriol.* **173**: 2739-2750.

Lee BR, Koprivova A, Kopriva S (2011) The key enzyme of sulfate assimilation, adenosine 5'-phosphosulfate reductase, is regulated by HY5 in Arabidopsis. *Plant J.* **67**: 1042-1054.

Lee SM, Leustek T (1999) The affect of cadmium on sulfate assimilation enzymes in *Brassica juncea*. *Plant Sci.* **141**: 201-207.

Leustek T, Saito K (1999) Sulfate transport and assimilation in plants. *Plant Physiol.* **120**: 637-643.

Lippemeier S, Hintze R, Vanselow KH, Hartig P, Colijn F (2001) In-line recording of PAM fluorescence of phytoplankton cultures as a new tool for studying effects of fluctuating nutrient supply on photosynthesis. *European Journal of Phycology* **36** 89-100

Loenen WAM (2006) S-adenosylmethionine: jack of all trades and master of everything? *Biochem. Soc. Trans.* **34**: 330-333.

Logan BA, Demmig-Adams B, Rosenstiel TH, Adams WW (1999) Effect of nitrogen limitation on foliar antioxidants in relationship to other metabolic characteristics. *Planta* **209**: 213-220.

Lovelock JE, Maggs RJ, Rasmusse RA (1972) Atmospheric dimethyl sulfide and natural sulfur cycle *Nature* **237**: 452-453.

Malin G, Wilson WH, Bratbak G, Liss PS, Mann NH (1998) Elevated production of dimethylsulphide resulting from viral infection of cultures of *Phaeocystis pouchetii*. *Limnology and Oceanography* **43**: 1389-1393.

Mann DG, Droop SJM (1996) Biodiversity, biogeography and conservation of diatoms. *Hydrobiologia* **336**: 19-32.

Mann KH (1993) Physical oceanography, food chains, and fish stocks - A review. *ICES J. Mar. Sci.* **50**: 105-119.

Martin M, Tarczynski M, Shen B, Leustek T (2005) The role of 5′-adenylylsulfate reductase in controlling sulfate reduction in plants. *Photosynthesis Res.* **86**: 309-323.

McCoy JG, Bailey LJ, Ng YH, Bingman CA, Wrobel R, Weber APM, Fox BG, Phillips GN, Jr. (2009) Discovery of sarcosine dimethylglycine methyltransferase from *Galdieria sulphuraria*. *Proteins-Structure Function and Bioinformatics* **74**: 368-377.

Miller R, Wu GX, Deshpande RR, Vieler A, Gartner K, Li XB, Moellering ER, Zauner S, Cornish AJ, Liu BS, Bullard B, Sears BB, Kuo MH, Hegg EL, Shachar-Hill Y, Shiu

SH, Benning C (2010) Changes in transcript abundance in *Chlamydomonas reinhardtii* following nitrogen deprivation predict diversion of metabolism. *Plant Physiol.* **154**: 1737-1752.

Milligan AJ, Harrison PJ (2000) Effects of non-steady-state iron limitation on nitrogen assimilatory enzymes in the marine diatom *Thalassiosira weissflogii* (Bacillariophyceae). *J. Phycol.* **36**: 78-86.

Mock T, Kroon BMA (2002) Photosynthetic energy conversion under extreme conditions - I: important role of lipids as structural modulators and energy sink under N-limited growth in Antarctic sea ice diatoms. *Phytochemistry* **61**: 41-51.

Mock T, Samanta MP, Iverson V, Berthiaume C, Robison M, Holtermann K, Durkin C, BonDurant SS, Richmond K, Rodesch M, Kallas T, Huttlin EL, Cerrina F, Sussmann MR, Armbrust EV (2008) Whole-genome expression profiling of the marine diatom *Thalassiosira pseudonana* identifies genes involved in silicon bioprocesses. *PNAS* **105**: 1579-1584.

Moellering ER, Benning C (2010) RNA interference silencing of a major lipid droplet protein affects lipid droplet size in *Chlamydomonas reinhardtii*. *Eukaryot. Cell* **9**: 97-106.

Napier JA (2007) The Production of Unusual Fatty Acids in Transgenic Plants. *Annu. Rev. Plant Biol.* **58** 295-319.

Nelson DM, Treguer P, Brzezinski MA, Leynaert A, Queguiner B (1995) Production and dissolution of biogenic silica in the ocean - Revised global estimates, comparison with regional data and relationship to biogenic sedimentation. *Global Biogeochem. Cy.* **9**: 359-372.

Neuenschwander U, Suter M, Brunold C (1991) Regulation of sulfate assimilation by light and O-acetyl-L-serine in *Lemna minor* L. *Plant Physiol.* **97**: 253-258.

Nishiguchi MK, Somero GN (1992) Temperature- and concentration-dependence of compatibility of the organic osmoylte β-dimethylsulfoniopropionate. *Cryobiology* **29**: 118-124.

Noctor G, Foyer CH (1998) Ascorbate and Glutathione: Keeping active oxygen under control. *Annual Review of Plant Physiology Plant Molecular Biology* **49**.

Noctor G, Queval G, Mhamdi A, Chaouch S, Foyer CH (2011) Glutathione. In H Millar, eds, The Arabidopsis Book. The American Society of Plant Biologists, Rockville, MD, pp e0142.

North KA, Ehlting B, Koprivova A, Rennenberg H, Kopriva S (2009) Natural variation in Arabidopsis adaptation to growth at low nitrogen conditions. *Plant Physiol. Biochem.* **47**: 912-918.

Nunn BL, Aker JR, Shaffer SA, Tsai YH, Strzepek RF, Boyd PW, Freeman TL, Brittnacher M, Malmstrom L, Goodlett DR (2009) Deciphering diatom biochemical pathways via whole-cell proteomics. *Aquat. Microb. Ecol.* **55**: 241-253.

Nyyssölä A, Kerovuo J, Kaukinen P, von Weymarn N, Reinikainen T (2000) Extreme halophiles synthesize betaine from glycine by methylation. *J. Biol. Chem.* **275**: 22196-22201.

Ohkama N, Takei K, Sakakibara H, Hayashi H, Yoneyama T, Fujiwara T (2002) Regulation of sulfur-responsive gene expression by exogenously applied cytokinins in *Arabidopsis thaliana*. *Plant and Cell Physiology* **43**: 1493-1501.

Ominato K, Akita H, Suzuki A, Kijima F, Yoshino T, Yoshino M, Chiba Y, Onouchi H, Naito S (2002) Identification of a short highly conserved amino acid sequence as the functional region required for posttranscriptional autoregulation of the cystathionine gamma-synthase gene in *Arabidopsis*. *J. Biol. Chem.* **277**: 36380-36386.

Palmer JD, Soltis DE, Chase MW (2004) The plant tree of life: An overview and some points of view. *Am. J. Bot.* **91**: 1437-1445.

Palmucci M, Ratti S, Giordano M (2011) Ecological and evolutionary implications of carbon allocation in marine phytoplankton as a function of nitrogen availability: A fourier transform infrared spectroscopy approach. *J. Phycol.* **47**: 313-323.

Pappin DJC, Hojrup P, Bleasby AJ (1993) Rapid identification of proteins by peptide-mass fingerprinting. *Curr. Biol.* **3**: 327-332.

Park S, Imlay JA (2003) High levels of intracellular cysteine promote oxidative DNA damage by driving the Fenton reaction. *J. Bacteriol.* **185**: 1942-1950.

Parker MS, Armbrust EV (2005) Synergistic effects of light, temperature, and nitrogen source on transcription of genes for carbon and nitrogen metabolism in the centric diatom *Thalassiosira pseudonana* (Bacillariophyceae). *J. Phycol.* **41**: 1142-1153.

Parker MS, Mock T, Armbrust EV (2008) Genomic insights into marine microalgae. *Annu. Rev. Genet.* **42**: 619-645.

Patron NJ, Durnford DG, Kopriva S (2008) Sulfate assimilation in eukaryotes: fusions, relocations and lateral transfers. *BMC Evol. Biol.* **8**: 39.

Paul VJ, Van Alstyne KL (1992) Activation of chemical defenses in the tropical green algae *Halimeda* spp. *Journal of Experimental Marine Biology and Ecology* **160** 191-203.

Peers G, Milligan AJ, Harrison PJ (2000) Assay optimisation of urease activity in two marine diatoms. *J. Phycol.* **36**: 523-528.

Peng MS, Bi YM, Zhu T, Rothstein SJ (2007) Genome-wide analysis of *Arabidopsis* responsive transcriptome to nitrogen limitation and its regulation by the ubiquitin ligase gene *NLA*. *Plant Mol. Biol.* **65**: 775-797.

Pokerny M, Marchenko E, Keglevic D (1970) Comparative studies of L- and D-methionine metabolism in lower and higher plants. *Phytochemistry* **9**: 2175-2188.

Porter KG, Feig YS (1980) The use of DAPI for identifying and counting aquatic microflora. *Limnol. Oceanogr.* **25**: 943-948.

Poulsen N, Kroger N (2005) A new molecular tool for transgenic diatoms - Control of mRNA and protein biosynthesis by an inducible promoter-terminator cassette. *FEBS J.* **272**: 3413-3423.

Queval G, Thominet D, Vanacker H, Miginiac-Maslow M, Gakiere B, Noctor G (2009) H_2O_2-Activated up-regulation of glutathione in *Arabidopsis* involves induction of genes encoding enzymes involved in cysteine synthesis in the chloroplast. *Molecular Plant* **2**: 344-356.

Rajagopal S, Joly D, Gauthier A, Beauregard M, Carpentier R (2005) Protective effect of active oxygen scavengers on protein degradation and photochemical function in photosystem I submembrane fractions during light stress. *FEBS J.* **272**: 892-902.

Ratti S, Knoll AH, Giordano M (2011) Did sulfate availability facilitate the evolutionary expansion of chlorophyll a+c phytoplankton in the oceans? *Geobiology* **9**: 301-312.

Raven JA (1985) Regulation of pH and generation of osmolarity in vascular plants - A cost-benefit analysis in relation to efficiency of use of energy, nitrogen and water. *New Phytol.* **101**: 25-77.

Roberts K, Granum E, Leegood RC, Raven JA (2007) C_3 and C_4 pathways of photosynthetic carbon assimilation in marine diatoms are under genetic, not environmental, control. *Plant Physiol.* **145**: 230-235.

Robertson DL, Alberte RS (1996) Isolation and characterization of glutamine synthetase from the marine diatom *Skeletonema costatum*. *Plant Physiol.* **111**: 1169-1175.

Robertson DL, Smith GJ, Alberte RS (1999) Characterization of a cDNA encoding glutamine synthetase from the marine diatom *Skeletonema costatum* (Bacillariophyceae). *J. Phycol.* **35**: 786-797.

Robertson DL, Tartar A (2006) Evolution of glutamine synthetase in heterokonts: Evidence for endosymbiotic gene transfer and the early evolution of photosynthesis. *Mol. Biol. Evol.* **23**: 1048-1055.

Ruffet ML, Droux M, Douce R (1994) Purification and kinetic-properties of serine acetyltransferase free of O-acetylserine(thiol)lyase from spinach chloroplasts. *Plant Physiol.* **104**: 597-604.

Saito K, Kurosawa M, Tatsuguchi K, Takagi Y, Murakoshi I (1994) Modulation of Cysteine Biosynthesis in Chloroplasts of Transgenic Tobacco Overexpressing Cysteine Synthase [O-Acetylserine(thiol)-Iyase]. *Plant Physiol.* **106**: 887-895.

Sauer J, Dirmeier U, Forchhammer K (2000) The *Synechococcus* strain PCC 7942 glnN product (glutamine synthetase III) helps recovery from prolonged nitrogen chlorosis. *J. Bacteriol.* **182**: 5615-5619.

Scheerer U, Haensch R, Mendel RR, Kopriva S, Rennenberg H, Herschbach C (2010) Sulphur flux through the sulphate assimilation pathway is differently controlled by adenosine 5'-

phosphosulphate reductase under stress and in transgenic poplar plants overexpressing *γ-ECS*, *SO*, or *APR*. *J. Exp. Bot.* **61**: 609-622.

Schmid A-MM (2003) Endobacteria in the diatom *Pinnularia* (Bacillariophyceae). I. "Scattered ct-nucleoids" explained: DAPI-DNA complexes stem from expplastidial bacteria boring into the chloroplasts. *J. Phycol.* **39**: 122-138.

Schupp R, Rennenberg H (1988) Diurnal changes in the glutathione content of spruce needled (*Picea Abies* L). *Plant Sci.* **57**: 113-117.

Schwender J, Shachar-Hill Y, Ohlrogge JB (2006) Mitochondrial metabolism in developing embryos of *Brassica napus*. *J. Biol. Chem.* **281**: 34040-34047.

Sheets EB, Rhodes D (1996) Determination of DMSP and other onium compounds in *Tetraselmis subcordiformis* by plasma desorption mass spectrometry. In RP Kiene, PT Visscher, MD Keller, GO Kirst, eds, Biological and Environmental Chemistry of DMSP and Related Sulfonium Compounds. Plenum, New York, pp 55-63.

Shibagaki N, Grossman A (2008) The state of sulfur metabolism in algae: from ecology to genomics. In R Hell, C Dahl, D Knaff, T Leustek, eds, Sulfur Metabolism in Phototrophic Organisms. Springer, Dordrecht. **27**, pp 231-267.

Siaut M, Heijde M, Mangogna M, Montsant A, Coesel S, Allen A, Manfredonia A, Falciatore A, Bowler C (2007) Molecular toolbox for studying diatom biology in *Phaeodactylum tricornutum*. *Gene* **406**: 23-35.

Sieburth JM (1960) Acrylic acid, an "antibiotic" principle in *Phaeocystis* blooms in Antarctic waters *Science* **132**: 676-677.

Simó R (2001) Production of atmospheric sulfur by oceanic plankton: biogeochemical, ecological and evolutionary links. *Trends in Ecology & Evolution* **16**: 287-294.

Simó R, Archer SD, Pedros-Alio C, Gilpin L, Stelfox-Widdicombe CE (2002) Coupled dynamics of dimethylsulfoniopropionate and dimethylsulfide cycling and the microbial food web in surface waters of the North Atlantic. *Limnol. Oceanogr.* **47**: 53-61.

Simó R, Pedrós-Alió C (1999) Role of vertical mixing in controlling the oceanic production of dimethyl sulphide. *Nature* **402**: 396-399.

Sims PA, Mann DG, Medlin LK (2006) Evolution of the diatoms: insights from fossil, biological and molecular data. *Phycologia* **45**: 361-402.

Sorhannus U (2007) A nuclear-encoded small-subunit ribosomal RNA timescale for diatom evolution. *Mar. Micropaleontol.* **65**: 1-12.

Stefels J (2000) Physiological aspects of the production and conversion of DMSP in marine algae and higher plants. *Journal of Sea Research* **43**: 183-197.

Stefels J, Dacey JWH, Elzenga JTM (2009) In vivo DMSP-biosynthesis measurements using stable-isotope incorporation and proton-transfer-reaction mass spectrometry (PTR-MS). *Limnology and Oceanography-Methods* **7**: 595-611.

Stefels J, Dijkhuizen L (1996) Characteristics of DMSP-lyase in *Phaeocystis* sp. (Prymnesiophyceae). *Marine Ecology Progress Series* **131**: 307-313.

Stefels J, Steinke M, Turner S, Malin G, Belviso S (2007) Environmental constraints on the production and removal of the climatically active gas dimethylsulphide (DMS) and implications for ecosystem modelling. *Biogeochemistry* **83**: 245-275.

Stefels J, Van Leeuwe MA (1998) Effect of iron and light stress on the biochemical composition of Antarctic *Phaeocystis* sp. (Prymnesiophyceae). I. Intracellular DMSP concentrations. *Journal of Phycology* **34**: 486-495.

Summers PS, Nolte KD, Cooper AJL, Borgeas H, Leustek T, Rhodes D, Hanson AD (1998) Identification and stereospecificity of the first three enzymes of 3-dimethylsulfoniopropionate biosynthesis in a chlorophyte algae. *Plant Physiol.* **116**: 369-378.

Sunda W, Kieber DJ, Kiene RP, Huntsman S (2002) An antioxidant function for DMSP and DMS in marine algae. *Nature* **418**: 317-320.

Sung D-Y, Lee D, Harris H, Raab A, Feldmann J, Meharg A, Kumabe B, Komives EA, Schroeder JI (2007) Identification of an arsenic tolerant double mutant with a thiol-mediated component and increased arsenic tolerance in phyA mutants. *Plant J.* **49**: 1064-1075.

Suzuki K, Kuwata A, Yoshie N, Shibata A, Kawanobe K, Saito H (2011) Population dynamics of phytoplankton, heterotrophic bacteria, and viruses during the spring bloom in the western subarctic Pacific. *Deep-Sea Research Part I-Oceanographic Research Papers* **58**: 575-589.

Sweetlove LJ, Beard KFM, Nunes-Nesi A, Fernie AR, Ratcliffe RG (2010) Not just a circle: Flux modes in the plant TCA cycle. *Trends Plant Sci.* **15**: 462-470.

Takabayashi M, Wilkerson FP, Robertson D (2005) Response of glutamine synthetase gene transcription and enzyme activity to external nitrogen sources in the diatom *Skeletonema costatum* (Bacillariophyceae). *J. Phycol.* **41**: 84-94.

Takahashi H, Kopriva S, Giordano M, Saito K, Hell R (2011) Sulfur Assimilation in Photosynthetic Organisms: Molecular Functions and Regulations of Transporters and Assimilatory Enzymes. In SS Merchant, WR Briggs, D Ort, eds, Annu. Rev. Plant Biol. **62**, pp 157-184.

Tanaka R, Oster U, Kruse E, Rudiger W, Grimm B (1999) Reduced activity of geranylgeranyl reductase leads to loss of chlorophyll and tocopherol and to partially geranylgeranylated chlorophyll in transgenic tobacco plants expressing antisense RNA for geranylgeranyl reductase. *Plant Physiol.* **120**: 695-704.

Thomas D, Cherest H, Surdinkerjan Y (1991) Identification of the structural gene for glucose-6-phosphate-dehydrogenase in yeast. Inactivation Leads to a nutritional-requirement for organic sulfur. *EMBO J.* **10**: 547-553.

Thompson GA, Datko AH, Mudd SH, Giovanelli J (1982) Methionine biosynthesis in *Lemna* - Studies on the regulation of cystathionine gamma-synthase, O-phosphohomoserine sulfhydrylase, and O-acetylserine suldhydrylase. *Plant Physiol.* **69**: 1077-1083.

Todd JD, Curson ARJ, Dupont CL, Nicholson P, Johnston AWB (2009) The *dddP* gene, encoding a novel enzyme that converts dimethylsulfoniopropionate into dimethyl sulfide, is widespread in ocean metagenomes and marine bacteria and also occurs in some Ascomycete fungi. *Environ. Microbiol.* **11**: 1376-1385.

Tolonen AC, Aach J, Lindell D, Johnson ZI, Rector T, Steen R, Church GM, Chisholm SW (2006) Global gene expression of *Prochlorococcus* ecotypes in response to changes in nitrogen availability. *Mol. Syst. Biol.* **2**: 53.

Trossat C, Nolte KD, Hanson AD (1996) Evidence that the pathway of dimethylsulfoniopropionate biosynthesis begins in the cytosol and ends in the chloroplast. *Plant Physiology* **111**: 965-973.

Udvardi MK, Czechowski T, Scheible W-R (2008) Eleven golden rules of quantitative RT-PCR. *Plant Cell* **20**: 1736-1737.

Vairavamurthy A, Andreae MO, Iverson RL (1985) Biosynthesis of dimethylsulfide and dimethylpropiothetin by *Hymenomonas carterae* in relation to sulfur source and salinity variations. *Limnology and Oceanography* **30**: 59-70.

Van Bergeijk S, Van Der Zee C, Stal L (2003) Uptake and Excretion of dimethylsulphoniopropionate is driven by salinity changes in the benthic diatom *Cylindrotheca closterium*. *European Jounal of Phycology* **38**: 341-349.

van Rijssel M, Gieskes W (2002) Temperature, light, and the dimethylsulfoniopropionate (DMSP) content of *Emiliania huxleyi* (Prymnesiophyceae). *Journal of Sea Research* **48**: 17-27.

Vandesompele J, De Preter K, Pattyn F, Poppe B, Van Roy N, De Paepe A, Speleman F (2002) Accurate normalization of real-time quantitative RT-PCR data by geometric averaging of multiple internal control genes. *Genome biology* **3**: RESEARCH0034.

Vardi A, Berman-Frank I, Rozenberg T, Hadas O, Kaplan A, Levine A (1999) Programmed cell death of the dinoflagellate *Peridinium gatunense* is mediated by CO_2 limitation and oxidative stress. *Current Biology* **9**: 1061-1064.

Vauclare P, Kopriva S, Fell D, Suter M, Sticher L, von Ballmoos P, Krähenbühl U, den Camp RO, Brunold C (2002) Flux control of sulphate assimilation in *Arabidopsis thaliana*: adenosine 5'-phosphosulphate reductase is more susceptible than ATP sulphurylase to negative control by thiols. *The Plant Journal* **31**: 729-740.

Vergara JJ, Berges JA, Falkowski PG (1998) Diel periodicity of nitrate reductase activity and protein levels in the marine diatom *Thalassiosira weissflogii* (Bacillariophyceae). *J. Phycol.* **34**: 952-961.

Waditee R, Tanaka Y, Aoki K, Hibino T, Jikuya H, Takano J, Takabe T (2003) Isolation and functional characterization of N-methyltransferases that catalyze betaine synthesis from glycine in a halotolerant photosynthetic organism *Aphanothece halophytica*. *J. Biol. Chem.* **278**: 4932-4942.

Wang ZT, Ullrich N, Joo S, Waffenschmidt S, Goodenough U (2009) Algal lipid bodies: Stress induction, purification, and biochemical characterization in wild-type and starchless *Chlamydomonas reinhardtii*. *Eukaryot. Cell* **8**: 1856-1868.

Watson AJ, Liss PS (1998) Marine biological controls on climate via the carbon and sulphur geochemical cycles. *Philosophical Transactions of the Royal Society London B* **353**: 41-51.

Westerman S, Stulen I, Suter M, Brunold C, De Kok LJ (2001) Atmospheric H_2S as sulphur source for *Brassica oleracea*: Consequences for the activity of the enzymes of the assimilatory sulphate reduction pathway. *Plant Physiol. Biochem.* **39**: 425-432.

Wingler A, Purdy S, MacLean JA, Pourtau N (2006) The role of sugars in integrating environmental signals during the regulation of leaf senescence. *J. Exp. Bot.* **57**: 391-399.

Wirtz M, Hell R (2006) Functional analysis of the cysteine synthase protein complex from plants: Structural, biochemical and regulatory properties. *J. Plant Physiol.* **163**: 273-286.

Wolfe GV, Steinke M (1996) Grazing-activated production of dimethylsulfide (DMS) by two clones of *Emiliania huxleyi*. *Limnology and Oceanography* **41**: 1151-1160.

Wolfe GV, Steinke M, Kirst GO (1997) Grazing-activated chemical defence in unicellular marine algae. *Nature* **387**: 894-897.

Wolfe GV, Strom SL, Holmes JL, Radzio T, Olson MB (2002) Dimethylsulfoniopropionate cleavage by marine phytoplankton in response to mechanical, chemical, or dark stress. *J. Phycol.* **38**: 948-960.

Wykoff DD, Davies JP, Melis A, Grossman A (1998) The regulation of photosynthetic electron transport during nutrient deprivation in *Chlamydomonas reinhardtii*. *Plant Physiol.* **117**: 129-139.

Yamamoto Y (2001) Quality Control of Photosystem II. *Plant and Cell Physiology* **42**: 121-128.

Yoon HS, Hackett JD, Ciniglia C, Pinto G, Bhattacharya D (2004) A molecular timeline for the origin of photosynthetic eukaryotes. *Mol. Biol. Evol.* **21**: 809-818.

Zadykowicz E, Robertson D (2005). Phylogenetic relationships amongst glutamate synthase enzymes. 44th Northeast Algal Symposium, Rockland, Maine, pp 41.

Zehr JP, Ward BB (2002) Nitrogen cycling in the ocean: New perspectives on processes and paradigms. *Appl. Environ. Microbiol.* **68**: 1015-1024.

Zolla L, Rinalducci S (2002) Involvement of Active Oxygen Species in Degradation of Light-Harvesting Proteins under Light Stresses. *Biochemistry* **41**: 14391-14402.

Appendix Table 1

Proteins that changed (>1.5 fold, P<0.005) in abundance in nitrogen starved Thalassiosira pseudonana, compared to nitrogen replete cultures. Identification was made by mass fingerprint and the calibrated spectra were searched against a monthly updated copy of the SPtrEMBL database, using an in-house version (v2.2) of the MASCOT search tool (reference: http://www.matrixscience.com), a mascot score > 53 indicates a possitive identification. In cases where a predicted protein was returned a function was assigned manually (M) using PFAM conserved domains (C) and NCBI BlastP (B). * indicates that more than one protein was identified in a spot and the fold change should therefore not be concidered accurate.

UniProt ID	JGI Protein ID	Protein name	Protein Mass (kD)	Protein isoelectric point	Spot	Number of peptides	% cover of Peptides	Mascot Score	Fold Change			t-test (P)		
									N	S	L	N	S	L
B8LET6	bd1563	ATP synthase subunit beta	51168	4.7	ID: 02786	29	75	302	-1.7	-1.0	-1.2	0.0002	0.4137	0.0022
					ID: 02789	15	43	188	-2.0	-1.6	-1.2	0.0007	0.0388	0.1535
B8LEV1	bd1048	Photosystem I iron-sulfur center [MB]	9305	5.6	ID: 08933	6	54	80	1.0	-1.2	-2.6	0.2815	0.0132	0.0004
B5YLU3	30385	Fucoxanthin chlorophyll a/c protein-LI818 clad	21306	4.9	ID: 05948	6	32	72	-1.2	-1.2	-2.5	0.1386	0.1856	0.0002
B5YM25	25402	Fucoxanthin chl a/c light-harvesting protein	21698	5.1	ID: 06516	5	36	69	-1.0	1.2	-3.6	0.3946	0.3275	0.0001
B5YMM4	270312	1-deoxy-D-xylulose-5-phosphate synthase [MB]	81321	5.7	ID: 01635	11	16	144	-2.1	1.3	-1.4	0.0004	0.0162	0.0124
B5YMQ0	258111	Glutamate-1-semialdehyde aminotransferase [MB]	49604	5.4	ID: 03285	25	51	525	-1.6	1.0	1.5	0.0047	0.3800	0.0110
B5YMV4	23452	Predicted protein	23962	6.9	ID: 05366	6	30	54	-1.4	3.6	1.0	0.0775	0.0005	0.4497
B8BPY6	1093	Predicted protein	92131	5.2	ID: 04950	10	17	68	1.5	-1.4	-1.2	0.0027	0.0806	0.1079
B8BQI4	31636	Aldose-1-epimerase	30601	4.3	ID: 03860	7	30	91	-2.4	-1.2	1.0	0.0011	0.1541	0.4219
B8BQQ3	20797	S-adenosylmethionine (SAM)-dependent Methyltransferase [MBC]	65523	4.9	ID: 02108	17	35	132	-1.7	3.6	1.2	0.0153	0.0017	0.1000
					ID: 02177	19	39	165	-3.0	3.6	1.3	0.0136	0.0027	0.0535
B8BQU3	26678	Transketolase	78558	5.9	ID: 01532	13	20	108	1.6	1.1	-1.0	0.0025	0.2052	0.2801
B8BQU4	260934	Branched-chain-amino-acid aminotransferase	42523	6.6	ID: 03027	8	15	58	6.4	1.3	-1.2	0.0001	0.1580	0.1778
B8BR03	1456	Isocitrate dehydrogenase	74331	5.7	ID: 01338	24	41	192	1.6	1.5	-1.2	0.0035	0.0128	0.0567
B8BRD0	39187	T-complex protein 1 gamma subunit	62273	5.5	ID: 02032	18	28	112	-1.1	1.4	1.5	0.1809	0.0043	0.0014
B8BRY4	20993	Heat shock protein HslVU, ATPase	60517	5.1	ID: 03083	13	22	100	1.4	1.3	1.2	0.0013	0.0370	0.0008
B8BTJ8	26941	NADPH nitrite reductase	110842	5.0	ID: 00415	8	8	98	-3.0	1.6	-1.6	0.0001	0.0711	0.0408
B8BTR4	21175	Transketolase	72061	5.0	ID: 01527	28	48	242	-1.6	1.1	-1.2	0.0045	0.1595	0.0112
					ID: 01603	24	44	201	-1.1	-1.4	3.2	0.1264	0.0738	0.0023
B8BU42	21235	RS1, ribosomal protein 1 [MC]	42355	5.6	ID: 03933	14	39	184	-2.0	1.3	-1.0	0.0005	0.0153	0.4157
B8BUF7	21290	N-acetyl-gamma-glutamyl-phosphate reductase	38732	5.0	eID: 00030	7	23	105	1.7	-1.0	1.0	0.0005	0.3905	0.3087
B8BUM6	268280	Dihydrolipoamide s-acetyltransferase	52743	4.6	ID: 02250	10	21	135	1.9	-1.3	-1.5	0.0006	0.0839	0.1360
B8BVN4	268374	Pyruvate dehydrogenase	42216	6.1	ID: 03732	11	38	98	2.3	1.3	1.1	0.0022	0.0697	0.2393
					eID: 00021	9	30	67	1.8	1.2	1.3	0.0008	0.0885	0.0356
B8BVR6	31912	Cyclophilin-type peptidyl-prolyl cis-trans isomerase	18740	4.9	ID: 06620	7	48	71	1.0	-1.9	-2.9	0.4197	0.0982	0.0005
					ID: 06656	6	52	79	1.7	-1.1	-1.0	0.0046	0.2868	0.3994
B8BVS6	27273	Methylenetetrahydrofolate reductase	42718	5.0	ID: 03284	14	46	128	1.0	1.9	1.5	0.4366	0.0031	0.0020
B8BW15	270378	Magnesium-protoporphyrin IX methyltransferase [MBC]	29696	5.4	ID: 05572	9	34	86	-2.7	1.0	-1.3	0.0001	0.4490	0.0924
B8BWJ8	32805	ATPase AAA [MBC]	23235	5.5	ID: 02195	8	39	91	1.8	1.1	1.1	0.0017	0.1903	0.0986
					ID: 07071	12	56	108	1.6	1.3	-1.1	0.0011	0.1727	0.2215
B8BWS4	21595	PDZ domain containing protein [MC]	119695	4.6	ID: 00886	16	19	74	2.2	-1.1	2.3	0.0039	0.3856	0.0008
					ID: 00890	9	7	56	2.1	-1.2	1.5	0.0025	0.1754	0.0053
					ID: 00863	18	19	122	1.9	-1.5	1.7	0.0020	0.1433	0.0089
B8BWT1	39767	5-hydroxyisourate hydrolase	38224	5.4	ID: 03818	11	38	90	2.0	-1.2	1.2	0.0002	0.0595	0.1432
B8BX37	21640	Isocitrate dehydrogenase [MBC]	62818	6.1	ID: 02652	14	30	100	1.5	1.2	1.2	0.0042	0.0928	0.0369
					ID: 02653	24	43	200	1.7	1.2	1.3	0.0001	0.0525	0.0363
B8BXV5	3463	Predicted protein	27309	4.4	ID: 04351	8	38	78	1.1	-1.5	2.4	0.2128	0.0077	0.0002
B8BY55	21815	S-adenosylmethionine synthetase	50954	5.1	ID: 02825	29	72	311	-1.4	2.9	1.1	0.0122	0.0001	0.1684
B8BYQ5	21916	Predicted protein	59917	5.1	ID: 02405	13	31	113	1.6	-1.2	1.1	0.0019	0.1308	0.1144
B8BYV1	21939	Predicted protein	58248	6.2	ID: 06361	6	19	58	1.9	-1.1	-1.3	0.0037	0.0266	0.1272
B8BYW8	268546	Phosphoenolpyruvate carboxylase	98264	5.5	ID: 00564	35	40	299	2.5	1.7	1.4	0.0010	0.0726	0.0120
					ID: 00587	16	20	107	2.0	1.5	1.4	0.0140	0.0903	0.0088
					ID: 00573	34	39	322	1.8	1.3	1.3	0.0021	0.0698	0.0017
					ID: 00569	31	35	281	2.5	1.2	1.6	0.0001	0.0005	0.0006
					eID: 00032*	32	40	399	1.6	1.7	1.5	0.0027	0.0040	0.0259
B8LCG0	30193	Urease	86349	5.2	eID: 00032*	19	32	399	1.6	1.7	1.5	0.0027	0.0040	0.0259
B8BZ06	262125	Nitrite reductase-ferredoxin dependent	60279	5.5	ID: 02043	9	21	91	-2.0	1.3	1.7	0.0010	0.0126	0.0025
					ID: 02033	19	37	184	-3.0	1.4	-1.4	0.0000	0.0136	0.0035
					eID: 00011	21	44	152	-1.7	1.4	1.3	0.0011	0.0415	0.1090
					ID: 02015	26	47	299	-3.7	2.2	-1.3	0.0001	0.0004	0.0165
B8BZ35	22208	Class V aminotransferase [MBC]	51899	6.2	ID: 03429	9	23	84	1.9	1.0	-1.1	0.0020	0.4020	0.1054
					eID: 00041	22	56	210	1.7	-1.5	-1.3	0.0106	0.0099	0.0016
B8BZ41	22213	Phosphofructokinase	44168	5.5	ID: 03214	20	63	219	1.4	1.5	-1.1	0.0042	0.0093	0.0519
B8BZ70	27850	Phosphoglycerate mutase	32559	5.9	ID: 04977	14	43	176	1.8	1.0	-1.1	0.0024	0.4059	0.0759
B8BZG6	13254	RNA helicase	50273	7.3	ID: 01041	16	40	127	-2.3	1.2	-1.2	0.0012	0.3104	0.2812
B8BZI8	270365	Suphite reductase [MBC]	76723	6.2	ID: 02276	31	45	276	1.6	1.2	1.1	0.0016	0.1578	0.2229
B8BZK1	22301	Phosphomannomutase	28573	4.8	ID: 04849	16	67	182	1.7	1.1	-1.2	0.0004	0.2421	0.1340
B8BZT5	40391	Enolase	46973	4.8	ID: 02947	19	58	242	1.5	-1.0	-1.1	0.0025	0.3591	0.0078
B8BZX9	33709	RNA binding protein [MBC]	8770	5.3	ID: 03876	7	64	79	-1.9	-1.3	1.1	0.0005	0.0368	0.0627
B8C0H3	22464	Fumarate hydratase	68151	6.1	ID: 02295	11	28	139	2.5	-1.0	1.1	0.0001	0.3556	0.1640

B8C0L1	40522	Vacuolar ATPase	56085	5.8	ID: 02722	26	63	267	1.5	-1.0	1.1	0.0019	0.3838	0.2814
B8C1A4	262083	ABC cassette-containing protein	104747	6.1	ID: 00283	28	31	179	-1.9	2.0	-1.1	0.0044	0.1153	0.3425
B8C247	28241	Glyceraldehyde 3-phosphate dehydrogenase	36504	5.8	ID: 03925	12	35	182	1.1	1.4	1.4	0.0035	0.0065	0.0241
					ID: 03950	11	40	136	1.8	-2.2	-1.3	0.0832	0.0005	0.1008
B8C2G9	22671	Predicted Protein	70858	5.4	ID: 01668	16	31	98	2.0	1.4	1.5	0.0186	0.0108	0.0119
B8C2J5	40713	Superoxide dismutase	25940	6.2	ID: 05533	4	23	57	1.9	1.2	1.3	0.0031	0.0949	0.0342
B8C2Y4	22747	Fucoxanthin chlorophyll a/c light-harvesting protein	23343	6.5	ID: 06393	8	48	72	-1.0	1.0	-3.5	0.4740	0.4651	0.0002
B8C303	28334	Glyceraldehyde-3-phosphate dehydrogenase	36949	5.9	ID: 03819	16	53	160	1.8	-2.9	-1.6	0.0598	0.0015	0.0564
					ID: 03827	10	44	90	1.7	-4.1	-1.6	0.0833	0.0014	0.1013
B8C306	22763	Predicted protein	91375	4.7	ID: 00786	7	8	59	1.8	-1.2	2.2	0.0046	0.2661	0.0227
B8C3V9	268965	Aconitase hydratase 2	95104	4.8	ID: 00568	32	44	254	1.7	1.1	1.3	0.0007	0.2612	0.0548
					ID: 00586	33	46	309	1.6	1.4	1.2	0.0009	0.0416	0.1270
B8C469	269148	Translation factor tu domain 2	92739	5.9	ID: 00796	11	13	115	-1.9	1.1	-1.1	0.0027	0.1808	0.2896
					ID: 00801	19	26	101	-1.7	-1.4	-1.2	0.0050	0.0066	0.1992
B8C4A8	269160	Glutamate synthase, NADH/NADPH, small subunit [MB]	51537	5.2	ID: 02241	11	23	108	2.9	-2.6	1.8	0.0012	0.0017	0.0110
					ID: 02242	9	17	91	1.7	-1.1	1.0	0.0003	0.2708	0.4555
					ID: 02252	18	40	197	1.8	1.1	1.1	0.0031	0.3174	0.0312
B8C4K5	34592	Oxidoreductase [MBC]	32394	6.3	ID: 03725	11	46	113	1.7	1.2	-1.0	0.0002	0.1110	0.3725
B8C553	28496	Adenosylhomocysteinase	53073	5.1	eID: 00034	33	61	338	-1.7	2.6	1.3	0.0022	0.0023	0.0243
B8C5E0	28544	Dihydrodipicolinate reductase [MBC]	31856	4.7	ID: 03994	20	85	221	1.6	1.1	1.1	0.0021	0.2026	0.0839
B8C631	270288	Fructose-bisphosphate aldolase [MBC]	43473	5.4	ID: 03460	7	15	70	1.8	-1.1	1.2	0.0036	0.0873	0.0219
					ID: 03417	12	28	124	1.8	-1.1	1.0	0.0006	0.0185	0.2027
					ID: 03418	15	35	102	1.7	1.1	-1.0	0.0019	0.1341	0.3520
					ID: 03444	13	38	122	1.8	1.1	1.2	0.0033	0.2039	0.0564
B8C637	6285	HSP90 family member	80647	4.7	ID: 01239	12	21	127	-1.0	2.3	1.1	0.3630	0.0031	0.2137
B8C663	23175	Acetolactate synthase [MB]	90246	5.5	ID: 01262	8	10	92	-2.0	1.4	-1.5	0.0048	0.0828	0.0172
B8C7D5	29228	1-hydroxy-2-methyl-2-(E)-butenyl-4-diphosphate synthase [MBC]	76371	4.9	ID: 01616	20	30	154	-2.0	-1.2	1.1	0.0005	0.1084	0.3160
B8C7T0	7883	Predicted protein	32398	4.9	ID: 04937	9	30	109	1.8	-2.1	1.3	0.0046	0.0331	0.0028
B8C871	644	Adenosine kinase	36444	4.7	eID: 00002	9	42	104	1.1	2.3	1.2	0.1847	0.0000	0.0129
B8C8K9	15259	RS1, ribosomal protein 1	31921	4.6	ID: 03217	9	35	96	-2.9	-1.6	1.4	0.0014	0.0539	0.0206
					ID: 03167	12	48	147	-3.4	-1.3	1.2	0.0000	0.0196	0.0082
B8C8L8	24060	Oxidoreductase [MC]	48598	4.9	ID: 02971	9	23	72	-2.0	1.1	1.0	0.0014	0.2218	0.4107
					eID: 00027	8	18	69	-2.4	1.1	-1.8	0.0001	0.2012	0.0031
B8C8Q0	24080	Fucoxanthin chl a/c light-harvesting protein, Ihcr type	21823	5.1	ID: 06190	5	28	61	-1.1	1.2	-2.4	0.2963	0.3389	0.0024
B8CB34	37071	Orotate phosphoribosyltransferase [MB]	23899	5.5	ID: 02500	9	56	75	1.7	1.1	-1.0	0.0004	0.2273	0.4754
B8CBE7	9467	Predicted protein	28683	5.5	ID: 05329	11	49	121	1.4	-1.4	1.4	0.0491	0.0031	0.0016
B8CC92	24812	Oxidoreductase [MC]	48349	6.0	eID: 00035	13	43	115	2.1	1.4	1.5	0.0049	0.0123	0.0088
B8CCN5	37294	Putative uncharacterized protein; Flags: Fragm	63400	8.3	ID: 01353	19	30	133	-1.7	-1.1	-1.7	0.0006	0.0967	0.0030
B8CCT7	42475	Succinate dehydrogenase flavoprotein subunit	69717	5.6	ID: 02077	9	16	57	1.9	-1.1	1.3	0.0042	0.0276	0.0209
					ID: 02072	16	27	121	1.8	-1.2	1.1	0.0020	0.0060	0.2887
B8CDB3	10234	Geranyl-geranyl reductase [MB]	47599	5.8	eID: 00012	17	46	208	-2.3	1.1	-1.3	0.0006	0.1314	0.0450
					ID: 02974	24	70	221	-1.9	-1.0	-1.1	0.0025	0.4072	0.1679
B8CDN8	10270	Predicted protein	46528	9.9	ID: 05573	7	16	59	-2.5	2.2	2.6	0.0021	0.0515	0.0026
B8CEC4	25299	Nitrate reductase [MBC]	102141	5.8	ID: 00667	13	12	122	-8.8	2.9	-1.1	0.0000	0.0623	0.2973
					ID: 00662	9	11	78	-10.7	3.3	-1.2	0.0000	0.0642	0.2884
					ID: 00660	16	19	152	-9.7	2.1	1.1	0.0000	0.0705	0.3166
B8CEG2	11411	Citrate synthase	52578	6.2	ID: 03207	11	21	113	1.8	1.4	1.0	0.0004	0.0171	0.4388
					ID: 03234	9	21	126	2.2	-1.3	1.0	0.0043	0.1413	0.4636
B8CF37	38428	Mitochondrial alternative oxidase	25599	6.3	ID: 03877	10	47	55	2.2	-1.0	1.2	0.0011	0.4563	0.0270
B8CFH4	30659	Metallo-beta-lactamase family protein [MBC]	32592	4.8	ID: 04361	18	54	183	1.6	1.6	1.0	0.0041	0.0458	0.4122
					ID: 04362	16	55	172	1.7	1.1	1.0	0.0001	0.1320	0.4859
B8CFW3	38583	Fucoxanthin chlorophyll a/c protein 1	20341	4.5	eID: 00065	5	40	69	1.0	-1.4	-2.4	0.4380	0.0006	0.0001
B8CGH5	270136	N-acetylornithine aminotransferase	51285	5.6	ID: 03184	13	31	185	2.4	1.5	-1.0	0.0001	0.0110	0.2526
B8CGK1	270138	Glutamine synthetase type III [MBC]	69526	5.1	ID: 01701	17	37	138	1.6	1.5	1.2	0.0023	0.0060	0.1263
					ID: 01666	33	59	284	1.6	1.3	-1.1	0.0009	0.0029	0.0892
					ID: 01678	25	41	216	1.5	1.5	-1.0	0.0006	0.0068	0.1509
B8CGM1	866	ATP-dependent Clp protease proteolytic subunit	21727	4.2	ID: 05251	8	43	81	1.1	-2.9	-1.2	0.1983	0.0067	0.0143
B8LBP8	8672	Predicted protein	28333	5.7	ID: 04982	6	24	87	2.4	1.3	1.0	0.0002	0.0398	0.4625
B8LC08	8778	Pyruvate dehydrogenase	36762	4.7	ID: 04155	9	38	99	1.8	1.3	1.2	0.0000	0.0074	0.0459
					eID: 00016	11	34	115	2.1	1.3	1.1	0.0001	0.0083	0.2493
B8LCI4	25130	D-isomer specific 2-hydroxyacid dehydrogenase [MBC]	50169	6.3	ID: 03315	18	47	148	-1.7	2.5	1.1	0.0021	0.0027	0.1979
B8LDQ8	15093	Serine carboxypeptidase	44464	4.7	eID: 00033	7	26	67	2.0	-1.1	-1.1	0.0009	0.1526	0.2477
B8LE80	bd1806	Aminotransferase, DegT/DnrJ/EryC1/StrS family [MBC]	48294	5.3	ID: 03168	8	27	72	-2.3	2.2	1.4	0.0000	0.0160	0.0945
					ID: 03140	9	27	76	1.7	1.9	1.2	0.0016	0.0076	0.1778

Appendix Table 2A

A comparison of changes in transcript levels associated with nitrogen deprivation in *T. pseudonana* (Mock et al 2008), as depicted in figure 7. Isoforms are gived as Protein IDs from the Joint Genome Institute *T. pseudonana* genome version 3 (http://genome.jgi-psf.org/Thaps3/Thaps3.home.html). Red indicates that the transcript level increased, while green indicates that the transcript decreased (fold change>2, P<0.05). X indicates no representative

Protein description and EC number	Isoform 1	Isoform 2	Isoform 3	Isoform 4	Isoform 5	Isoform 6	Isoform 7	Isoform 8	Isoform 9
6-phosphofructokinase [EC:2.7.1.11]	22213								
fructose-bisphosphate aldolase, class I [EC:4.1.2.13]	428	21748	35048	270288					
glyceraldehyde-3-phosphate dehydrogenase (NAD(P)) [EC:1.2.1.59]	x								
glyceraldehyde 3-phosphate dehydrogenase [EC:1.2.1.12]	28241	28334	31383	35816					
phosphoglycerate kinase [EC:2.7.2.3]	25116	35712	39901	42577	269057				
phosphoglycerate mutase [EC:5.4.2.1]	5573	17651	17735	27850	28350	260919	263035	263036	263397
enolase [EC:4.2.1.11]	40391	40771							
pyruvate kinase [EC:2.7.1.40]	4875	22345	31810	40393	264583				
pyruvate dehydrogenase E1 component [EC:1.2.4.1]	8778	16169	16241	32067	32983	41005	268374		
pyruvate dehydrogenase E2 component (dihydrolipoamide acetyltransferase) [E	547	21033	21177	38957	268280				
dihydrolipoamide dehydrogenase [EC:1.8.1.4]	21619	24399	36716	264440	268657				
pyruvate carboxylase [EC:6.4.1.1]	11075	11076	269908						
citrate synthase [EC:2.3.3.1]	11411								
aconitate hydratase 1 [EC:4.2.1.3]	268965								
isocitrate dehydrogenase [EC:1.1.1.42]	21640	1456							
isocitrate dehydrogenase (NAD+) [EC:1.1.1.41]	x								
2-oxoglutarate dehydrogenase E1 component [EC:1.2.4.2]	269718								
2-oxoglutarate dehydrogenase E2 component (dihydrolipoamide succinyltransfe	36971								
dihydrolipoamide dehydrogenase [EC:1.8.1.4]	21619	24399	36716	264440	268657				
succinyl-CoA synthetase alpha subunit [EC:6.2.1.5]	31362								
succinyl-CoA synthetase alpha subunit [EC:6.2.1.4]	411								
succinate dehydrogenase flavoprotein subunit [EC:1.3.99.1]	269017								
succinate dehydrogenase (ubiquinone) flavoprotein subunit [EC:1.3.5.1]	9849	32945	42475						
fumarate hydratase, class I [EC:4.2.1.2]	22464	24123							
malate dehydrogenase [EC:1.1.1.37]	20726	25953	41425						

Appendix Table 2B

A comparison of changes in transcript levels associated with nitrogen deprivation in *C. reinhardtii* (Miller et al 2010), as depicted in figure 7. Isoforms are gived as Protein IDs from the Joint Genome Institute *C. reinhardtii* genome version 4 (http://genome.jgi-psf.org/Chlre4/Chlre4.home.html). Red indicates that the transcript level increased, while green indicates that the transcript decreased (fold change>2, False Discovery<0.05).

Protein description and EC number	Isoform 1	Isoform 2	Isoform 3	Isoform 4	Isoform 5	Isoform 6	Isoform 7
6-phosphofructokinase [EC:2.7.1.11]	x						
fructose-bisphosphate aldolase, class I [EC:4.1.2.13]	24459	29185	152892	196304			
glyceraldehyde-3-phosphate dehydrogenase (NAD(P)) [EC:1.2.1.59]	x						
glyceraldehyde 3-phosphate dehydrogenase [EC:1.2.1.12]	93758	129019	140618	196837	403741		
phosphoglycerate kinase [EC:2.7.2.3]	132210						
phosphoglycerate mutase [EC:5.4.2.1]	8761	161085					
enolase [EC:4.2.1.11]	83064						
pyruvate kinase [EC:2.7.1.40]	104490	107530	118203	119280	122254	136854	196263
pyruvate dehydrogenase E1 component [EC:1.2.4.1]	139515	155587	190446	193810			
pyruvate dehydrogenase E2 component (dihydrolipoamide acetyltran	149206	149709	182542	196500	393418	420162	
dihydrolipoamide dehydrogenase [EC:1.8.1.4]	57890						
pyruvate carboxylase [EC:6.4.1.1]	402089						
citrate synthase [EC:2.3.3.1]	194915						
aconitate hydratase 1 [EC:4.2.1.3]	129025						
isocitrate dehydrogenase [EC:1.1.1.42]	196567						
isocitrate dehydrogenase (NAD+) [EC:1.1.1.41]	196042	196044					
2-oxoglutarate dehydrogenase E1 component [EC:1.2.4.2]	79471						
2-oxoglutarate dehydrogenase E2 component (dihydrolipoamide suc	x						
dihydrolipoamide dehydrogenase [EC:1.8.1.4]	57890						
succinyl-CoA synthetase alpha subunit [EC:6.2.1.5]	x						
succinyl-CoA synthetase alpha subunit [EC:6.2.1.4]	x						
succinate dehydrogenase flavoprotein subunit [EC:1.3.99.1]	145357						
succinate dehydrogenase (ubiquinone) flavoprotein subunit [EC:1.3.5	142231	195511	329709	394775	409053		
fumarate hydratase, class I [EC:4.2.1.2]	x						
malate dehydrogenase [EC:1.1.1.37]	60444	126023	137163	158129			

Appendix Table 2C

A comparison of changes in transcript levels associated with nitrogen deprivation in *A. thaliana* (Peng et al 2007), as depicted in figure 7. Isoforms are gived as AGI IDs from the *A. thaliana* Tair database (www.arabidopsis.org). Red indicates that the transcript level increased, while green indicates that the transcript decreased (fold change>2, False Discovery<0.005).

Protein description and EC number	Isoform 1	Isoform 2	Isoform 3	Isoform 4	Isoform 5	Isoform 6	Isoform 7	Isoform 8	Isoform 9	Isoform 10
6-phosphofructokinase [EC:2.7.1.11]	AT2G22480	AT4G26270	AT4G29220	AT4G32840	AT5G47810	AT5G56630	AT5G61580			
fructose-bisphosphate aldolase, class I [EC:4.1.2.13]	AT2G21330	AT4G38970	AT1G18270	AT2G01140	AT2G36460	AT3G52930	AT4G26520	AT4G26530	AT5G03690	
glyceraldehyde-3-phosphate dehydrogenase (NAD(P)) [EC:1.2.1.59]	AT2G24270									
glyceraldehyde 3-phosphate dehydrogenase [EC:1.2.1.12]	AT3G26650	AT1G12900	AT3G04120	AT1G13440	AT1G79530	AT1G16300				
phosphoglycerate kinase [EC:2.7.2.3]	AT1G56190	AT3G12780	AT1G79550							
phosphoglycerate mutase [EC:5.4.2.1]	AT1G09780	AT3G08590	AT1G22170							
enolase [EC:4.2.1.11]	AT1G74030	AT2G29560	AT2G36530							
pyruvate kinase [EC:2.7.1.40]	AT2G36580	AT3G04050	AT3G25960	AT3G52990	AT3G55650	AT3G55810	AT4G26390	AT5G08570	AT5G56350	AT5G63680
pyruvate dehydrogenase E1 component [EC:1.2.4.1]	AT1G01090	AT1G24180	AT1G30120	AT1G59900	AT5G50850					
pyruvate dehydrogenase E2 component (dihydrolipoamide acetyltransferase) [E	AT1G34430	AT1G54220	AT3G13930	AT3G25860						
dihydrolipoamide dehydrogenase [EC:1.8.1.4]	x									
pyruvate carboxylase [EC:6.4.1.1]	x									
citrate synthase [EC:2.3.3.1]	AT2G44350	AT2G42790	AT3G58740	AT3G58750	AT3G60100					
aconitate hydratase 1 [EC:4.2.1.3]	AT4G35830	AT4G26970	AT2G05710							
isocitrate dehydrogenase [EC:1.1.1.42]	AT1G54340	AT5G14590	AT1G65930							
isocitrate dehydrogenase (NAD+) [EC:1.1.1.41]	AT5G03290	AT3G09810	AT4G35260	AT2G17130	AT4G35650					
2-oxoglutarate dehydrogenase E1 component [EC:1.2.4.2]	x									
2-oxoglutarate dehydrogenase E2 component (dihydrolipoamide succinyltransfe	AT4G26910	AT5G55070								
dihydrolipoamide dehydrogenase [EC:1.8.1.4]	x									
succinyl-CoA synthetase alpha subunit [EC:6.2.1.5]	AT2G20420	AT5G08300	AT5G23250							
succinyl-CoA synthetase alpha subunit [EC:6.2.1.4]	x									
succinate dehydrogenase flavoprotein subunit [EC:1.3.99.1]	AT4G32210	AT2G18450	AT3G27380	AT5G09600	AT5G65165					
succinate dehydrogenase (ubiquinone) flavoprotein subunit [EC:1.3.5.1]	AT2G18450	AT3G27380	AT5G65165							
fumarate hydratase, class I [EC:4.2.1.2]	AT5G50950	AT2G47510								
malate dehydrogenase [EC:1.1.1.37]	AT1G04410	AT1G53240	AT2G22780	AT3G15020	AT3G47520	AT5G09660	AT5G43330	AT5G56720		

Appendix Table 2D

A comparison of changes in transcript levels associated with 12 hr nitrogen deprivation in *P. marinus* (MED4) (Tolonen et al. 2006), as depicted in figure 7. Isoforms are gived as locus IDs from the *Prochlorococcus marinus pastoris* CCMP1986 genome, JGI intergrated microbial genomes (http://img.jgi.doe.gov/cgi-bin/w/main.cgi). Red indicates that the transcript level increased, while green indicates that the transcript decreased (fold change>2, False Discovery<0.01).

Protein description and EC number	Isoform 1	Isoform 2	Isoform 3
6-phosphofructokinase [EC:2.7.1.11]	x		
fructose-bisphosphate aldolase, class I [EC:4.1.2.13]	PMM0781		
glyceraldehyde-3-phosphate dehydrogenase (NAD(P)) [EC:1.2.1.59]	PMM0023		
glyceraldehyde 3-phosphate dehydrogenase [EC:1.2.1.12]	PMM0713		
phosphoglycerate kinase [EC:2.7.2.3]	PMM0195		
phosphoglycerate mutase [EC:5.4.2.1]	PMM0515	PMM1434	
enolase [EC:4.2.1.11]	PMM0208		
pyruvate kinase [EC:2.7.1.40]	PMM0912		
pyruvate dehydrogenase E1 component [EC:1.2.4.1]	PMM0930	PMM1229	PMM1288
pyruvate dehydrogenase E2 component (dihydrolipoamide acetyltransferase) [EC:2.3.1.12]	PMM0405		
dihydrolipoamide dehydrogenase [EC:1.8.1.4]	PMM1298		
pyruvate carboxylase [EC:6.4.1.1]	x		
citrate synthase [EC:2.3.3.1]	PMM0161		
aconitate hydratase 1 [EC:4.2.1.3]	PMM1700		
isocitrate dehydrogenase [EC:1.1.1.42]	x		
isocitrate dehydrogenase (NAD+) [EC:1.1.1.41]	PMM1596		
2-oxoglutarate dehydrogenase E1 component [EC:1.2.4.2]	x		
2-oxoglutarate dehydrogenase E2 component (dihydrolipoamide succinyltransferase) [EC:2.3.1	x		
dihydrolipoamide dehydrogenase [EC:1.8.1.4]	PMM1298		
succinyl-CoA synthetase alpha subunit [EC:6.2.1.5]	x		
succinyl-CoA synthetase alpha subunit [EC:6.2.1.4]	x		
succinate dehydrogenase flavoprotein subunit [EC:1.3.99.1]	x		
succinate dehydrogenase (ubiquinone) flavoprotein subunit [EC:1.3.5.1]	x		
fumarate hydratase, class I [EC:4.2.1.2]	PMM1466		
malate dehydrogenase [EC:1.1.1.37]	x		